



**REPUBLIC OF IRAQ
MINISTRY OF HIGHER EDUCATION AND
SCIENTIFIC RESEARCH
AL-FURAT AL-AWSAT TECHNICAL UNIVERSITY
ENGINEERING TECHNICAL COLLEGE- NAJAF**

**EXPERIMENTAL STUDY OF SOLAR FLAT PLATE
COLLECTOR WITH V-GROOVES AND MANY SHAPE
TUBES DESIGN**

**ABDULABBAS ABDULNABI WALI HAMMADI
AL QARAGHULI**

**M.TECH.
IN MECHANICAL ENGINEERING TECHNIQUES
OF POWER**

2023



**EXPERIMENTAL STUDY OF SOLAR FLAT PLATE
COLLECTOR WITH V-GROOVES AND MANY SHAPE
TUBES DESIGN**

A THESIS

**SUBMITTED TO THE DEPARTMENT OF MECHANICAL
ENGINEERING TECHNIQUES OF POWER
IN PARTIAL FULFILLMENT OF THE REQUIREMENTS FOR THE
DEGREE OF MASTER THERMAL TECHNOLOGIES IN
MECHANICAL ENGINEERING TECHNIQUES OF POWER
(M.TECH.)**

BY

**ABDULABBAS ABDULNABI WALI HAMMADI
ALQARAGHULI**

Supervised by:

Prof.

Dr. Ahmad Hashim Yousif

January/ 2023

بِسْمِ اللَّهِ الرَّحْمَنِ الرَّحِيمِ
(قَالُوا سُبْحَانَكَ لَا عِلْمَ لَنَا إِلَّا
مَا عَلَّمْتَنَا إِنَّكَ أَنْتَ الْعَلِيمُ
الْحَكِيمُ)

صدق الله العلي العظيم

DISCLAIMER

I confirm that the work submitted in this thesis is my own work and has not been submitted to another organization or for any other degree.

Abdulabbas Abdalnabi Wali

Signature:

Date: / /2022

ACKNOWLEDGMENT

Full thanks to the Almighty God for the divine interference in a modest effort. Candid thanks are hereby extended to the following Never desisted in contributing to this thesis, Prof. Dr. Ahmad Hashim Yousif, my supervisor, support me for his guidance and unlimited support during the research period. Present of mine gratitude with appreciation for every one of the employers of the Power Techniques Department, College of Technical Engineering-Najaf Grateful and Special thanks for my parents, my late father, my mum, for mine brothers and for them unceasing assistance, inducement and Diligence in the hard time of my working life. Special thanks to the Dean of Engineering Technical College- Najaf Asst.Prof. Dr. Hassanain Ghani Hameed, Special thanks to the Head of Department of Mechanical Engineering Techniques of Power Asst. Prof. Dr. Adel A. Eidan in the Technical Engineering College /Al-Najaf, Al-Furat Al-Awsat Technical University, for their support and advice.

Abdulabbas Abdunabi Wali

November - 2022

DEVOTION

To my late father.....The symbol of giving and sacrifice

To my dear mother.....The Symbol of tenderness and passion

I dedicate my tiny effortto my beloved brothers and sisters,
who are my source of strength.

Abdulabbas

November - 2022

SUPERVISOR CERTIFICATION

We certify that this thesis titled " experimental study of solar flat plate collector with V- grooves and many shape tubes design" which is being submitted by **Abdulabbas Abdulnabi Wali** was prepared under our supervision at the Mechanical Engineering Techniques of Power Department, Engineering Technical College/Najaf, AL-Furat Al-Awsat Technical University, as a partial fulfillment of the requirements for the degree of Master in Thermal Mechanical Engineering.

Signature:

Name: Prof. Dr. Ahmad Hashim Yousif

(Supervisor)

Date: / / 202

In view of the available recommendation, we forward this thesis for debate by the examining committee.

Signature:

Name: Ass. Prof. Dr. Adel A. Eidan

Head of Mechanical Eng. Tech. of Power. Dept.

Date: / / 202

COMMITTEE REPORT

We certify that we have read this thesis titled “**EXPERIMENTAL STUDY OF SOLAR FLAT PLATE COLLECTOR WITH V-GROOVES AND MANY SHAPE TUBES DESIGN**” which is being submitted, by Abdulabbas Abdulnabi Wali, and as Examining Committee, examined the student in its contents. In our opinion, the thesis is adequate for the degree, of Master of Technical in Thermal Engineering.

Signature: 

Name: Prof. Dr. Ali Shakir Baqir
(Chairman)

Date: / /2023

Signature: 

Name: Prof. Dr. Ahmad Hashim Yousif
(Supervisor)

Date: 12 / 1 /2023

Signature: 

Name: Asst. Prof. Dr. Ali Najah Kazem
(Member)

Date: / /2023

Signature: 

Name: Asst. Prof. Dr. Haider Sami Saleh
(Member)

Date: 12 / 1 /2023

Approval of the Engineering Technical College-Najaf

Signature:

Name: Asst. Prof. Dr. Hassanain Ghani Hameed
Dean of Technical College-Najaf

Date: / /2023

ABSTRACT

The goal of this study is Experimental Study of Solar Flat Plate Collector with V- Grooves and Many Shape Tubes Design, the study on the heat transfer in terms of the Nusselt number (Nu), pressure loss in terms of friction factor(f), thermal performance factor TPF and the efficiency (η) of a flat plate solar collector. This research focuses with process of energy conversation under steady-state status in the laminar flow situation for uses drinkable water as the working fluid.

Experimental side includes design and construction of a V- grooves solar collector and triangular riser tubes, flat plate solar collector and circular riser tubes. The measuring instruments used in this experiment were solar radiation meter, volumetric flowmeter, manometer, temperature record meter, and temperature sensors. The experiments are carried out in Nasr City in Dhi Qar,Iraq with latitude 31.54° N and longitude 46.12° E, the volumetric flow rates used are (2,3,5 and 7)LPM.

The experimental result showed that the decrease in flow rate was found to increase the difference in water temperature between the outlet and the inlet of tubes, and the higher difference in temperature was (10.8° C) in the triangular riser tubes inside the grooves at volumetric flow rate 2 L / min, and at the same time the maximum outlet temperature of the triangular riser tubes inside the grooves 89% .In addition , heat transfer in term Nusselt number(Nu) and pressure loss in friction factor (f) improved compared to other cases in the triangular tubes inside the grooves, the Nusselt Number in triangular tubes inside the grooves enhanced to 30%,35.5%,40% and 52.7% with respect to circular tubes at laminar flow at ($500 < Re < 1900$). And the friction factor (f) increases as the Reynolds number Re decreases in triangular tubes inside the grooves comparing with circular tubes, the friction factor (f) in the triangular tubes inside the grooves 15% -25% above the circular tubes. The experimental results also showed that the TPF thermal performance factor for triangular tubes inside the grooves. The highest

thermal performance was 2.6, greater than the circular cylinder with same pumping capacity., the maximum efficiency of the triangular tubes inside the grooves was 53.4%.

CONTENTS

DISCLAIMER.....	II
ACKNOWLEDGMENT.....	III
DEVOTION.....	IV
SUPERVISOR CERTIFICATION.....	V
COMMITTEE REPORT.....	VI
ABSTRACT.....	VII
CONTENTS.....	IX
LIST OF TABLES.....	XIII
LIST OF FIGURES.....	XIV
LIST OF NOMENCLATURE.....	XIX
ABBREVIATIONS.....	XXII
Chapter One.....	1
Introduction.....	1
1.1 preface.....	1
1.2 Solar collectors.....	2
1.3 Flat plate solar collector.....	6
1.4 Research problem and objectives of the thesis.....	6
Chapter Two.....	8
Literature Review.....	8
2.1 Introduction.....	8
2.2 Geometric shapes of rising tubes in solar collectors.....	8
2.3 Influence of the triangular tubes.....	13
2.4 Influence of the used plate.....	19
2.5 The influence of different flow.....	26

2.6 Scope of the present work.....	41
Chapter Three.....	45
Theoretical Analysis.....	45
3.1 Introduction.....	45
3.2 Triangular tubes.....	41
3.3 The V- grooves absorber plate.....	46
3.4 Heat transfer and flowing fluid in circular tubes.....	49
3.5 The performance of solar collector.....	50
3.6 The gross coefficient of heat loss for flat plate collector U_L	52
3.7 The internal convection heat transfer coefficient of water flow (h_i) in riser tubes.....	57
3.8 The useful of energy and the efficiency of solar collector.....	57
3.9 Thermal performance factor (performance ratio) (TPF).....	58
Chapter Four.....	59
Experimental Work.....	59
4.1 Introduction.....	59
4.2 Experimental Work Description.....	60
4.2.1 Specifications of Flat Plate Solar collector.....	61
4.2.2 Specifications V-grooves Plate Solar collector.....	65
4.2.3 Experimental setup of the system.....	67
4.2.4 Water pumps.....	71
4.2.5 Pipes.....	71
4.2.6 Valves.....	72
4.2.7 The insulators.....	73
4.2.8 The measuring devices.....	73
Chapter Five.....	81

Results and Discussions.....	81
5.1 Introduction.....	81
5.2 Experimental results.....	81
5.3 The results of solar radiation.....	82
5.4 The result of outlet temperature.....	83
5.4.1 Outlet temperature comparison of the circular and triangular riser tubes inside the grooves.....	83
5.4.2 Outlet temperature comparison of the circular and triangular riser tubes beside the grooves.....	85
5.4.3 Outlet temperature comparison of the circular and triangular riser tubes over the grooves.....	86
5.4.4 The outlet temperature comparison for the T_t inside and T_t beside and T_t over grooves.....	88
5.5 The results of temperature difference.....	92
5.6 The heat transfer variation.....	94
5.7 The Results of pressure loss	98
5.8 Thermal Performance factor TPF.....	101
5.9 Collector efficiency.....	104
5.10 Compare the results obtained with the results of previous research.....	105
Chapter Six.....	107
Conclusions and Recommendation.....	107
6.1 The conclusion.....	107
6.2 The recommendations.....	109
References.....	110
Appendices.....	A-1
A. The calibration of the experiment-related equipment.....	A-1
A.1 Calibration of solar collector meter.....	A-1

A.2 Calibration of volumetric flow meter.....	A-1
A.3 Calibration of temperature sensors of 8- channel data logger and 4K type thermocouples with digital thermometers.....	A-3
A.4 Calibration differential pressure manometer.....	A-6
B. Uncertainties analysis.....	B-1
B.1 Friction factor derivation.....	B-2
B.2 Nusselt number derivation.....	B-3
B.3 collector efficiency derivation.....	B-4
B.4 Uncertainty analysis for forced circulation condition.....	B-5
B.4.1 Friction factor evaluated.....	B-5
B.4.2 The Nusselt number calculation.....	B-6
B.4.3 Efficiency calculation.....	B-6
C. List of publications.....	C-1

LIST OF TABLES

Table	Page
No.	No.
Table-2.1: The summary	41
Table-4.1: The specification of flat plate and V-grooves plate solar collectors.....	64
Table-4.2: The specifications of centrifugal pumps.....	71
Table-A.1: calibration results of first 8- channels data logger with 8 sensors..	A-3
Table-A.2: Calibration results of second 8- channels data logger with 8 sensors.....	A-4
Table-A.3: The calibration of 4 k- type.....	A-5
Table-B.1: The errors in the instruments used in experiments.....	B-5

LIST OF FIGURES

Figure	Page
No.	No.
Fig. 1.1: Evacuated tube collector.....	3
Fig. 1.2: Flat plate solar collectors.....	4
Fig. 1.3: Line Focus Collectors.....	5
Fig. 1.4: A point focus solar collector.....	5
Fig. 2.1 a: Variation heat transfer coefficient with mass flow rate for circular and rectangular tube.....	9
Fig. 2.1 b: Variation Nusselt number with mass flow rate for circular and rectangular tube.....	10
Fig. 2.1 c: Variation of pressure drop with mass flow rate for circular and rectangular tube.....	10
Fig. 2.2: models A, B of solar water collector of circular and elliptical tubes respectively.....	11
Fig. 2.3: Schematic layout of experimental system.....	12
Fig. 2.4: Schematic Diagram of the Thermal Collector with Flat Solar Radiation Reflectors.....	13
Fig. 2.5: various shapes of tubes circular, elliptical, triangular & square.....	14
Fig. 2.6: Triangular Tube Configuration.....	15
Fig.2.7: Top Views of the Risers for Both cases.....	16
Fig. 2.8: Photo of the triangular flat plate collector.....	17
Fig. 2.9 a: distribution in circular riser's tubes.....	18
Fig. 2.9 b: distribution in triangular riser's tubes.....	18
Fig. 2.9 c: distribution in square riser's tubes.....	19
Figure.2.10: Cross-sectional schematic of rectangular solar water heater with corrugated surface.....	20

Fig.2.11: The absorbers with different structure.....	21
Fig. 2.12: Solar water heating system with (a) flat-plate absorber plate(b) V-shaped absorber plate.....	22
Fig.2.13: Solar FPC with V corrugated absorber plate.....	23
Fig. 2.14: Experimental setup of the integrated solar water heater showing measurement points.....	24
Fig.2.15: Schematic of experiment and heat exchange in Solar Collector.....	25
Fig.2.16: Sketch and photograph of experimental rig for TSAC.....	26
Fig.2.17: Installation of the solar water heater.....	28
Fig.2.18: Developed arrangement of the pipe.....	29
Fig.2.19: Solar collector models with 3,4,5, and 6 mm glass thick, respectively.....	30
Fig.2.20: Pictorial View of a Flat- Plate Solar Collector.....	31
Fig.2.21: Scheme of data collection.....	32
Fig.2.22: Pictorial view of the experimental setup and roughness elements.....	33
Fig.2.23: FPC with Aerofoil and Circular absorber tubes.....	34
Fig. 2.24 a: A schematic view of an open system.....	35
Fig.2.24b: A schematic of the closed system of solar collector.....	35
Fig.2.25: flat plate solar collector.....	36
Fig. (2.26 a-b): (a) Schematic diagram of the experimental rig and (b) Schematic diagram of the flat plate solar collector with water pipes.....	37
Fig.2.27: Pictorial view of the experimental rigs.....	38
Fig.2.28: Flat plate collector.....	39
Fig.2.29: Photograph for the test rig.....	40
Fig. 3.1 Triangular riser tubes.....	46
Fig. 3.2 The V- grooves absorber plate.....	47

Fig. 3.3: schematic diagram of the solar collectors that contain circular tubes and triangular tubes.....	48
Fig. 3:4. distribution of solar irradiance over solar collector.....	51
Fig. 3.5: solar collector thermal resistance system with two layers.....	55
Fig. 4.1: Schematic of test rig construction and the measurement devices.....	61
Fig. 4.2: flat plate solar collector components.....	63
Fig. 4.3 V- grooves plat solar collector components.....	66
Fig. 4.4: FPC and V-grooves plate solar collector with measurements device...	68
Fig. 4.5: The flat plate solar collector that contains circular tubes.....	69
Fig. 4.6: The V-grooves plate solar collector that contains triangular tubes inside the grooves.....	69
Fig. 4.7: The V-grooves plate solar collector that contains triangular tubes beside the grooves.....	70
Fig. 4.8: The V-grooves plate collector that contains triangular tubes over the grooves.....	70
Fig. 4.9 Water pumps.....	71
Fig. 4.10 Plastic pipes (1/2 inch) covered by insulators.....	72
Fig. 4.11 Ball valves.....	72
Fig. 4.12 Data Logger.....	74
Fig. 4.13 Seventeen temperature sensors type K.....	74
Fig. 4.14 Positions of temperature sensors.....	76
Fig. 4.15 Volumetric water flow meter.....	77
Fig. 4.16: Manometer.....	77
Fig. 4.17: solar power meter.....	78
Fig. 4.18: Wind speed.....	78
Fig. 5.1: solar radiation for (1-12)/ September /2022.....	83

Fig. 5.2: Comparing between Tout circular tubes and Tout triangular tubes inside the grooves at flow water (2,3,5 and 7) LPM for (1-4)/ September /2022 respectively.....	84
Fig. 5.3: Comparing between Tout circular tubes and Tout triangular tubes beside the grooves at flow water (2,3,5 and 7) LPM for (5-8)/ September /2022 respectively.....	86
Fig. 5.4: Comparing between Tout circular tubes and Tout triangular tubes over the grooves at flow water (2,3,5 and 7) LPM for (9-12)/ September /2022 respectively.....	88
Fig. 5.5: Comparing between To for ($T_{t_{inside}}$, $T_{t_{beside}}$, $T_{t_{over}}$) V grooves plate at flow water 2 Lpm.....	90
Fig. 5.6: Comparing between To for ($T_{t_{inside}}$, $T_{t_{beside}}$, $T_{t_{over}}$) V grooves plate at flow water 3 Lpm.....	90
Fig. 5.7: Comparing between To for ($T_{t_{inside}}$, $T_{t_{beside}}$, $T_{t_{over}}$) V grooves plate at flow water 5 Lpm.....	91
Fig. 5.8: Comparing between To for ($T_{t_{inside}}$, $T_{t_{beside}}$, $T_{t_{over}}$) V grooves plate at flow water 7 Lpm.....	91
Fig. 5.9: Temperature Difference for Triangular tubes inside the grooves.....	92
Fig. 5.10: Temperature Difference for Triangular tubes beside the grooves.....	93
Fig. 5.11: Temperature Difference for Triangular tubes over the grooves.....	93
Fig. 5.12: Temperature Difference for Circular tubes.....	94
Fig. 5.13: The variation of Nusselt Number with local Time For 2L/min.....	95
Fig. 5.14: The variation of Nusselt Number with local Time For 3L/min.....	96
Fig. 5.15: The variation of Nusselt Number with local Time For 5L/min.....	96
Fig. 5.16: The variation of Nusselt Number with local Time For 7L/min.....	97
Fig. 5.17: Nusselt number (Nu) variation with Reynolds Number Re for (circular tubes, triangular tubes inside the grooves, triangular tubes beside the grooves and triangular tubes over the grooves).....	97
Fig. 5. 18: The Friction Factor variation with Local Time For 2 LPM.....	99

Fig. 5. 19: The Friction Factor variation with Local Time For 3 LPM.....	99
Fig. 5. 20: The Friction Factor variation with Local Time For 5 LPM.....	100
Fig. 5. 21: The Friction Factor variation with Local Time For 7 LPM.....	100
Fig. 5.22: The Friction Factor variation with Reynolds Number Re for (circular tubes, triangular tubes inside the grooves, triangular tubes beside the grooves and triangular tubes over the grooves).....	101
Fig. 5.23: Thermal Performance Factor (TPF) with Local Time For 2LPM...	102
Fig. 5.24: Thermal Performance Factor (TPF) with Local Time For 3LPM...	102
Fig. 5.25: Thermal Performance Factor (TPF) with Local Time For 5LPM....	103
Fig. 5.26: Thermal Performance Factor (TPF) with Local Time For 7LPM....	103
Fig. 5.27: Thermal Performance Factor with Reynolds Number Re for triangular tubes inside the grooves, triangular tubes beside the grooves and triangular tubes over the grooves).....	104
Fig. 5.28: the efficiency of solar collector with Reynolds number Re for (triangular tubes inside the grooves, triangular tubes beside the grooves, triangular tubes over the grooves and circular tubes placed on the flat plate).....	105
Fig. A.1 sun radiation meter calibration.....	A-1
Fig. A.2 calibration of differential pressure manometer.....	A-7

LIST OF NOMENCLATURE

A_c	The area of solar collector	m^2
A_i	Inside surface area	m^2
A_o	Outside surface area	m^2
C_{pw}	Specific heat of water	J/kg.K
r	Circular tube radius	m
d_i	Inner diameter of circular tube	m
d_o	Outlet diameter of riser tube	m
X	side length of triangle tube	m
h'	The height of the triangular tube	m
D_h	The hydraulic diameter of the triangle tube	m
f	Friction factor	Dimensionless
F_R	The Heat removal factor	Dimensionless
G_T	Global radiation	W/ m^2
h	heat transfer coefficient	W/ $m^2 \cdot K$
h_i	Internal convection heat transfer coefficient	W/ $m^2 \cdot K$
h_c	Convection heat transfer coefficient	W/ $m^2 \cdot K$
h_r	Radiation heat transfer coefficient	W/ $m^2 \cdot K$
h_w	The wind loss coefficient	W/ $m^2 \cdot K$
I_T	Total solar radiation	W/ m^2
k	Thermal conductivity	W/ m. K
k_e	Thermal conductivity of insulation at edges	W/ m. K
k_b	Thermal conductivity of insulation at bottom	W/ m. K
k_p	Thermal conductivity of absorber plate	W/ m. K

k_w	Thermal conductivity of water	W/ m. K
L	Length of the collector	m
l	Distance between plate and covers	m
\dot{m}	Mass flow rate	Kg/sec
Nu	Nusselt number	Dimensionless
P	Pressure of water	N/ m ²
Q	Thermal energy	W
Q_u	Useful thermal energy	W
$q_{loss,top}$	Heat loss from the top of collector	W/m ²
S	Solar radiation absorption	W/m ²
t_e	Thickness of insulation at edges	m
t_b	Thickness of insulation at bottom	m
T_a	Ambient temperature	° C
T_i	Inlet water temperature	K
T_p	Plate temperature	K
T_{pm}	mean Temperature of the plate	K
T_o	Outlet water temperature	K
U_L	Overall heat coefficient	W/ m ² . K
U_e	Heat coefficient from edges	W/ m ² . K
U_b	Heat coefficient from bottom	W/ m ² . K
U_o	Outside overall heat transfer coefficient	W/ m ² . K
U	Velocity of water	m/sec
u	Wind speed	m/sec
W	Distance between two riser tubes	m

Greek Symbols		
$(\tau\alpha)_{av}$	Average transmittance-absorptance product	Dimensionless
τ	The transmittance of a single cover	Dimensionless
τ_r	Transmittance with only reflection losses	Dimensionless
$\tau\alpha$	Transmittance with only absorption losses	Dimensionless
α_n	Absorptance at normal incident angle	Dimensionless
β	The tilt angle of collector	Degree
β'	Volumetric coefficient	K^{-1}
δ_p	Thickness of absorber plate	m
ΔP	pressure drop across riser tube	N/m^2
ε_p	The emissivity of plate	Dimensionless
ε_c	The emissivity of glass (cover)	Dimensionless
η	collector efficiency	Dimensionless
η_i	instantaneous collector efficiency	Dimensionless
θ_1	The incidence angle of solar radiation	Degree
θ_2	The refraction angle of solar radiation	Degree
θ_e	Effective incidence angle	Degree
ω	solar hour angle	Degree
ϑ	The latitude of city	Degree
μ_w	Dynamic viscosity of water	$Pa \cdot s$
ρ_w	Density of water	Kg/m^3
ν	kinematics viscosity of air	m^2/sec

ABBREVIATIONS

Symbol	Description
N	Number of glass (covers)
Tt_{inside}	Temperature of triangular tubes inside the grooves
Tt_{beside}	Temperature of triangular tubes beside the grooves
Tt_{over}	Temperature of triangular tubes over the grooves
Tt_{circular}	Temperature of circular tubes
$f(t)$	Friction factor in triangular tubes
$f(c)$	Friction factor in circular tube
Nu(t)	Nusselt number in triangular tubes
Nu(c)	Nusselt number in circular tube
$Nu_{\text{triangular}}$	Nusselt number for flow in a triangular tube
Nu_{circular}	Nusselt number of flows in circular tubes
$f_{\text{triangular}}$	friction factor for flow in a triangular tube
f_{circular}	Friction factor for flow in circular tubes.
FPC	The flat plate solar collector
VGPC	The V-grooves plate solar collector
Pr	Prandtl number
Ra	Rayleigh number
Re	Reynolds number

CHAPTER ONE

INTRODUCTION

Chapter One

Introduction

1.1 Preface

There are many different sources of energy in the world, including coal and fossil fuels, but solar energy has become a practical energy source, particularly since the Industrial Revolution. Many scientists and researchers have proven that renewable energy sources offer many benefits, including being ecologically friendly, having a low maintenance requirement compared to harmful emissions, and being an energy source that can be produced again. It is also referred to as a fossil fuel since coal and natural gas are sources of solar energy that are created through photosynthetic processes and then decompose under extreme pressure and temperature. As a result of temperature variations in the earth's regains, wind and tide are also solar phenomena. Solar energy may be converted using solar collectors and photovoltaic cells. into electricity and heat, respectively. [1]

Solar energy can also be used to solve the issue of not having enough water supply by solar-distilling sea water. Imagine a heat exchanger as a solar collector that converts, expends, and recovers heat. Chemicals, agronomic products, air and liquid chilling schemes in engines, and liquid evaporating and precipitation in air conditioners and refrigerators all undergo thermal processing., as well as numerous other home, commercial, and industrial uses are among them. When temperature is already being transferred between two surfaces, the solar thermal collector is collecting solar irradiance and transforming it into internal energy. There is liquid inside the heat exchanger. a way to make heat transfer better. Three factors influence a thermal system's coefficients. The Mechanisms are: active, passive, and compound. It falls into three categories: exhaust power, powerlessness, and the use of both of the above methods. You can use one or more of the following heat transfer enhancement techniques [2]

- 1) Increasing the interaction surface area between the tube and the plate by changing the tube shape in the solar collectors which can increase the heat transfer more efficiently.
- 2) Using the grooves in flat plates to expand the interaction of surface area, between the tube and the plate, which can increase the efficiency of the solar collector.
- 3) Using fins in order to boost contact area of contact with the fluid to be heated or cooled increasing the slowness of the fluid due to the inclusion of secondary heat transfer surfaces
- 4) It's excellent to increase the effective area between the insertion device edges and the tube wall.
- 5) Short or long fins and rough surfaces cause more disturbances in the lamellar boundary layers

Heat transfer technology has a significant impact on heat exchangers as it handles high heat flows and minimizes size. The result is a cost-effective heat transfer enhancement technique that allows the heat exchanger to operate with higher heat transfer coefficients and at low speeds.

1.2 Solar collectors

An apparatus that gathers and focuses solar radiation from the sun is called a solar collector. These gadgets provide both personal water heating and active solar heating. These collectors need to be exceptionally durable because they are frequently mounted on roofs and subjected to many types of weather. A number of these collectors can also be utilized to generate energy in solar thermal power stations for home purposes.

Types of solar collectors

A. variety of solar panels are available of sizes and shapes, but they are all built on the same basic premise. For the purpose of heating water, a number of materials are often used to collect and concentrate solar energy. The most basic of these tools is a black substance-enclosed tube through which water flows. The black material efficiently absorbs sunlight, warming the water nearby. Although the design is rather simple, the collector can be a little complicated. Systems that focus sunlight with reflectors typically experience greater temperature increases. When considerable temperature increases are not required, absorber panels can be employed.

B. Stationary collectors

A fixed condensing collector is a form of condensing collector that transmits solar energy from a wide tolerance to the companion absorber or opening using a composite parabolic reflector and a flat reflector. This reflector's wide opening angle makes a sun tracker unnecessary. This category of collectors includes solar cookers, flat plate collectors with parabolic sensitizers, and flat plate collectors with parabolic troughs. The usage of solar cookers is widespread, particularly in underdeveloped nations.

- **Evacuated tube collector**

This kind of solar collector heats water for usage using a network of vacuum tubes as showing in fig. (1.1). These tubes minimize heat loss to the environment by absorbing solar energy in a vacuum or vacuum region. They act as absorbers and have a heat pipe connected to an inner metal tube that allows the light of the sun to be transferred to the water. This heat pipe is essentially a tube that contains a liquid that is compressed to a specific degree. At this pressure, the "cold" end of the tube is filled with condensed vapor, and the "hot" end is filled with boiling liquid. This enables efficient transfer of heat energy from the tube's inner to outer ends. As heat from the sun moves from the heated end of the temperature pipe to the condensed end, it is transmitted to the water, which then is heated and absorbed.

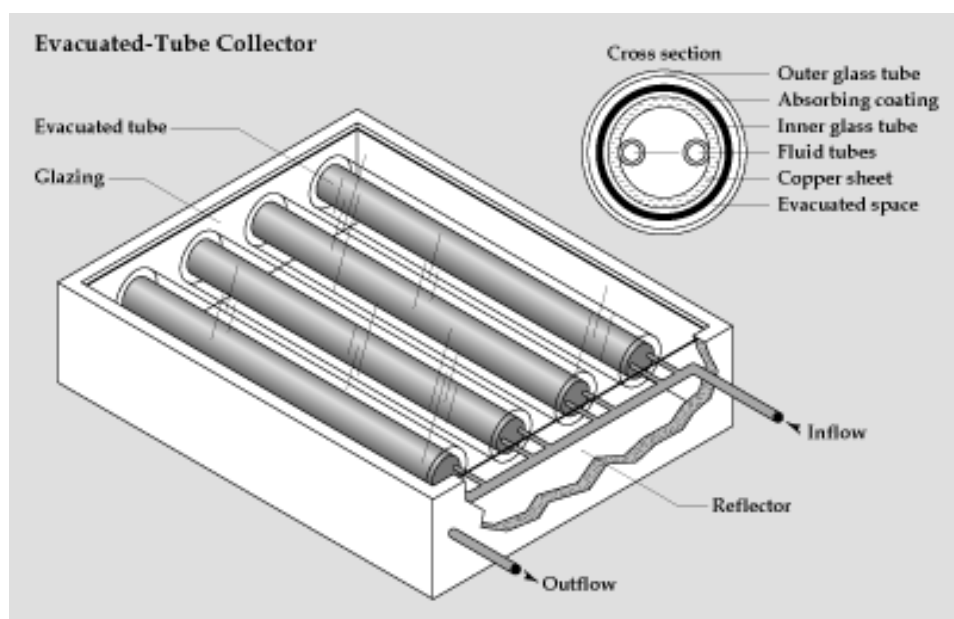


Fig. 1.1: Evacuated tube collector [1]

- **Flat plate solar collector**

These collectors are simple metal boxes with a clear glass top over a dark absorber as showing in fig. (1.2). The side and bottom of the collector are designed to minimize heat loss of the collector which are usually coated with insulation. Transparent glass allows solar rays to reach the absorber. This heated panel radiates heat to any liquid or gas that is sandwiched between the absorber panel and the glazing. It is possible to paint these heat absorber plate with a black paint to absorb and holds onto heat.



Fig. 1.2: Flat plate solar collectors [2]

C. Sun tracking concentrating collectors:

- **Line Focus Collectors**

These collectors, also known as parabolic troughs as showing in fig. (1.3), absorb and concentrated generate heat from solar radiation using highly reflecting materials. These collectors include a long trough and a parabolic reflecting portion. This bathtub's water is heated via a water-carrying tube in the center. The reflecting material attracts the sunlight, which is then focused

on the tube. Since they are particularly effective collectors, they are typically utilized to produce steam from solar thermal power plants rather than homes.

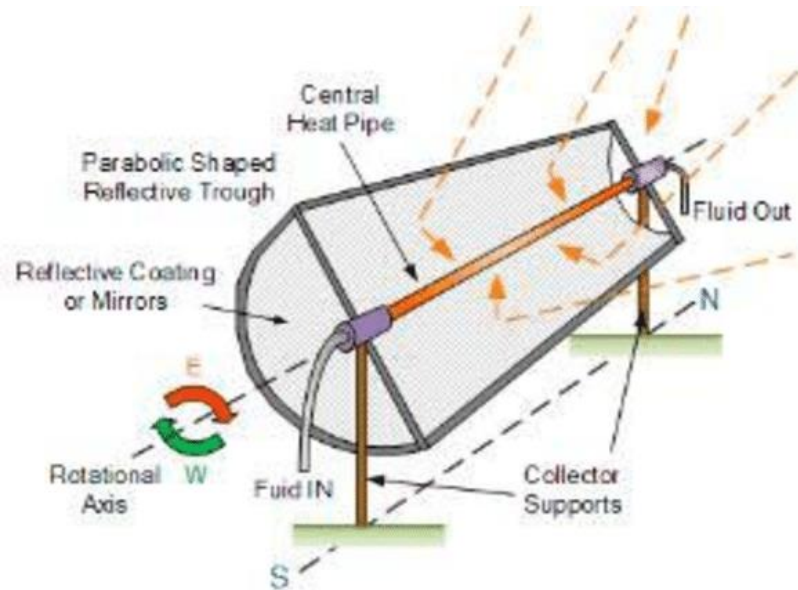


Fig. 1.3: Line Focus Collectors [3]

- **Point focus collectors**

Large parabolic dishes made of reflective material, called collectors, concentrate the sun's energy in one place as showing in fig. (1.4). The Stirling engine is frequently run-on heat from these collectors.



Fig. 1.4: A point focus solar collector [4]

1.3 Flat plate solar collector

A Flat plate collector is a solar panel device that uses solar energy to generate thermal energy. It converts solar power into thermal energy, i.e., cheaper energy utilizing water as an operating fluid. A Flat plate solar collector takes in solar radiation and transmits heat to the functioning medium. It is suitable for several thermal applications. The FPC devices are the backbone of solar thermal devices. They have diverse applications from household to commercial sectors. Flat plate collector devices are commonly used for active space heating and water heating for further usage, and the solar collector consists of the following parts:

- container: It is an external cover for the system to protect it from external atmospheric influences and contains the parts of the system inside, allowing the entry of solar radiation from the top.
- Glassing cover: This is a single or several sheets of glass that allows solar energy to pass through to the system.
- The headers pipes: Two tubes are placed above and below the system for the entry and exit of liquid through them.
- Tubes: They are connecting tubes between the two main tubes that handover fluid from the creek tube to the outlet tube, where they exchange heat between the fluid inside them with solar radiation outside the tubes. It is made of conductive materials.
- Absorber plate: It is a metal that is flat or contains grooves, which may be copper, aluminum, or the like.
- Insulations: They are thermal insulators that reduce heat loss between the system and the outside environment.

1.4 Research problem and objectives of the thesis

The major objective of that study is to promote an experimental research tool to investigate the flowing fluid-structure, and the heat transfer characteristic of water in riser tubes, for double glass covers of solar collectors equipped with triangular riser tubes with V- grooves absorber plate, and in three cases (the triangular tubes inside the grooves, the triangular tubes beside the grooves and the triangular tubes over the grooves) under laminar flow ($500 < Re < 1900$).), at volumetric flowmeter (2, 3, 5 and 7) LPM. This study includes investigating the effect of triangular riser tubes with V- grooves absorber plate on the thermal rate in term number of Nusselt, friction parameter, and performance of solar collector, this goal is to achieve through several steps.

The first step involves design, manufacture and installation of the experimental test rig with all necessary instruments required to evaluate the augment in heat and measuring the conditions of the experiment such as (mass flow rate, solar radiation, pressure difference). The second step is to evaluate the improvement in the rate of heat transfer for triangular riser tube equipped with V- grooves absorber plate and compare with circular riser tubes and study, then developing a relationship to evaluate the Nusselt number (Nu), factor of friction (f).

CHAPTER TWO

LITERATURE REVIEW

Chapter Two

Literature Review

2.1 Introduction

In addition to achieving the necessary goals described in the preceding chapter, advancement has been achieved in the literature review by comparing the performance of various tube shapes, such as triangular pipes and circular tubes, and by using corrugated absorber plates and flat plates in solar panels, respectively. In order to conduct a fruitful literature study, heat transmission needs to be increased. It is advised to make sure the historical context is considered., with an awareness of the categorization of several types of tubes employed and the various plates that the study paper is concerned with, as well as the chosen thermal transfer technique. The literature review makes progress in summarizing the techniques for enhancing heat transmission and the findings of earlier research; at least twenty of the current works on heat transfer are focused on mechanisms of improved heat transfer. The approach of enhancing heat transmission by utilizing various types of empirically and numerically tested pipes and panels used in solar panels has recently been the subject of extensive research and study. Also, example, the use of, the tubes that have the largest contact area between the riser tubes and the plates used inside the solar collector.

2.2 Geometric shapes of rising tubes in solar collectors

In addition to other important components, the increasing tubes used in solar collectors are a crucial component because they significantly affect the device's performance. To maximize the solar collector's efficiency, it is important to determine which one of the riser pipes has a bigger contact area with the flat plate. To get the most of the solar energy available, flat plate catchers, which utilize both direct and scattered radiation from the sun, are the easiest and least costly to construct, install, and maintain. Homes, apartments, buildings, schools, restaurants,

dairies, agricultural areas, and industrial areas all use it. The shallow of the absorber is tinted with black epoxy dye, and it is constructed of a metallic substance like copper, steel, or aluminum. Strong conductivity, low radiation, and high absorption characterize it.

(Priyanka et al. 2014)[5] compared of heat transfer between circular and rectangular tube using the simulation program Ansys Fluent, under similar operating conditions. Results indicated that circular pipe heat exchangers showed 2.5% increase in the heat transfer rate over the rectangular tube as shown in fig. (2.1 a), Simulation results also showed 8.5% increase in Nusselt number for the circular tube as shown in fig. (2.1 b), whereas pressure drop in case of circular tube is higher when compared to the rectangular tube as shown in fig. (2.1 c).

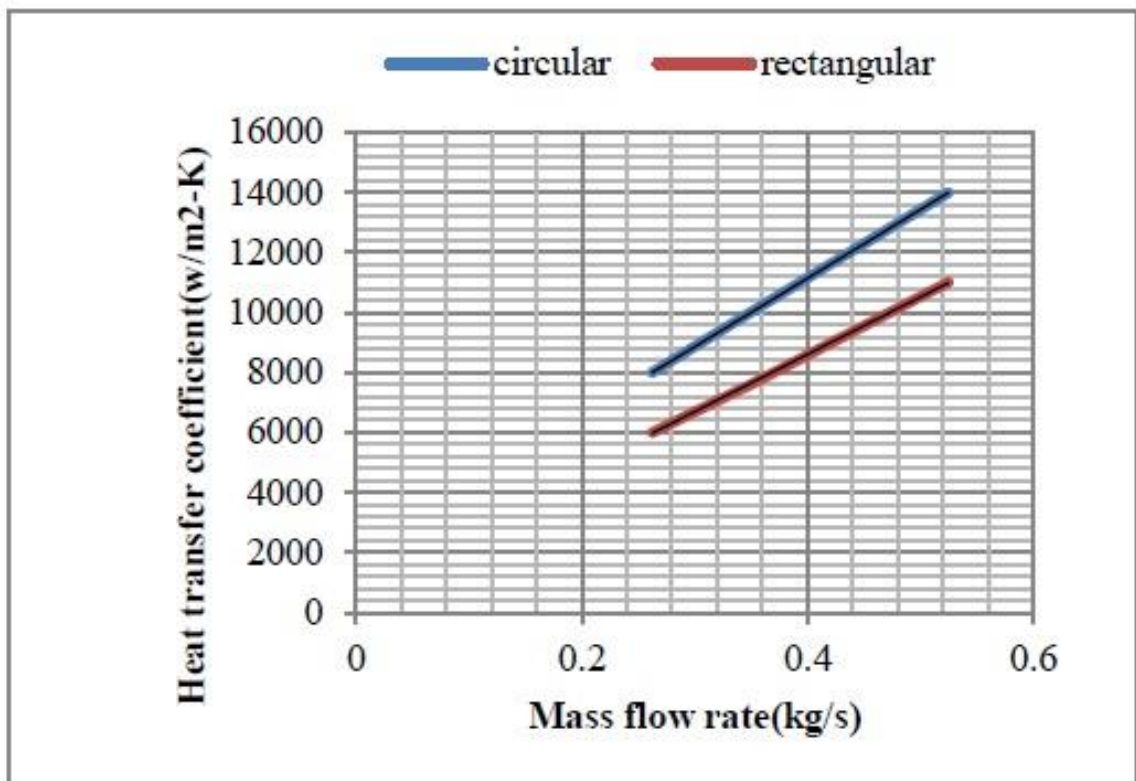


Fig. 2.1 a: Variation heat transfer coefficient with mass flow rate for circular and rectangular tube [5].

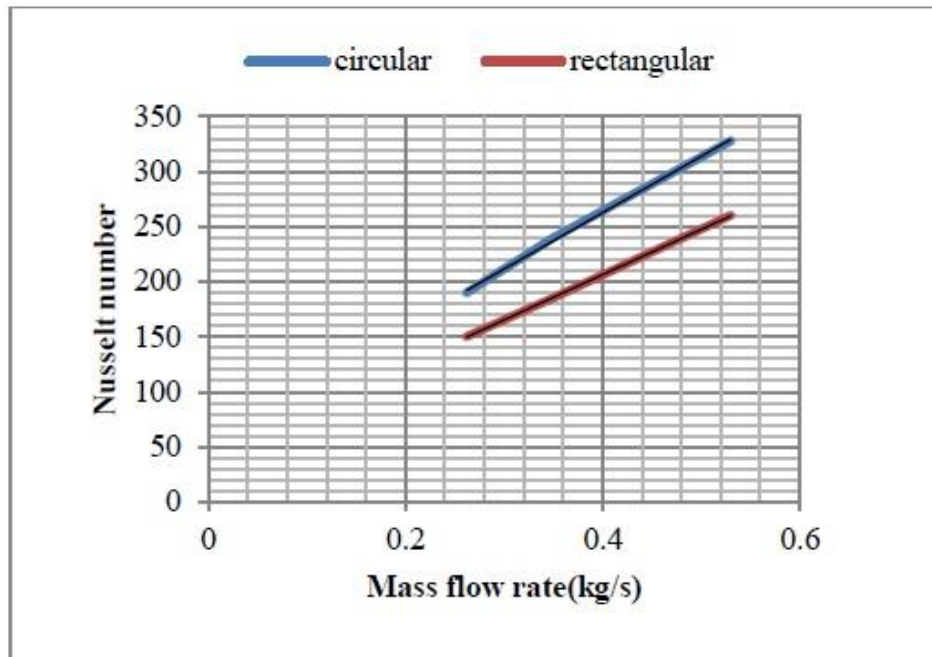


Fig. 2.1 b: Variation Nusselt number with mass flow rate for circular and rectangular tube [5].

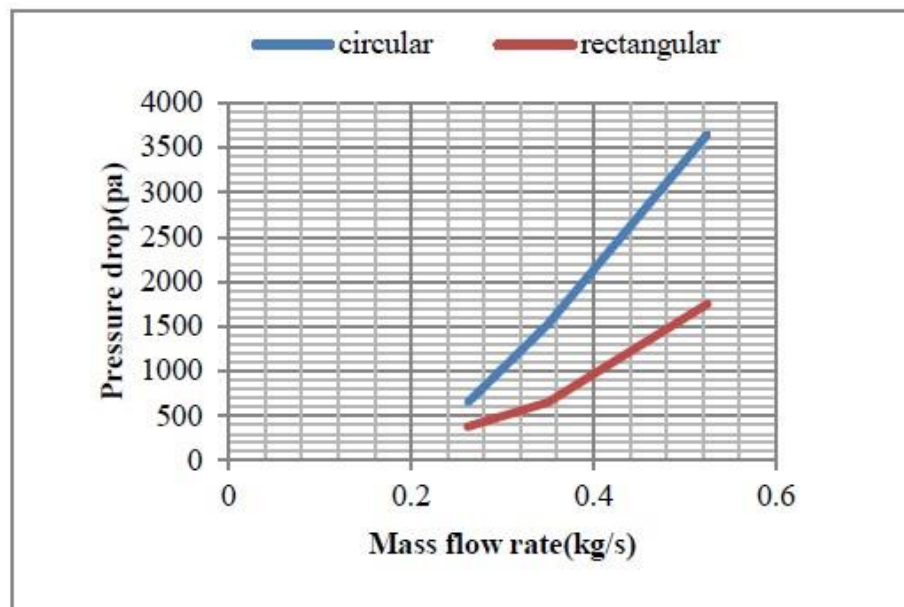


Fig. 2.1 c: Variation of pressure drop with mass flow rate for circular and rectangular tube [5].

(Vishal et al. 2015) [6] performed an analysis of the impact of tube form modifications for flat - plate solar water heaters., using two shapes of tubes, circular and elliptical as shown in fig. (2.2), for this study circular tube of 12.7 mm diameter was considered and numerical analysis is carried out with ANSYS CFD FLUENT

software. from this study it is concluded that elliptical tube gives the maximum outlet temperature of water for the same heat flux and inlet temperature in comparison with circular geometries. It also shows the peak outlet temperature difference between circular and elliptical tube is $4.17\text{ }^{\circ}\text{C}$. This shows that elliptical tube is beneficial in future for domestic purpose.

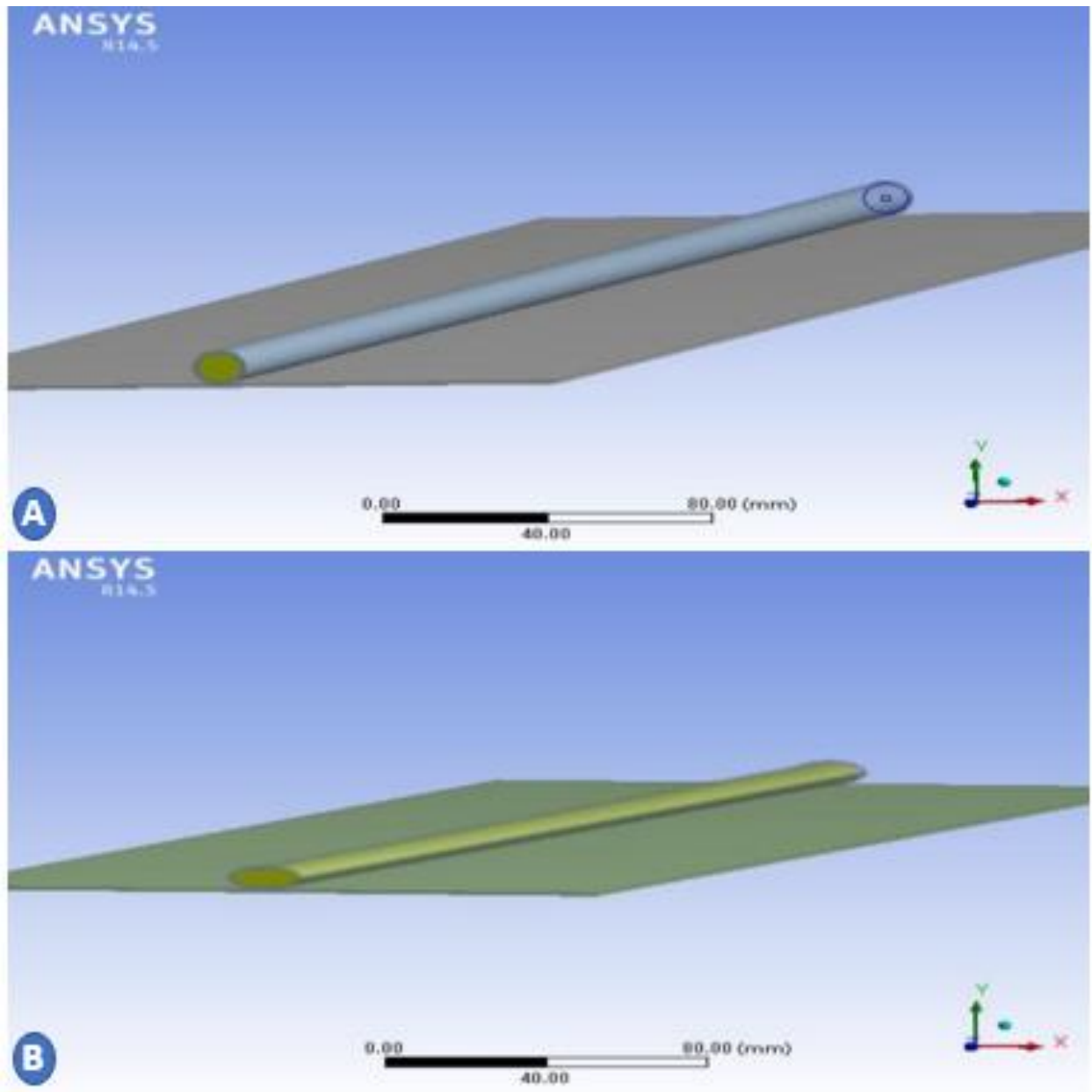


Fig. 2.2: models A, B of solar water collector of circular and elliptical tubes respectively [6].

(Mangesh et al. 2016)[7] Investigated of formed tubes of different geometry like circular, triangular, square, and oval for a flat plate solar collector, as shown in fig. (2.3). The purpose of this study was to focus on improving the performance of solar

flat plate collectors, by knowing which of the geometry of the pipes used is more efficient in heat conduction. The results showed that the efficiency of the efficiency of the triangular tube is the highest compared to other tubes. It is observed that efficiency is directly proportional to flow rate and depends on the intensity of sunlight also.

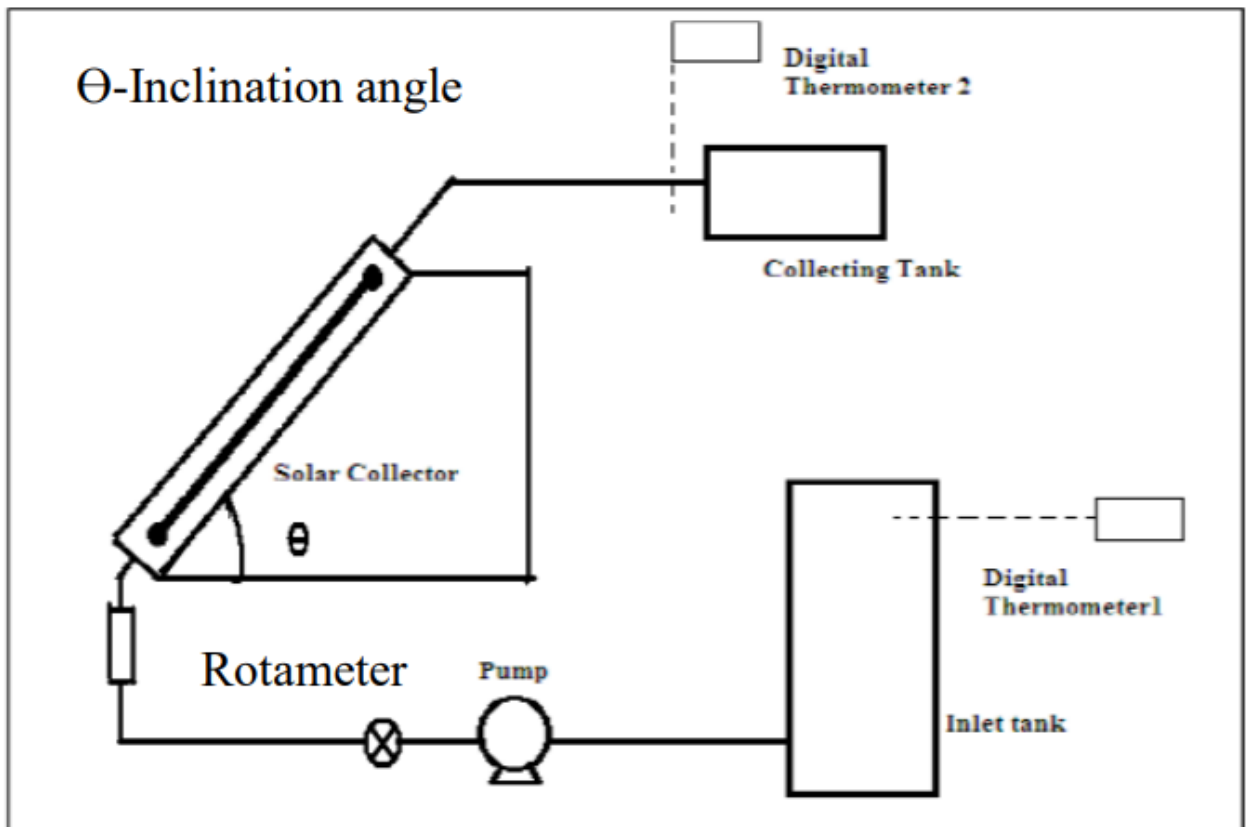


Fig. 2.3: Schematic layout of experimental system [7].

(Nilesh et al. 2018) [8] Found that the lots of research had been done in the advancements in design configurations to enhance efficiency and performance of flat plate collector. It has been found that flat plate collector enhancement widely investigated both analytically and experimentally. In some design advancement reverse flat plate, bifacial absorber or concentric collectors are used to reduce side and rear losses. Wind barriers are used to reduce losses from top whereas reflectors are used to improve the heat gain. In some papers there is advancement of absorber plate like changing its shape or making concavities on it which results in improvement of efficiency of flat plat collector. Some papers are related with design of riser tubes which include changing the geometry from circular to triangular one

or making the exit of riser almost half of the entrance for improvement of the efficiency. Some researchers studied the glazing material and their impact on performance of flat plate collector. In some papers tracking system is studied for the improvement of the efficiency of flat plate collector. Overall, the numerous researchers are trying to improve the performance of the flat plate collector by changing some sort of design of it. fig. (2.4), explain the schematic Diagram of the thermal collector with flat solar radiation reflectors.

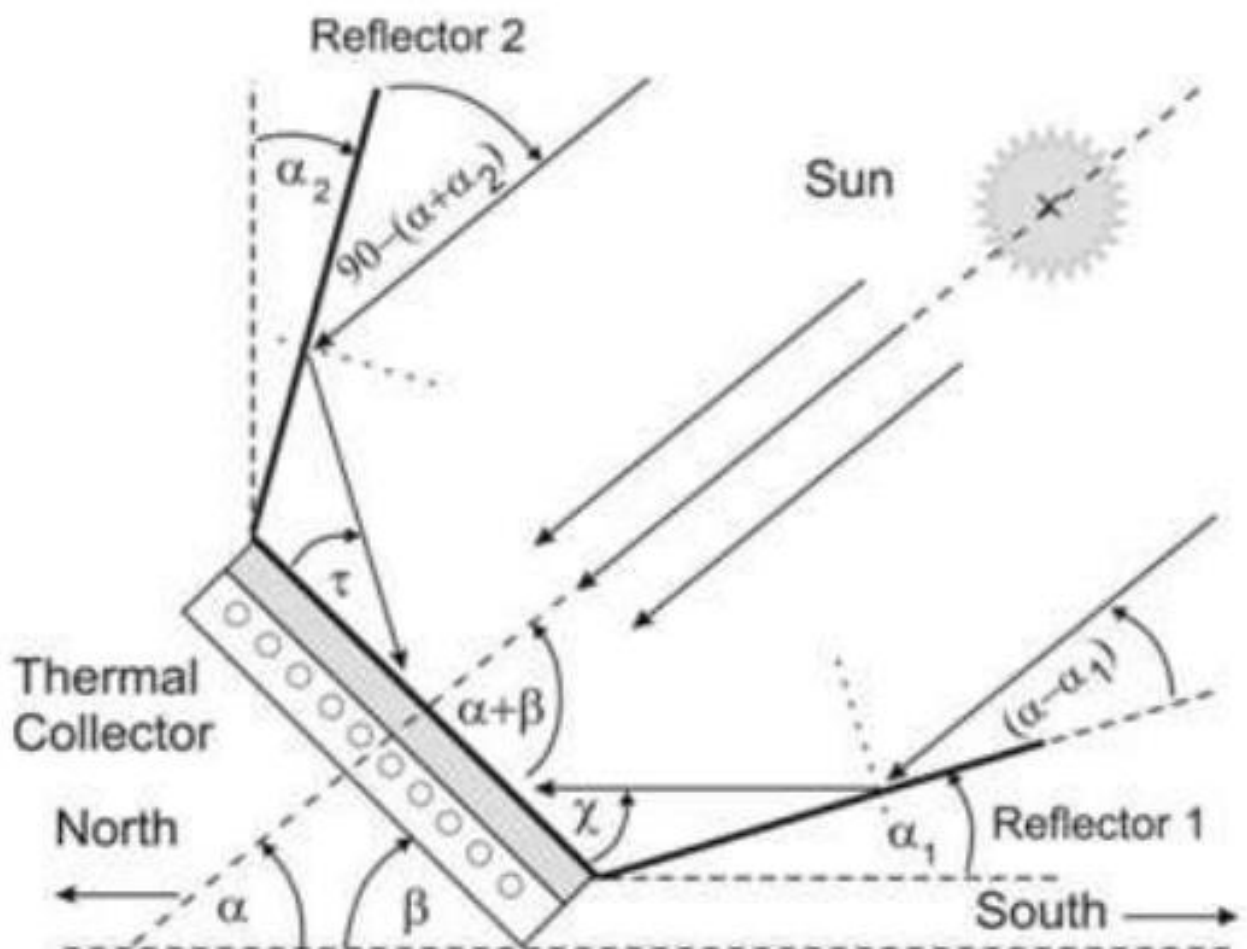


Fig. 2.4: Schematic Diagram of the Thermal Collector with Flat Solar Radiation Reflectors [8].

2.3 Influence of the triangular tubes

The change in the shape of the riser tubes in solar collectors is an important element, because it plays an important part in increasing the heating of the water used and thus increasing the efficiency of the solar collectors. Triangular tubes are

one of the most prominent types of riser tubes used in solar collectors, because they have a high contact rate between the riser tubes and the plate used in the solar collectors. The high contact rate between the riser tubes and the plate used in the solar collectors increases the amount of heat transferred from the plate to the riser tubes, which increases the efficiency of the solar collectors.

(Ganesh et al. 2007) [9] Changed geometry of absorber tube, by using various shapes of tubes as square, circular, semi-circular, triangular, oval and rectangular to performance analysis of flat plate collector as shown in fig. (2.5). The result was that the heat transfer rate in the semicircular tube is greater than the circular tube, the heat transfer efficiency in the triangle tube is the highest compared to the other used tubes, the efficiency of the solar collector is directly proportional to the flow rate of the fluid used, also the efficiency of the solar collector can be increased by changing the absorption using a substance high conductivity, also reducing the area of FPC with increasing diameter of tube by reducing riser tube length increases performance of collector. Through this work, it can be concluded that increasing the contact surface area between the flow tube and the liquid increases the efficiency of the flat plate solar collector.



Fig. 2.5: various shapes of tubes circular, elliptical, triangular & square [9].

(Basavanna et al. 2013)[10] Used the Computational Fluid Dynamics (CFD) so as to simulate the solar collector for better understanding of the heat transfer capabilities of the collector. In the present work shown in fig. (2.6), Fluid flow and heat transfer in the collector panel are studied by means of Computational Fluid Dynamics (CFD). The conjugate heat transfer phenomenon between collector and water is modeled using FLUENT CFD software. The solar radiation heat transfer is not modeled; however, radiation effects are taken in to consideration while calculating the heat flux boundary conditions for the collector area. The geometric model and fluid domain for CFD analysis is generated using ANSYS Design Modeler software, Grid generation is accomplished by ANSYS Meshing Software. The numerical results obtained using the experimentally measured temperatures are compared to the temperatures determined by the CFD model and found to have a good similarity between the measured and calculated results.

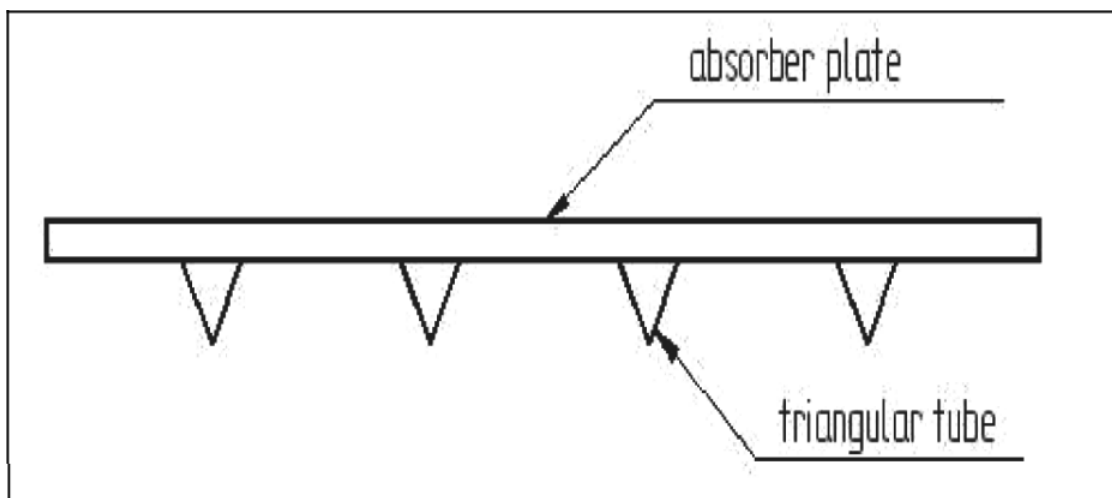


Fig. 2.6: Triangular Tube Configuration [10].

(Mohammed et al. 2021)[11] converted the shape of the cross section of the tube from the circle to the triangle with single fin along the tube which represented a segment of the solar collector operating in similar conditions as show in fig. (2.7), by using ANSYS 12 to achieve this. The objective, on the effort's objectives are to improve thermal efficiency and heat transport. the outcome was, the full temperature attained in circular tube riser (314.499 k) and in modified tube riser (324.109 k) .and

the percent temperature 12% increase in the collector .and the whole parameter like velocity, pressure is progress in the model than the conventional.

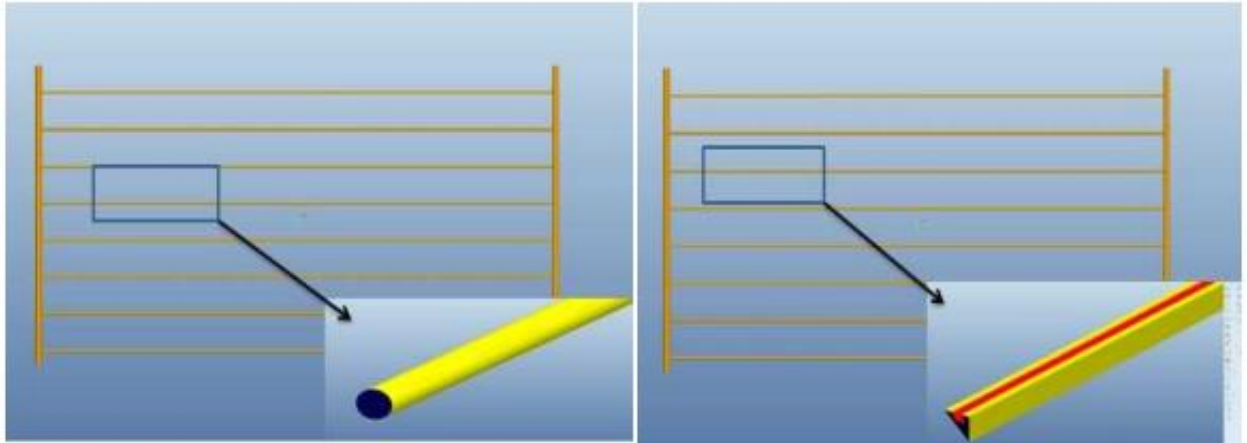


Fig. 2.7: Top Views of the Risers for Both cases [11].

(Mojtaba et al. 2021) [12] Studied the performance of a solar flat plate collector with triangular geometry and with zigzag and non-riser tubes was experimentally examined. To assess the collector, as shown in fig. (2.8), the ASHRAE standard was used in hot and dry climate conditions. The test site was located in southwestern Iran and was tested in the early months from March to June 2020. The measured parameters include the environmental and thermal parameters of the collector and the fluid, and the best data have been selected and presented. The results of the study showed that the collector had a suitable efficiency; the lowest recorded value was 32% and the highest was 58.9 %. Hence, It could be used as a solar water heating system in both domestic and industrial sectors. In the pressure drop testing, the results showed that in all flow rates used, the pressure drop in the collector was less than 0.1 bar. Also, the performance of the collector was presented based on environmental variables such as temperature and radiation, as well as fluid variables such as input temperature and flow rate.



Fig. 2.8: Photo of the triangular flat plate collector [12].

(Sunil et al. 2022) [13] Analyzed the effect of various shapes of riser tubes on flat plate solar water heater efficiency, by made a comparison between square and triangular tubes on the one hand with circular tubes on the other hand, in order to find out which of the tubes is more efficient in heat transfer, by using ANSYS CFD, where Result shows is an increase of about 8-10 % efficiency in case of square/triangular riser tubes in comparison with circular tubes, as shown in fig. (2.9 a), (2.9 b), (2.9 c).

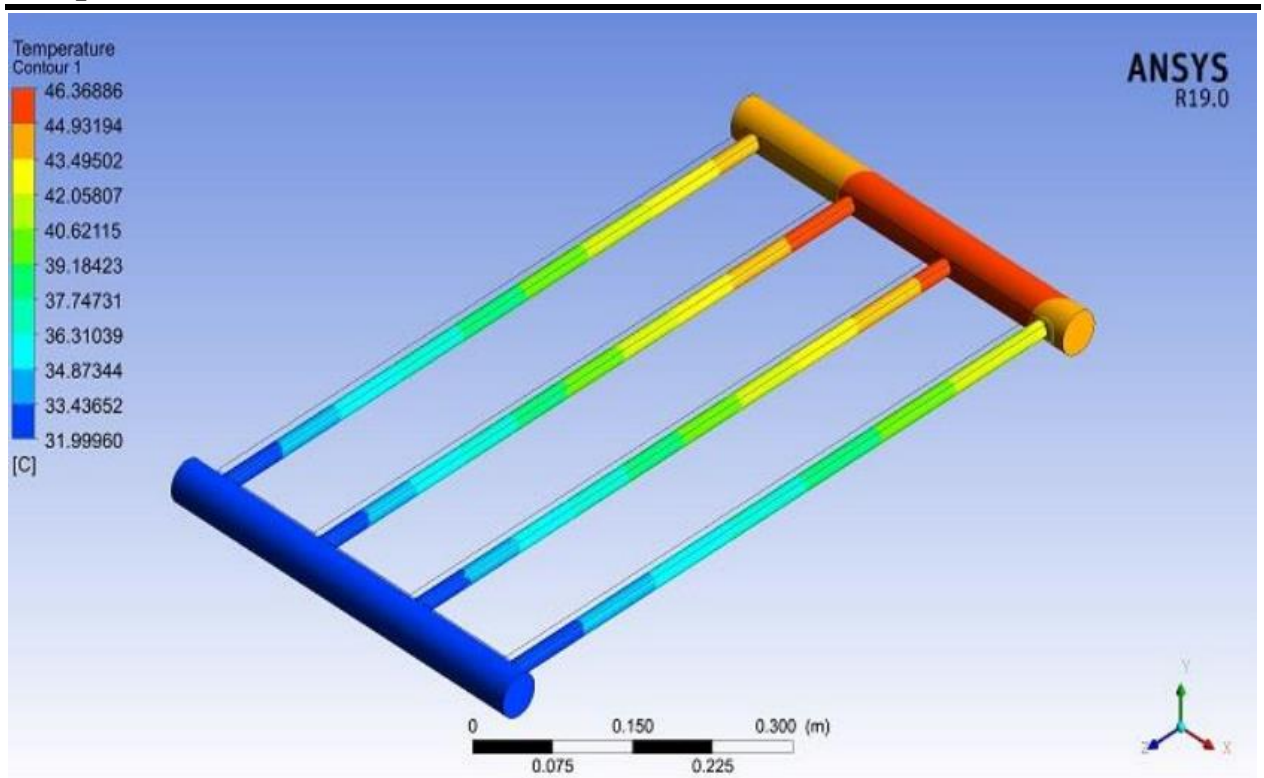


Fig. 2.9 a: Distribution in circular riser's tubes [13].

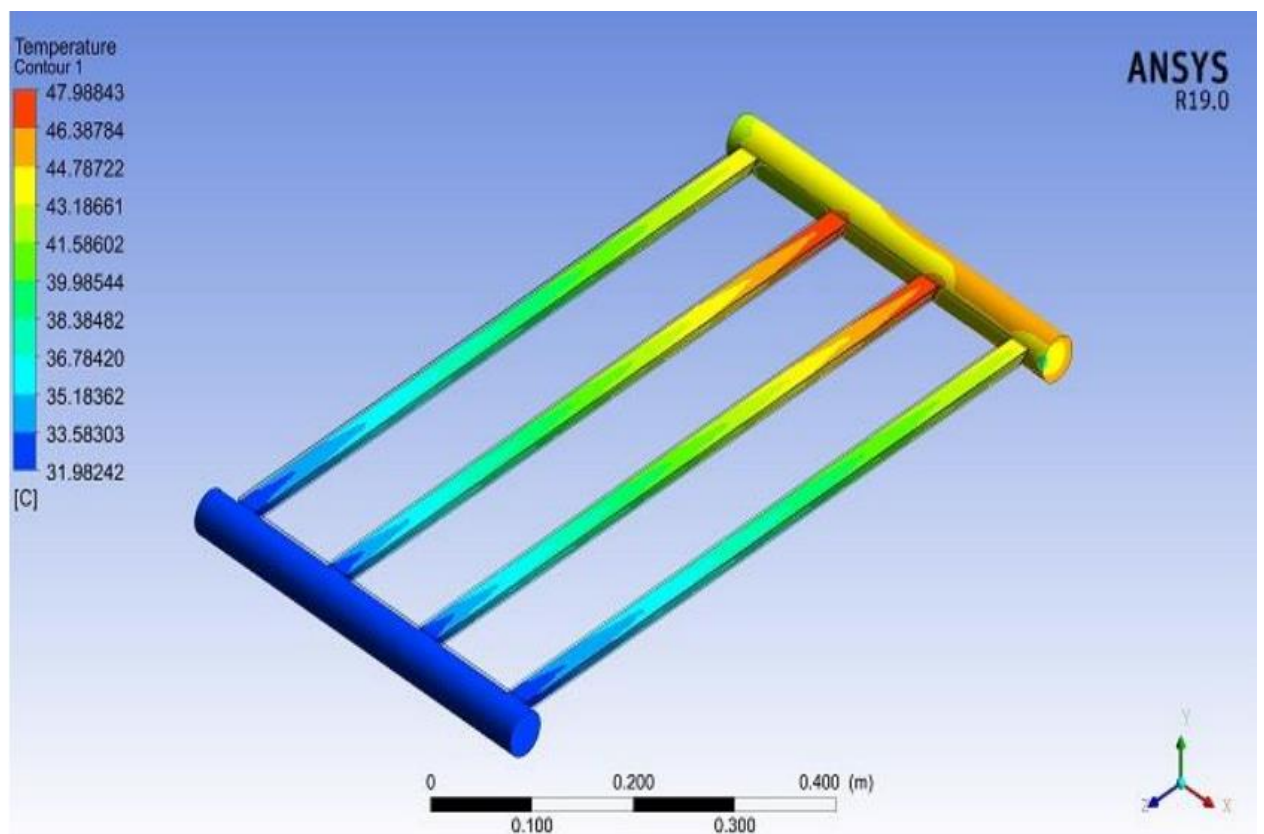


Fig. 2.9 b: Distribution in triangular riser's tubes [13].

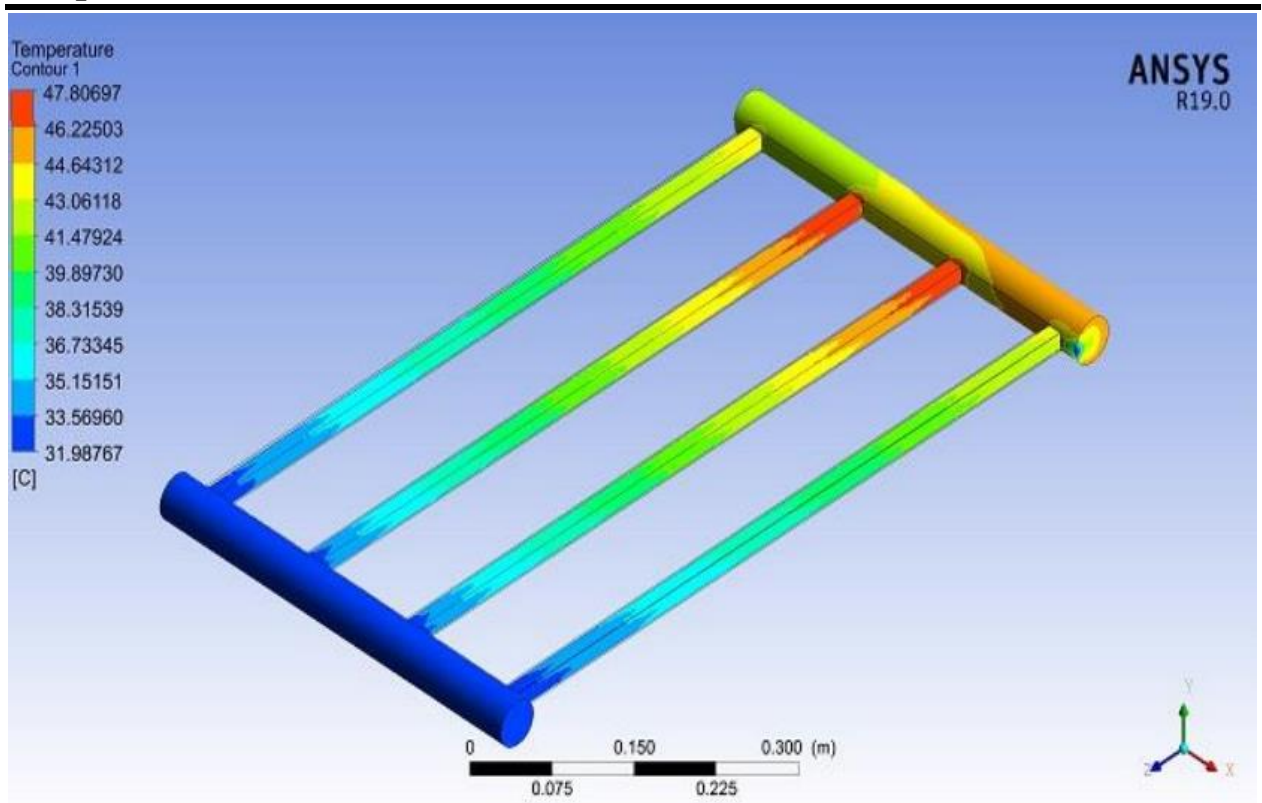


Fig. 2.9 c: Distribution in square riser's tubes [13].

2.4 Influence of the used plate

The used metal plate in solar collectors is considered as one of the main and important parts that affect the efficiency of solar collectors, because of their important role in heating the water used and thus increasing the efficiency of the solar collector. The V-grooves Because of its ability to absorb light, and absorber plates are regarded as one of the crucial kinds of materials panels in use in solar collectors. When using triangle riser tubes in grooves of the V- grooves absorber plate, the surface is greater than the surface area of flat plate, and the amount of sunlight falling on it is higher than the amount of radiation from the sun falling on the flat plate. As a result, these same amounts of heat transferred from of the V- grooves absorber tube to the riser pipes is higher than the amount of heat is transferred from the single plate to riser tubes. and the V- grooves the water in use in solar panels is heated by an absorber plate, which boosts the solar collector's effectiveness.

(Kumar et al. 2010)[14] investigated analytically the performance of a SWHs which was integrated with a corrugated absorber plate. The solar water heating system was

a rectangular collector as a storage solar water heater. The small corrugated depths were 0.4, 0.7, 0.9 and 1mm as shown in fig. (2.10), for 100 Liters of the constant volume water storage tank. The result was that 1mm corrugated depth had a higher water temperature than other depths. The gain in solar water heater efficiency for corrugated depth was found to be greater than 1mm. The system needed to continuously or sporadically withdraw the water flow rates. Additionally, throughout the majority of the day, the corrugated absorber plate's water temperature was greater than that of the flat absorber plate. The system's thermal efficiency did, however, somewhat decline. Withdrawing from the system could boost thermal efficiency in accordance with the findings of changing flow rates.

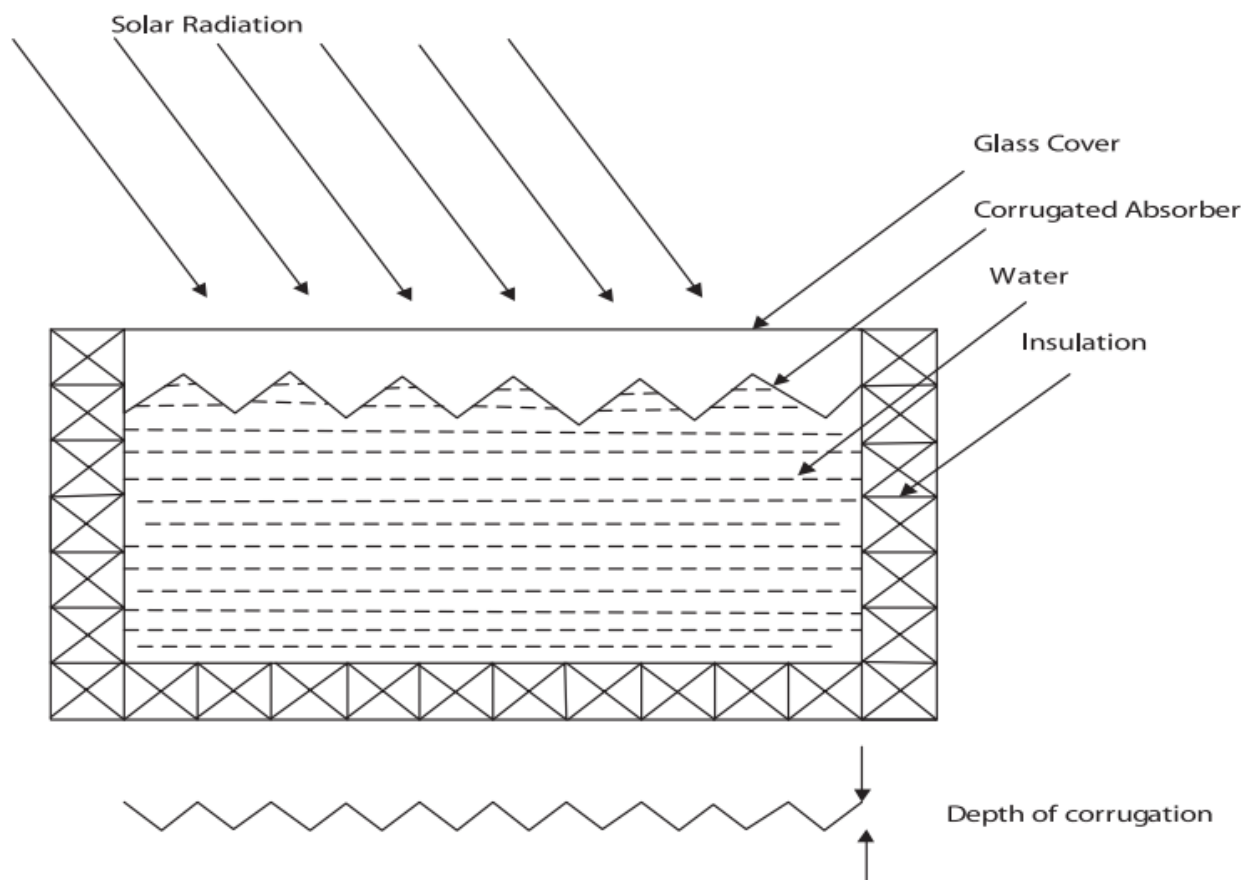


Fig. 2.10: Cross-sectional schematic of rectangular solar water heater with corrugated surface [14].

(Shuilian et al. 2016)[15] Studied comparative on the performance of a solar air collector with different surface shapes, as sinusoidal corrugated plate, protrusion plate, sinusoidal corrugated and protrusion plate, and a base flat-plate collector as shown in fig. (2.11). where the results were as follows, the efficiency of the solar collector increases by increasing the mass flow rate. The roughness of the

absorbing surface of the collector increases the efficiency of the solar collector due to the increase in the surface area of heat exchange. This means changing the shape of the absorbent plate more efficiently than the flat plate, which increases the efficiency of the solar collector.

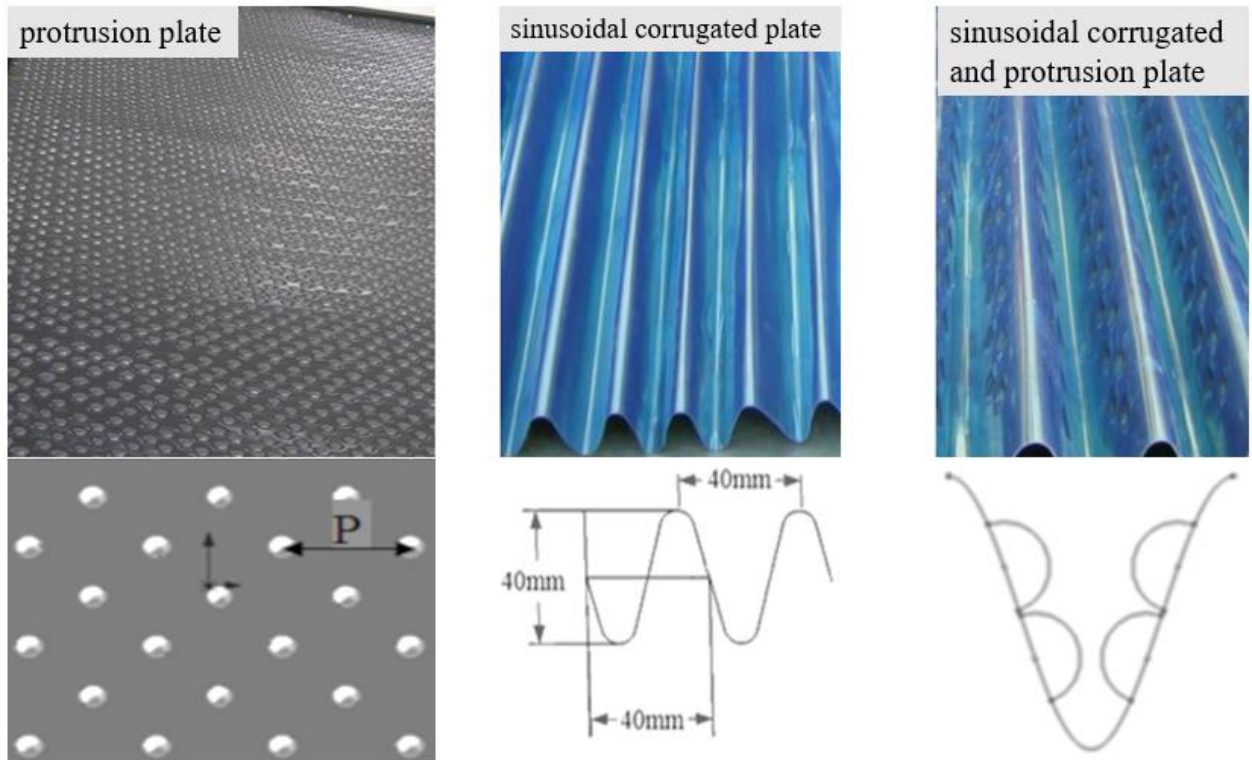


Fig. 2.11: The absorbers with different structure [15].

(Jalaluddin et al. 2016)[16] examined Experimentally the performance of a SWH with a flat absorber plate and a V-shape absorber plate with a variable angle in (August 2015 in Indonesia). The plates' absorptivity was first calculated analytically. For a V-shape with dimensions of $t = 4$ cm and $l = 4$ cm, the best angle was 21° from (21° , 27° , 32° , 40° , 41° , and 49°), as shown in fig. (2.12). The two solar water heating systems were tested at flow rates of 0.5 LPM and 2 LPM. According to the findings, the rising absorptivity of the V-shaped absorber plate makes it more efficient than flat absorber plates by 3.6% to 4.4%.



Fig. 2.12: Solar water heating system with (a) flat-plate absorber plate(b) V-shaped absorber plate [16].

(Manoj et al. 2016) [17] Studied the flow of the solar flat plate collector and record experimental observations. After completion of experiment a 3D mathematical model with single- and double-glazed covers of Solar Flat plate collector (SFPC) is prepared and model is analyzed for CFD flow and heat transfer. Moreover, in this project use of vortex generators as show in fig. (2.13) (V corrugation over absorber plate) and heat enhancement setups such as double glazing, optimum air gap, use of different gases (air, carbon dioxide and argon) is considered so as to increase the heat transfer rate between the interacting fluids. The basic geometrical dimensions for the 3D mathematical model are based on domestically available SFPC on which experiment was performed and CAD model is prepared using Ansys Design

Modeler. The prepared model is simulated in ANSYS Fluent 14.5 considering radiation, natural convection and conduction all modes of heat transfer in boundary conditions. A parametric study is done so as to understand the effect of air gap thickness and use of different gases on the heat transfer rate. A comparative study is carried on between models having V corrugation and model having double glazing and another similar model but without fins and glazing, it was concluded that Heat transfer Enhancement occurs for models with double glazing and also with the use of v corrugation over absorber plates

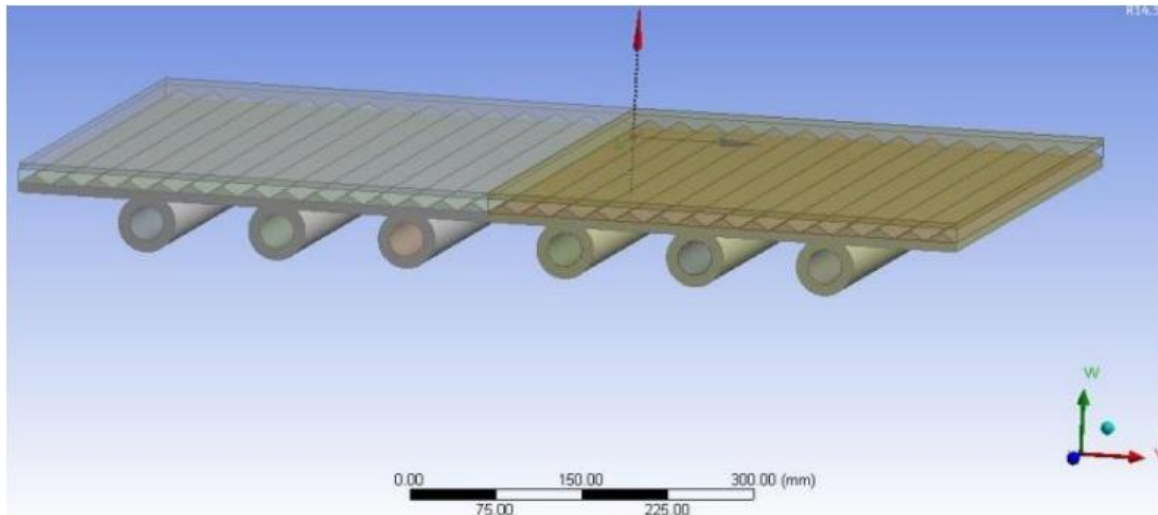


Fig. 2.13: Solar FPC with V corrugated absorber plate [17].

(Tadahmun et al. 2019)[18] Built an integrated solar water heater tested it experimentally to observe the temperature variation of water in the storage tank. The present solar water heater capacity is 140 liters. Two cases have been studied, which are with and without flow rate. In case of without flow rate, the maximum value of stored water temperature obtained is 58°C and 78°C during winter and spring seasons, respectively. The stored water temperature got in the present work is higher than for the previous work principally attributable to the corrugated absorber of the storage tank. In case of with load, the daily thermal efficiency values of the solar collector were 59%, 65%, and 67%, when the mass flow rate values were 0.005 kg/s, 0.0091 kg/s, and 0.013 kg/s, respectively. The outcomes demonstrate that a large thermal loss from the system was observed during the night hours. In addition, the present integrated solar water heater is success to provide hot water suitable to use by the human during the winter and spring seasons of Iraq.

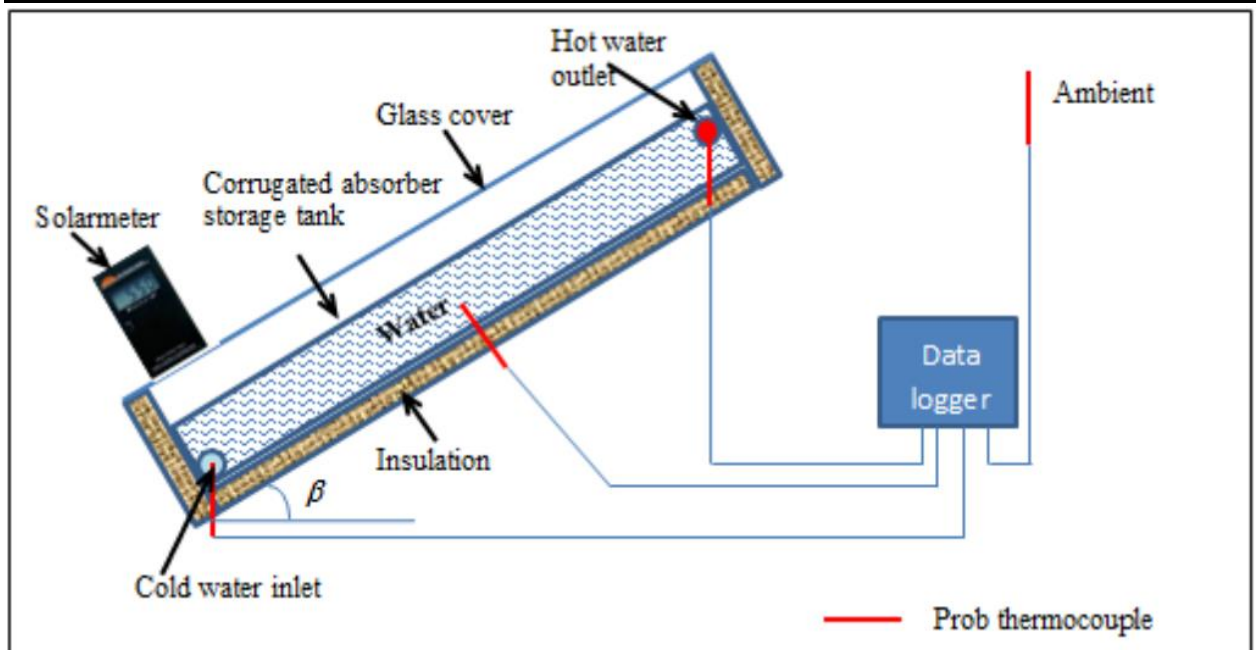


Fig. 2.14: Experimental setup of the integrated solar water heater showing measurement points [18].

(Muhammad et al. 2021) [19] Investigated the configuration of a v-corrugated solar collector with triangular channels for domestic water heating has been analytically. In the present study, a configuration of a v-corrugated solar collector with triangular channels for domestic water heating has been analytically. A mathematical model based on effectiveness-NTU (the number of transfer units is another dimensionless parameter used in the effectiveness). Additionally, the heat losses from the body of the collector, useful energy from the collector and solar efficiency have been calculated analytically over different operating parameters. The effects of mass flow rate and solar heat flux on water outlet temperature are evaluated analytically and compared with the experimental results. Moreover, the study includes the experimental and theoretical investigation of the heat exchange effectiveness and thermal efficiency of the proposed absorber. The study shows that high temperature and high performance can be obtained from this collector as more heat energy can be collected by using triangular channels because all the three sides of these channels are exposed to solar radiations at the same time. Therefore, these channels will enhance the collector exposed surface area and thereby increase the solar efficiency and overall performance of the system.

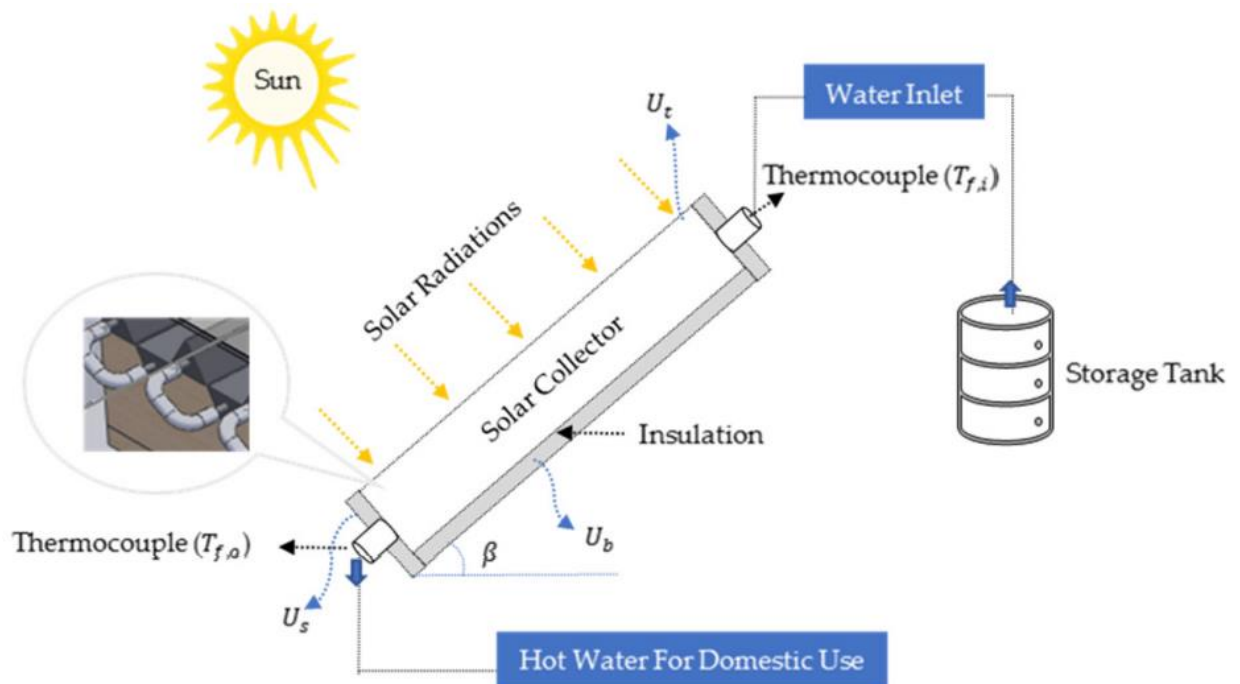


Fig. 2.15: Schematic of experiment and heat exchange in Solar Collector [19].

(Yan et al. 2021)[20] Conducted a Triangular solar air hoarders (TSAC) and flat plate solar air hoarders (FSAC) were compared and mathematically represented in order to confirm the findings of a comparison study on the effectiveness of a novel triangle solar air collectors with slanted translucent panel as shown in fig. (2.16). In this investigation, a type solar air collectors (FSAC) with the same perforation corrugated absorber and a triangle type solar collector (TSAC) with such a sloping translucent top plate with the same southern wall coverage were both employed (PCA). Compared and carried out various analyses operating circumstances. The findings indicate that: 60 The efficiency of thermal TSAC is to enhance the quantity of solar radiation. The gathered energy per units of TSAC Southern Wall Cover Area (CPUWA) with clear cover plate (TSAC60) is 100–130 W/m² greater than FSAC. It accelerates its growth with it. This is because the transparent cover panel has a wide surface area, increasing the solar heat fraction and heat absorption capacity of the TSAC60 by 11.7% and 24.3%, respectively, during in the hot season. that of the FSAC, specifically. As a result, TSAC may receive more solar light, which enhances its ability to capture heat.

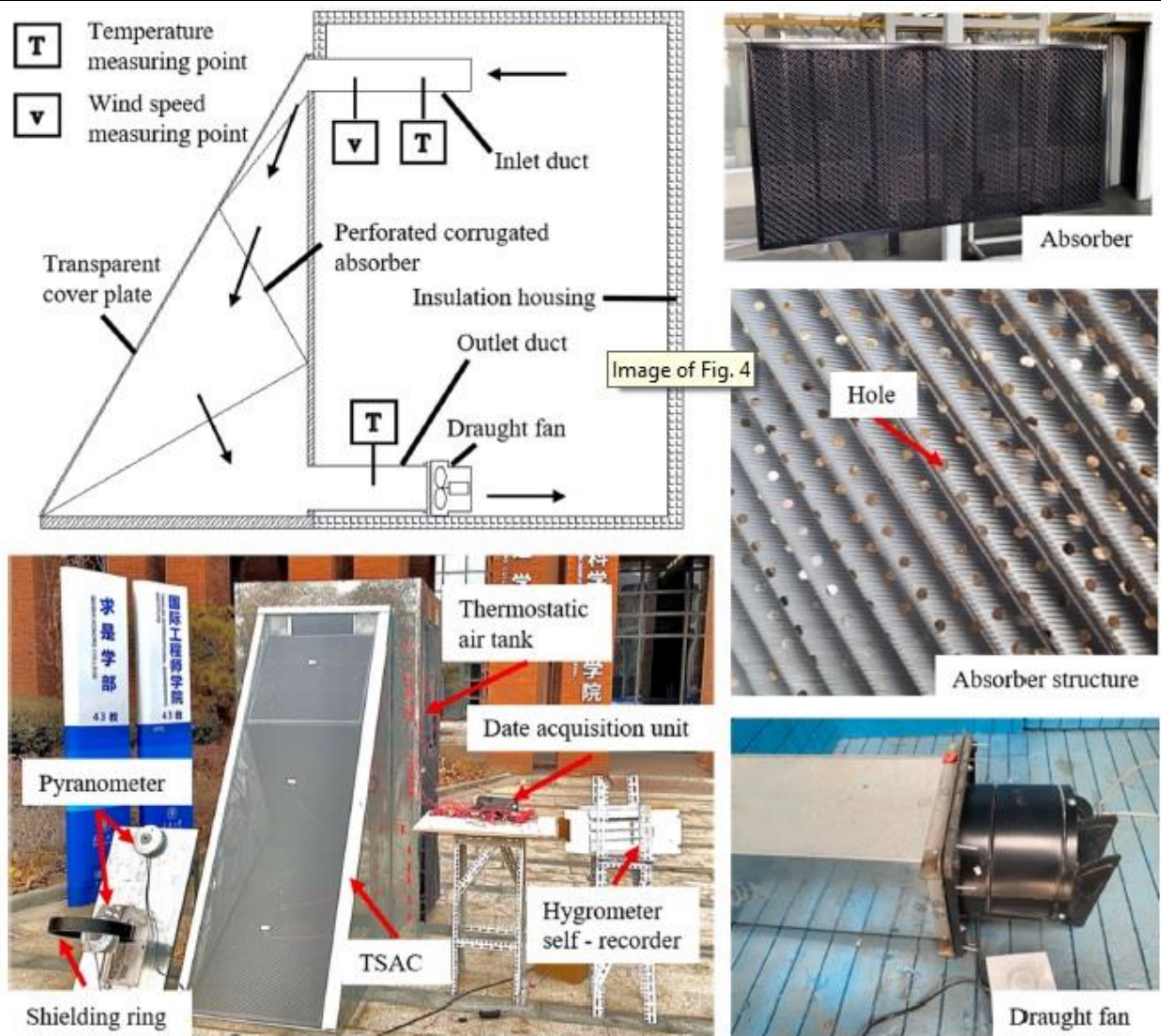


Fig. 2.16: Sketch and photograph of experimental rig for TSAC [20].

2.5 The influence of different flow

Many researchers used different flows of the fluids used in solar collectors in order to compare to the dissimilar flows and find out which of them is more efficient in fluid heating. Increasing the flow of the fluids used in closed solar collectors' system increases their efficiency of it, because when the flow increases the number of times fluid passes through the tubes increase compared to the lower flows in the same time period, and this increases the fluid's acquisition of thermal energy gained from the riser tubes through the flat plate used in the solar collectors. Because the liquid passage time at low velocities is longer than the liquid passage duration at high velocities, the lower flow of liquids used in open photovoltaic

systems boosts their efficiency. This improves the fluid's absorption of heat emitted to the fluids utilized by riser tubes.

(Ruchi et al. 2012)[21] presented a detailed review exclusively on the design aspects of SWH systems. where provided a consolidated summary on the development of various system components that includes the collector, storage tank and heat exchanger. The later part of the research covers the alternative refrigerant technology and technological advancements in improving the performance as well as the cost effectiveness of the SWH system. SWH systems are cost effective with an attractive payback period of 2–4 years depending on the type and size of the system. Extensive research has been performed to further improve the thermal efficiency of solar water heating.

(Maldonado et al. 2014)[22] Investigated the design, construction and instantaneous efficiency in solar water heater. A thermal analysis was developed, based on the energy balanced in the solar collector. The geometry and dimension in the collector were determine ate by the results of the thermal analysis and the thermal properties of the materials used for the collector construction. The dimension of solar collector was of 1.4 m² with a storage tank of 100 L. The highest temperature reached was 55.0 °C and decreased to 47.6 °C during the night. The flow rate was at range from 0.0038-0.04kg/s, and the global average efficiency was of 30.2%



Fig. 2.17: Installation of the solar water heater [22].

(Shouquat ET AL. 2014)[23] Investigated of the thermal performance of a flat plate solar water heater with a circulating absorber pipe surface. The thermal performance of the 2-side parallel serpentine flow solar water heater depends significantly on the heat transfer rate between the absorber surface and the water, and on the amount of solar radiation incident on the absorber surface. The modified pipe arrangement has a higher characteristic length for convective heat transfer from the absorber to the water, in addition to having more surface area exposed to solar radiation. It means during the operation of water heater; more solar energy is converted into useful heat. However, this modification has reduced the efficiency of the system marginally.



Fig.2.19:Solar collector models with 3,4,5, and 6 mm glass thick, respectively[24].

(Salim et al. 2014) [25] Developed the mathematical model and simulation of flat plate solar collector. The weather data, which used in the calculations of the performance of the collector, is for Mosul city. Detailed energy analyses were carried out for evaluating the efficiency and useful heat gain of a typical flat plate solar collector under certain operation and design conditions. In this analysis, different fluids and different absorbing materials were used to indicate their effect on the performance of flat plate solar collector. Operating parameters, which considered as variables, are the mass flow rate, the inlet and the outlet temperature difference and the total solar radiation flux. The simulation program had written by using EES (Engineering Equation Solver) software program. The results of this analysis show that the copper and aluminum give a good efficiency up to (0.6) with value (0.02) of collector performance coefficient when water as a working fluid, while the plain carbon steel gives efficiency (0.46) that stated previously because of low heat conductance. The results show also that the copper and the aluminum give the largest useful heat gain extracted from the collector as compared with plain carbon steel. It has been also showing that the solar collector efficiency is higher in case of using water as working fluid than that of propylene glycol solution.

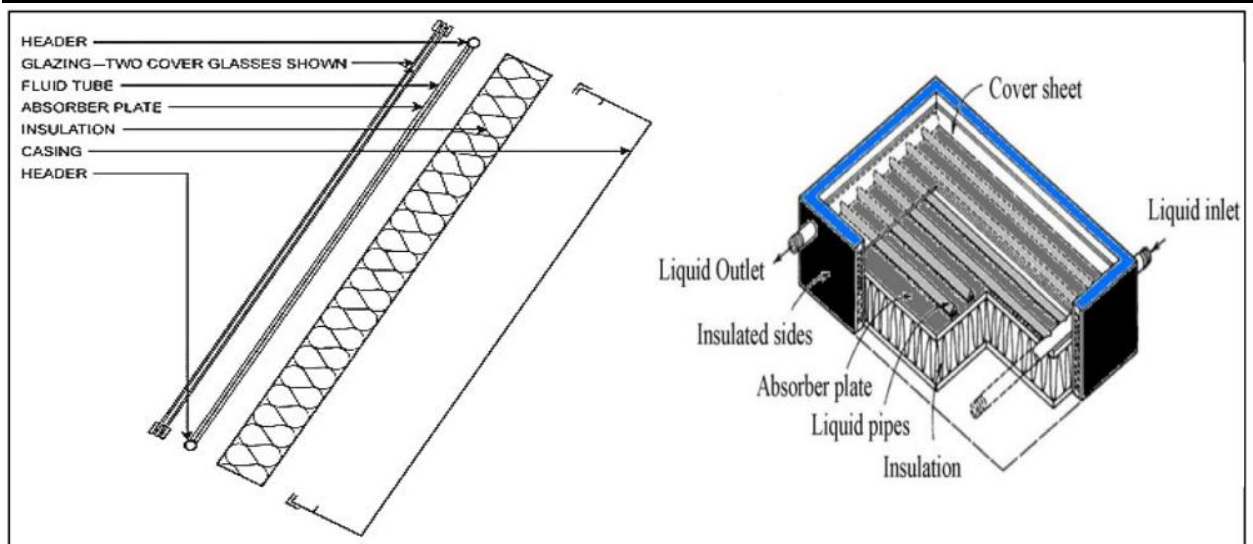


Fig. 2.20: Pictorial View of a Flat- Plate Solar Collector [25].

(Anderson et al. 2017)[26] The collected temperature data by PT100 sensors and solar radiation was measured with a pyranometer, coupled to a CR-1000 datalogger, with readings and collection every 5 minutes for 1 year. Data collection and analysis showed that the system presented monthly efficiency ranging between 33.7 and 53.54%, and energy absorbed between 30.79 and 75.29 kWh m⁻². month. Results show the system is a good option for use in residential or rural water heating due to decrease in the electric bill. The tested collector is a 1 m² flat plate. Experiments were conducted at the State University of Western Paraná (UNIOESTE), campus Cascavel, Paraná State, Brazil.

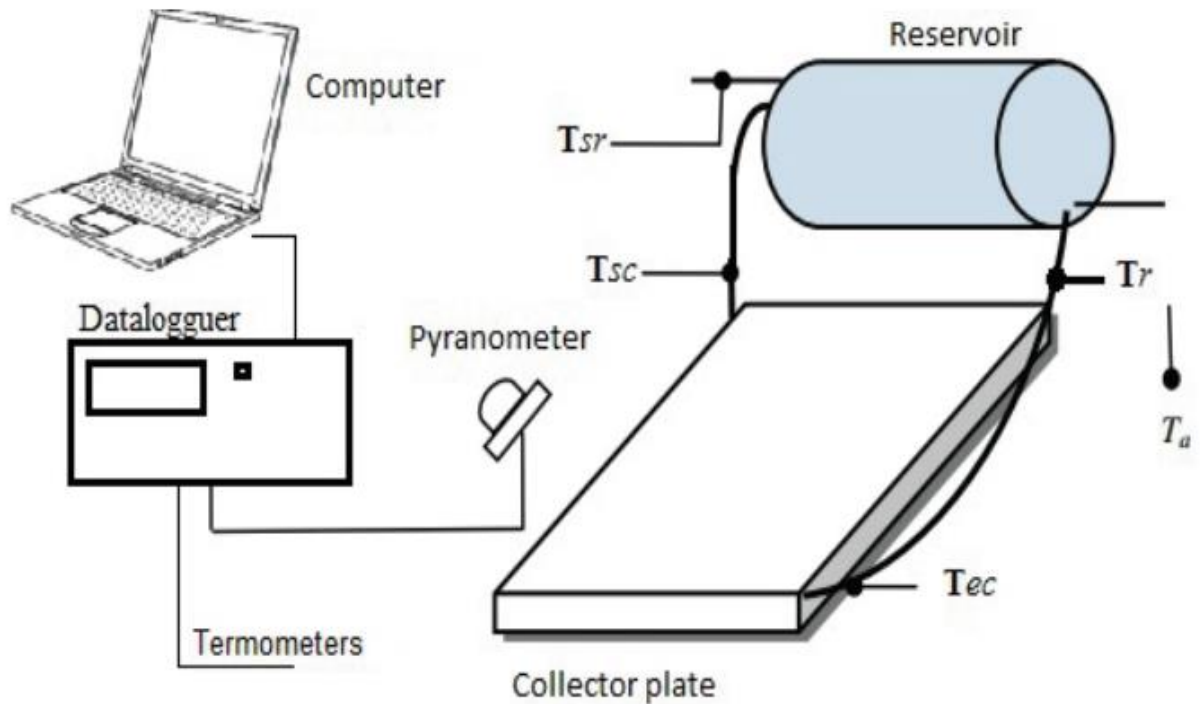
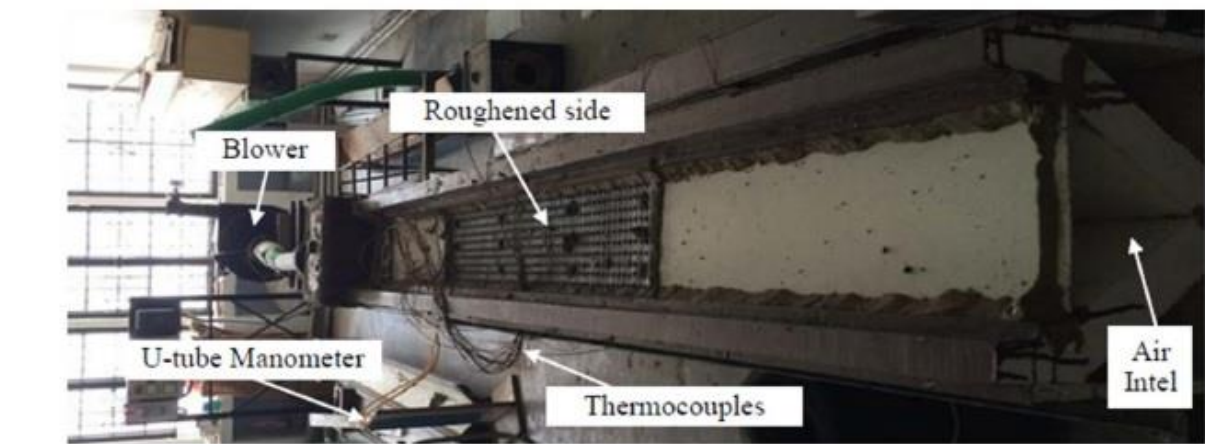
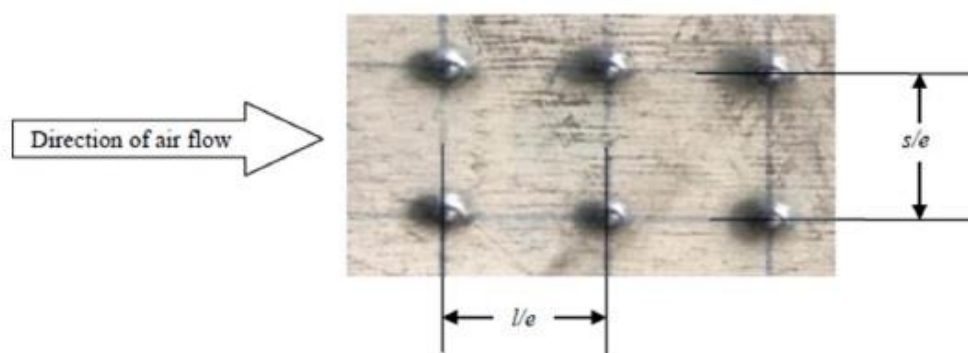


Fig. 2.21: Scheme of data collection [26].

(Varun et al. 2017) [27] Performed experiment to analyze the influence of apex angle on thermal and hydraulic characteristics of triangular duct for Reynolds number range from 2000 to 16,000. Four different triangular ducts of apex angle 30° , 60° , 90° and 110° were fabricated for the experimentation. The one side of the duct is roughened with dimple shaped roughness element. The both relative short way length (s/e) and relative long way length (l/e) of dimple shaped roughened element was kept constant (i.e., 10) but relative roughness height (e/D) is varied from 0.016 to 0.038. Result shows that apex angle plays an important role in heat transfer. The experimental results are presented in a form of correlation for Nusselt number (Nu) and friction factor (f).



(a). Pictorial view of experimental setup



(b). Pictorial view of absorber plate with roughness parameters

Fig. 2.22: Pictorial view of the experimental setup and roughness elements [27].

(Pankaj et al. 2018) [28] Used flat-plate collectors (FPC) to harness the solar radiations to heat the water specifically used for household purpose. The thermal efficiency of FPC is mainly affected by the shape of the absorber tubes and the absorbing capacity of absorber plate. The objective of the present paper is to evaluate and compare the thermal efficiency of flat plate solar thermal collector with varying shape of the absorber tubes. In the present study, the experiments were conducted on solar flat plate collectors having conventional circular and aerofoil shape absorber tubes. The experiments were carried out under identical conditions such as mass flow rate, intensity of solar radiations and size of collector for both types of flat plate collectors. The results obtained from both the collectors are compared and it is observed that there is increase in the outlet water temperature from aerofoil absorber tubes as compared with the conventional circular absorber tubes. It is observed that the flat plate thermal collector with aerofoil shape absorber tubes gives a 10 to 12% higher efficiency than the conventional circular absorber tubes under identical operating conditions. This is due to the fact that the aerofoil shape absorber tubes

provide more surface area for transferring the heat to the water which in turn gains more amount of heat as compared with the conventional circular shape absorber tubes.

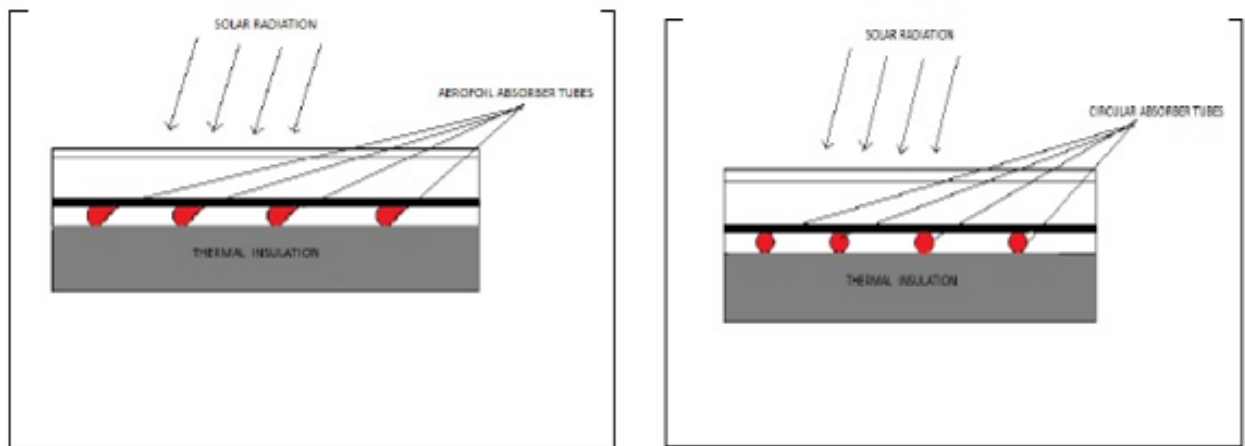


Fig. 2.23: FPC with Aerofoil and Circular absorber tubes [28].

(Hiba et al. 2020) [29] Studied the effect of air bubbles injection on the rate of heat exchange for solar water heating using a flat plate solar collector. Experiments were conducted to achieve the objectives of the research under the conditions of the city of Najaf in Iraq with the support of the Techniques Power Mechanic Engineering Department Experiments were conducted to test the performance of the solar water collector in two cases: first by using a single-phase flow (water only) and the second with a two-phase flow (injection of air bubbles in water) under open and closed systems circulation as show in figures (2.24 a), (2.24 b). In case of open system, several experiments were conducted with different flow rates of water. For the two cases (single and two phase), the flow rates were adjusted on 1, 1.5, 2 and 2.5L/min respectively under established inlet temperature. The enhancement of heat transfer and thermal efficiency of two phase compared with single-phase flow were 9.94% and 9.5% respectively. In case of closed system, several experiments were also conducted at different rates of air, moreover the water is circulated only by air bubbles. The used air flow rates in this experiment were 1, 1.5, 2 and 2.5L/min respectively. The results indicated that the maximum enhancement in the heat transfer rate in this system was 27.1% and the thermal efficiency was 11.5%. Moreover, the tank temperature increased from 27 to 71.7 °C in two-phase flow while at single phase flow from 24.3 to 35 °C in the same period and weather conditions. Finally, for the two systems characterized by a different flow of water and air rates results show that the solar collector in the two-phase flow has higher performance than the single-phase flow.

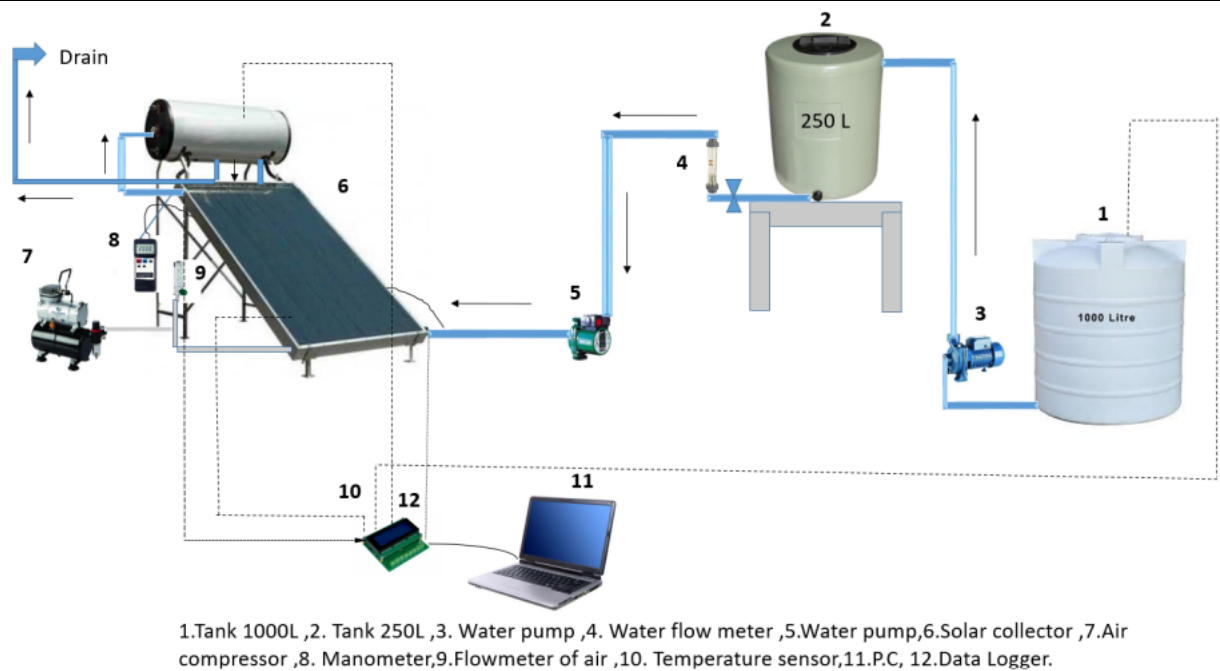


Fig. 2.24 a: A schematic view of an open system [29].

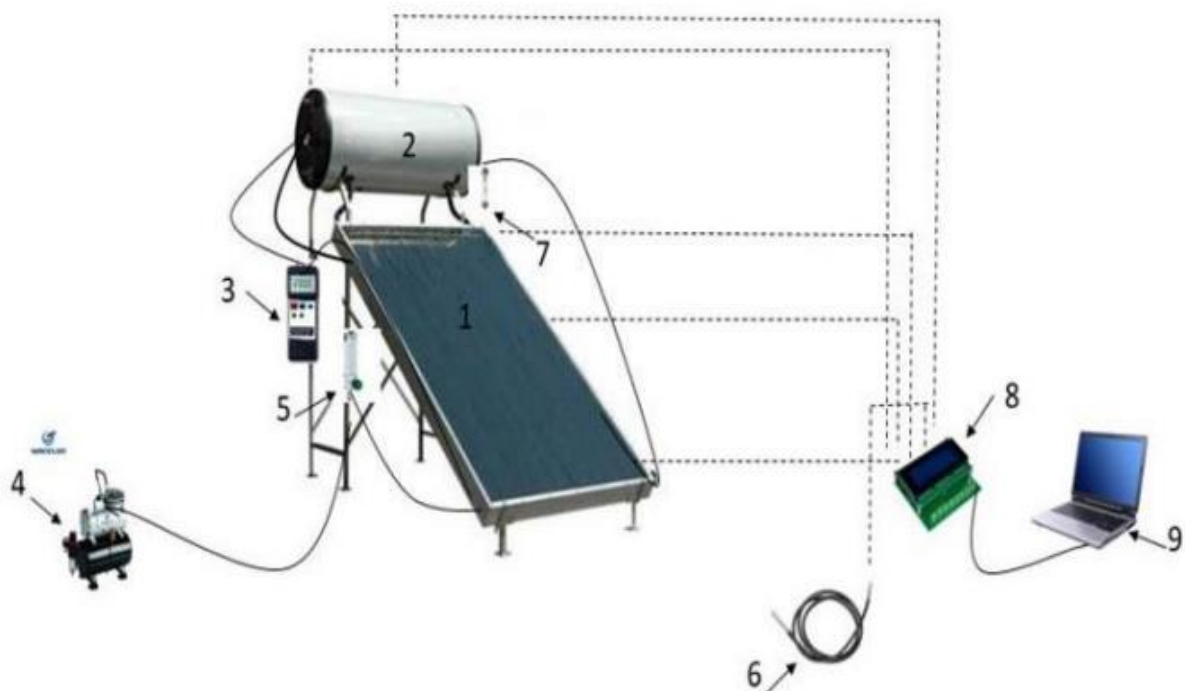


Fig. 2.24b: A schematic of the closed system of solar collector [29].

(Jafer et al. 2020) [30] Reviewed the most important studies that dealt with the development in the manufacture of collectors. Studies differed according to the type

of improvement discussed, such as use of obstacles, type of fin, absorber plate design, nanofluid as heat transfer fluid and use of enhancement devices. Researchers can take advantage of simulation programs to get the best experiences at the lowest cost and time. Where Solar thermal collectors are most frequent type of solar energy applications.

(Ali et al. 2020)[31] Investigated Experimentally to insert the twisted tapes for flat plate solar collector in laminar regime to study its effect on solar collector performance as show in fig. (2.25). Heat transfer rate and friction factor experimented were carried out with using twisted made from aluminum materials by using curvature vortex generators and fixed twist ratio($Y=2$). Twisted tapes insertion was, typical twisted tape (TT), twisted tape with curved vortex generation in facing flow (TTFF). In order to expand the experimental range, the solar collector was tested at four different values of mass flow rate, from 0.025kg/s to 0.117kg/s. at Reynolds number Re from 400 to 2000. The results obtained were compared with those obtained from plain tube published data the results clearly indicate the enhancement of the Nusselt number by insert device. The results show that the Nusselt increasing with (31.4%-54%) by using twisted tape with curvature vortex generator (TTFF).



Fig. 2.25: flat plate solar collector [31].

(Hiba et al. 2020) [32] Studied experimentally with and without the effects of small air bubble injection on the efficiency of a flat plate solar collector with tube risers for open flow system as show in fig. (2.26). The variation of the thermal efficiency of the solar flat plate collector due to both different of the water flow rate and due to the air bubbles injection with air flow rates are evaluated. A new experimental procedure for injecting small air bubbles into the riser tubes of solar flat plate collector is proposed. The comparison between the effects of forced water flow rates and air bubbles injection on the solar flat plate thermal efficiencies with a variation of solar radiation intensity were investigated. Water and air flow rate were changed between 1.5-2.5 LPM with inlet water temperature ranged between 19-23.5°C. Observations showed that the injecting of air bubbles inside the solar flat plate tubes risers play key roles on the effect of thermal efficiency more than that of using the water flow rate without air bubbles injection. Small air bubbles injecting into the riser's tubes of the flat solar collector causes enhancement of the thermal efficiency and it increased 3.5-5.25% depending on air flow rate.

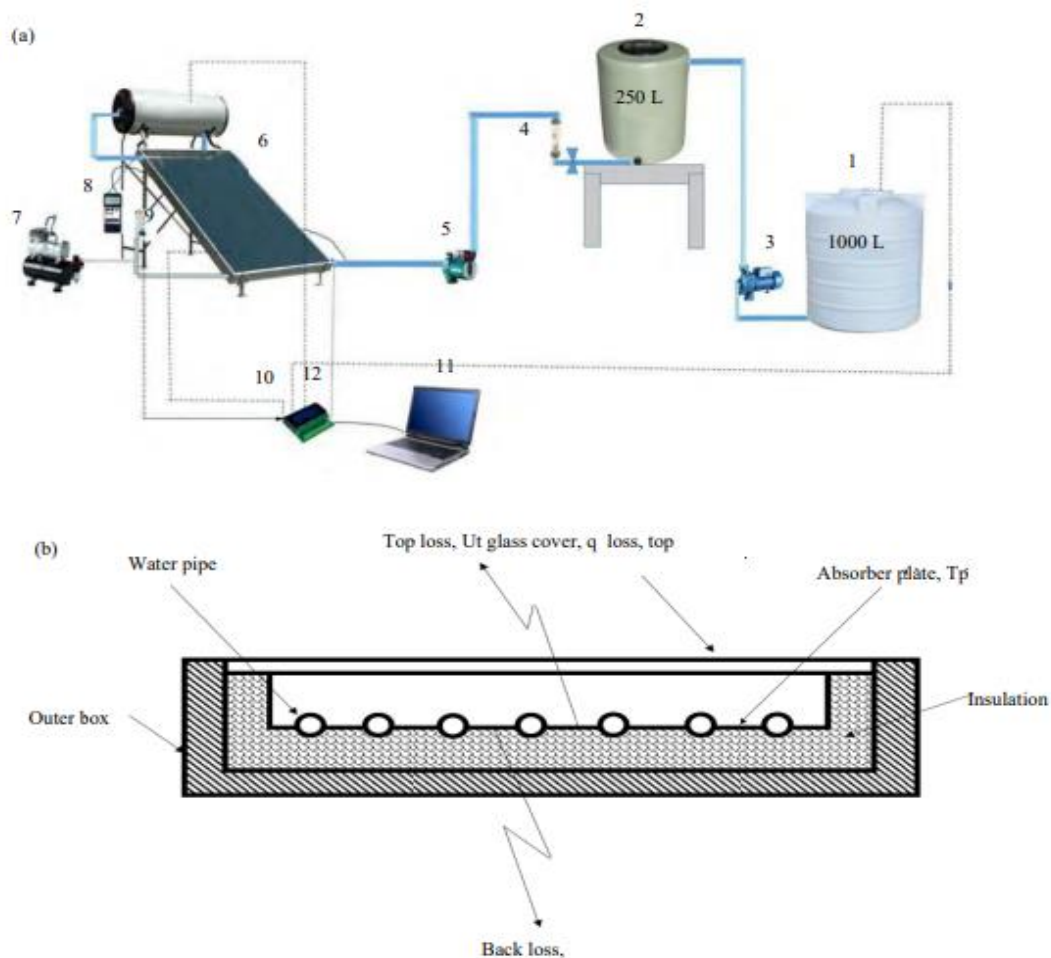


Fig. (2.26 a-b): (a) Schematic diagram of the experimental rig and (b) Schematic diagram of the flat plate solar collector with water pipes [32].

(Hassanain et al. 2021)[33] Tested experimentally to a new design for an air solar heater and its results are compared with the corresponding results of a conventional air solar heater (two-pass black flat plate) as show in fig. (2.27). Experimental measurements have been performed under Najaf city/Iraq (latitude and longitude are $32^{\circ} 03' N$ and $44^{\circ} 19' E$) prevailing weather conditions. The new design is a longitudinal aluminum radiator placed inside a fully isolated bed. The radiator is covered with black paint to increase the heat absorption of the solar radiation and then distribute it regularly to the passing air. In addition to test the activity of the new system, the current experiments shed a light on influence of the air mass flow rate on the air outlet temperature, thermal efficiency and pressure drop. Three air mass flow rates are selected: 0.0046, 0.0092 and 0.0138 kg/s. The results show that increasing in the air mass flow rate leads to decrease in the air outlet temperature and increase of the pressure drop and thermal efficiency for both current solar collectors. Moreover, the radiator air solar heater is 18.62% more efficient at the maximum point compared to the conventional one with 0.0138 kg/s leading to obtain 32.66% as the maximum enhancement in the thermal efficiency.



Fig. 2.27: Pictorial view of the experimental rigs [33].

(Mohammed et. al, 2021) Studied the numerical and experimental of the thermal performance of a flat plate collector (FPC) as show in fig. (2.28). They studied focuses on analyzing the performance of (FPC) in the climatic conditions of Najaf and calculating the thermal energy produced by the collector for domestic use, which reduces the electricity consumption that Iraq is witnessing a severe shortage in its supply. Also, various working fluids (water, oil engine, ethylene glycol-water mixture) were tested to determine the best working fluid that improves the collector's efficiency. The experiments were performed in Najaf, Iraq ($32^{\circ} 2' N / 44^{\circ} 18' E$) on January 9, 2019. The simulation study of the (FPC) is performed by COMSOL Multiphasic 5.3 software. The numerical results were validated with experimental results and there was good convergence between them. The results showed that the average daily efficiency of the solar collector (FPC) was 37.17%, and the highest outlet water temperature of the collector was $57.1^{\circ}C$. The collector achieved a useful cumulative useful heat during the day of about 3.3557 MW, this contributes to reducing the use of electricity and achieving the required economic feasibility of use (FPC). Finally, the engine oil gave better results in improving efficiency compared to other working fluids.



Fig. 2.28: Flat plate collector.

(azmi et al.2022) [34] Investigated the effect of four different fluids ethylene glycol, ethanol, methanol, and acetone as well as their aqua solutions on the performance of the thermosyphon evacuated tube heat pipe solar collector. Water is used as a heat transfer fluid with a volume flow rate of 1.95 l/min. Five modules each of three evacuated tube heat pipe solar collectors are used. The thermosyphon heat pipes are manufactured and charged with each working fluid and its aqua solution of volume concentration of 0, 0.25, 0.5, 0.75 and 1.0 respectively. The performance of the systems is illustrated by the solar collector efficiency and the overall system efficiency. The results showed that pure water gives higher solar collector efficiencies than that of ethylene glycol, ethanol, methanol, and their solutions while acetone gives higher solar collector efficiency than the pure water. Correlation equations for solar collector efficiency in terms of $(T_m - T_\infty)/G$ and concentration are deduced. The current results are validated with the previously experimental published correlations.



Fig. 2.29: Photograph for the test rig [34].

2.6 Scope of the present work

The objectives of this article are to investigate the effect of using multi pipes shapes on the thermal performance for the triangular tubes used in the V- grooves plate solar collectors and in three cases, when the triangular tubes (inside the grooves, beside the grooves, over the grooves), and show that action on heat transfer in term of the Nusselt number (Nu), pressure drop in term of friction factor (f), thermal performance factor (TPF) and the efficiency (η) of a simple V- grooves absorber plate solar collector. And comparison with circular riser tubes in the flat plate solar collector in close system forced flow with four flow rates (2, 3, 5 and 7) LPM for laminar flow $500 < Re < 1900$.

Table- 2.1: The summary

Author	Working fluid	The geometry shape of (tubes, plates)	Type of investigation	Results and Discussions
[9]	Water	square, circular, semi-circular, triangular, oval and rectangular) tubes	Experimental work	The result was that the heat transfer rate in the semicircular tube is greater than the circular tube, the heat transfer efficiency in the triangle tube is the highest compared to the other used tubes, the efficiency of the solar collector is directly proportional to the flow rate of the fluid used,
[5]	Pure water	circular and rectangular tubes	computational Fluid Dynamics (CFD)	Results indicated that circular pipe heat exchangers showed 2.5% increase in the heat transfer rate over the rectangular tube, Simulation results also showed 8.5% increase in Nusselt number for the circular tube,

				whereas pressure drop in case of circular tube is higher when compared to the rectangular tube
[6]	Water	circular and elliptical tubes	numerical analysis using ANSYS CFD FLUENT software	concluded the elliptical tube gives the maximum outlet temperature of water for the same heat flux and inlet temperature in comparison with circular geometries. And the outlet temperature difference between circular and elliptical tube is 4.17 °C
[7]	R.O Water	(Circular, triangular, square) tubes	Experimental Study	it is found that the efficiency of triangular tube is maximum as compared to other tubes. Also, it is observed that efficiency is directly proportional to flow rate and it is dependent on the intensity of sun light.
[15]	Air	different surface shapes, as sinusoidal corrugated plate, protrusion plate, sinusoidal corrugated and protrusion plate, and a	Experimental Study	the efficiency of the solar collector increases by increasing the mass flow rate. The roughness of the absorbing surface of the collector increases the efficiency of the solar collector due to the increase in the surface area of heat exchange. This means changing the shape of the absorbent plate more efficiently than the flat plate, which increases the efficiency of the solar collector.

		base flat-plate collector		
[16]	Water	flat absorber plate and a V-shape absorber plate with different angles (21°, 27°, 32°, 40°, 41°, and 49°)	Experimental analytical study	the rising absorptivity of the V-shaped absorber plate makes it more efficient than flat absorber plates by 3.6% to 4.4%, and the best angle of a V-shape was 21° from (21°, 27°, 32°, 40°, 41°, and 49°)
[28]	Water	circular and aerofoil shape absorber tubes	Experimental study	It is observed that the flat plate thermal collector with aerofoil shape absorber tubes gives a 10 to 12% higher efficiency than the conventional circular absorber tubes under identical operating conditions.
[32]	Water	Flat plate solar collector with circular riser tubes	Experimental	Observations showed that the injecting of air bubbles inside the solar flat plate tubes risers play key roles on the effect of thermal efficiency more than that of using the water flow rate without air bubbles injection. Small air bubbles injecting into the riser's tubes of the flat solar collector causes enhancement of the thermal efficiency and it increased 3.5-5.25% depending on air flow rate.

[35]	Water	v-corrugated solar collector with triangular channels	experimental and theoretical investigation	The study shows that high temperature and high performance can be obtained from this collector as more heat energy can be collected by using triangular channels because all the three sides of these channels are exposed to solar radiations at the same time. Therefore, these channels will enhance the collector exposed surface area and thereby increase the solar efficiency and overall performance of the system.
[33]	water, oil engine, ethylene glycol-water mixture	Flat plate collector with circular tubes	Numerical and experimental study	The results showed that the average daily efficiency of the solar collector (FPC) was 37.17%, and the highest outlet water temperature of the collector was 57.1°C. The collector achieved a useful cumulative useful heat during the day of about 3.3557 MW, this contributes to reducing the use of electricity and achieving the required economic feasibility of use (FPC). Finally, the engine oil gave better results in improving efficiency compared to other working fluids.

CHAPTER THREE

THEORETICAL ANALYSIS

Chapter Three

Theoretical Analysis

3.1 Introduction

Enhanced heat transfer at a heat exchange is widely used in domestic and industrial applications, due to the need for more compact heat exchanges, lower operating costs, energy savings and environmental benefits. Another typical method is the use of elevated pipes with various shapes. In heat exchangers, triangular tubes are frequently utilized as heat transfer enhancement tools. It's only wanted to raise the contact surface area between both the flat board with V-corrugations and the triangular tube and to increase the heat exchange between the wall and fluid flow [36].

May generate The use of triangular tubes in a wide range of Reynolds numbers is a preferred efficiency in the rate at which heat transference and the distance between the triangle tube and the metal plate used is wide compared to the interaction part between the circular tube and the metal plate used in the traditional way, due to the abundance of solar energy, it is the most promising source of energy and is environmentally friendly to protect The environment, where solar vigor can be transformed into usable vigor either through photovoltaic cells or through solar collectors and used as thermal energy, where the flat solar panel complex is the most commonly used and simplest type of collector, and the heat transfer factor in the rising triangular tubes of the solar panel complex is more efficient in heating Water from the used circular tubes [37].

3.2 Triangular tubes

Triangular riser tubes and as shown in figure (3.1) are considered one of the most important types of tubes used in solar collectors because of their shape that makes them more conductive of heat, due to the large contact area between the triangular tubes and the metal plate used in solar collectors. The amount of heat transferred from the triangular tubes to the water inside them rises as the flow rate rises. Because in the higher flow rate, the water pass through riser tubes more than lower flow rate, this increases the amount of heat gain from sunlight falling on the tubes used and the metal plate used in the solar collector [45]

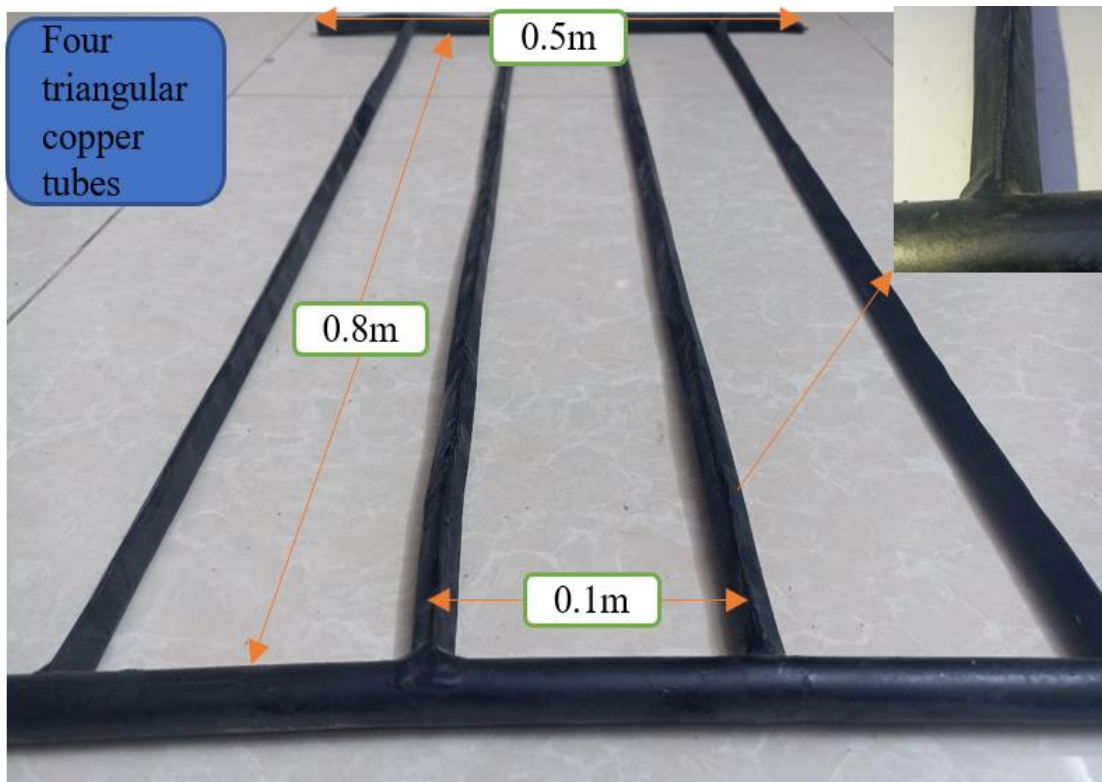


Fig. 3.1: Triangular riser tubes.

3.3 The V- grooves absorber plate

The V- corrugated absorbers pad is used in solar panels in order to increase contact region of the plate in use, increasing the amount of solar radiation that falls on it and is converted into heat energy that is transferred to the riser tubes in use, increasing the amount of heat is transferred to the tubes and from there to the

water in the solar hoarder, increasing the efficiency of the solar collector that contains the absorber plate.[38].

The following calculation was done since the triangular and circular riser tubes have to be identical in size but had different shapes in order for the comparison to be accurate:

$$\text{perimeter of a circle} = \pi * d = 3.14 * 0.0125\text{m} = 0.03925\text{m}$$

$$\text{perimeter of the triangle is equilateral} = X + X + X = 0.03925\text{m}$$

$$3X = 0.03925\text{m}$$

$$X = 0.01308\text{m}$$

$$X = 13.08\text{mm}$$

where X is an equilateral triangle's side length



Fig. 3.2: The V- grooves absorber plate

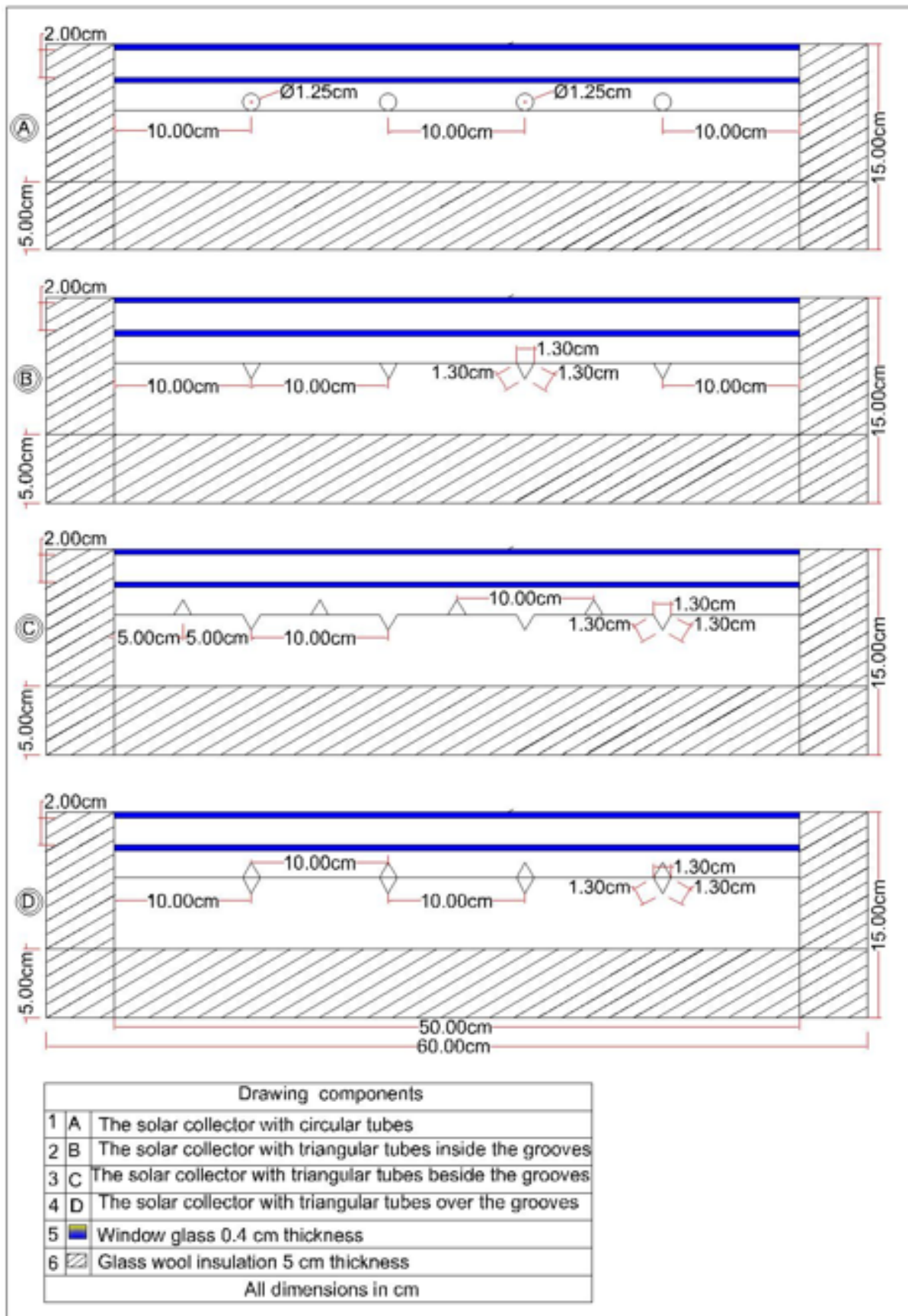


Fig. 3.3: schematic diagram of the solar collectors that contain circular tubes and triangular tubes

3.4 Heat transfer and flowing fluid in circular tubes

Since of heat transfer coefficient correlation and Research work provide the basis of laminar flow friction, the laminar regime is frequently used in practice. This really is expected to the correspondingly advanced coefficient of temperature transmission. The friction factor for smooth circular tube to calculate fluid velocity Darcy-Weisbach [39]

$$f = \frac{64}{Re} \quad (3.1)$$

or the friction factor calculated from the well-known Darcy-Weisbach equation which calculate the pressure drop.[40]

$$\Delta P = f \frac{L}{d_i} \frac{\rho u^2}{2} \quad (3.2)$$

And

$$f = \frac{\Delta P}{\frac{L}{d_i} \frac{\rho u^2}{2}} \quad (3.3)$$

The Nusselt number is calculated using the general relationship of forced convection heat transport in the following formula the coefficient are (h_i), (K_w) and, the internal riser tube diameter (d_i)

$$Nu = \frac{h_i d_i}{K_w} \quad \text{or} \quad Nu = \frac{h_i D_h}{K_w} \quad (3.4)$$

$$D_h = (\text{area} / \text{perimeter}) \quad (3.5)$$

Where D_h hydraulic diameter for Irregular shapes

$$A_i = \pi r^2 \quad (3.6)$$

The area of the triangular tube

$$A_i = \frac{1}{2} X h' \quad (3.7)$$

Where X the length of the side of the triangle, h' the height of the triangle tubes

Hydronic diameter D_h

$$D_h = A_i/P' \quad (3.8)$$

Where A surface area and P' perimeter of triangle

3.5 The performance of solar collector

At a steady-state, the energy balance indicated the distribution of solar energy incidence description of the solar collector efficiency, the division of solar power incidence to beneficial power gains, optical losses also heat losses.

The difference between solar irradiance incidence and optical losses represents solar radiation, which is absorbed by the solar collector(S), thermal losses in collectors at conductive form, infrared irradiance and convective, exemplified by the coefficient of heat transfer U_L , thermal losses equal the product U_L by the temperature difference of mean absorb plate temperature T_{pm} and ambient temperature T_a thus the term represents thermal energy, lose from the collector is $U_L(T_{pm} - T_a)$ per meter square of collector area A_C , therefore The difference between the solar irradiance absorption and the losses of heat represent the solar collector's useful energy or energy output in steady-state:

Useful energy $Q_u = A_C [S - U_L(T_{pm} - T_a)]$, the predicament of that equation of the mean temperature of the absorption plate T is difficult to predict because it related with three parameters, collector layout, fluid condition, and solar irradiance incidences which create a problem for beneficial energy equations.

The collector efficiency represents the solar collector output, which is defined as the ratio of the useful energy gain from solar energy incidence over the same time (John A. Duffie 2013)[41]

$$\eta = \frac{\int Q_u dt}{A_C \int G T dt} \quad (3.9)$$

And for stable condition-state, the collector efficiency becomes as

$$\eta = \frac{Q_u}{I_{TAC}} \quad (3.10)$$

The provision of minimum cost energy is a very important factor in the design of a solar energy device, so that the design of an efficient collector can be beneficial, lower than is technically feasible if the cost is significantly reduced, including the expectation that the solar collector output will in any event occur. A number of simplifying assumptions will make the simple physical condition the assumptions as follows model the condition in fig. (3.3) without opacity:

1. Performance is steady conditions.
2. The structure is in parallel form and surface-plated
3. The header cover areas are limited and small thus could be ignored.
4. The headers supply steady flow risers.
5. Solar irradiance does not absorb by a cover which causes extra heat losses.
6. In one dimension the heat flows through the cover.
7. Ignored the temperature decreases over the cover.
8. Glass covers are opaque for solar irradiance.
9. In one-dimension, thermal flows through the bottom insulation.
10. Consider the sky like a black body at equivalent black body temperature

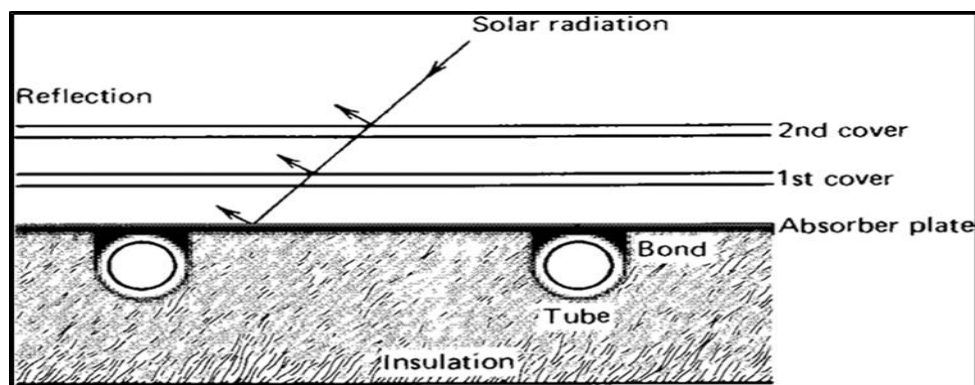


Fig. 3.4: distribution of solar irradiance over solar collector [42]

3.6 The gross coefficient of heat loss for flat plate collector U_L

Detailed analysis of solar collectors is a complex problem, and a relatively simple analysis will give very useful results, these results reveal important variables, how they are related and how they affect solar collector performance. To illustrate these basic concepts, a collector of liquid heat, as shown in fig. (3.3) the following developments will be tested first, it is hoped that the temperature distribution that exists in a solar collector constructed will be understood, an area between two tubes must be conducted along the plate to the tube region, in which some of the solar energy absorbed by the plate, and at midway between the tubes the temperature is higher than near the tubes, while the temperature above the tubes is approximately uniform due to the tube and weld metal relationship. An energy transferred to the fluid heats the fluid, which causes a temperature gradient in the direction of flow, since the local temperature in any region of the collector was governed by the general temperature level, having defined the temperature distribution over the flat plate collector, revealing the idea of a total loss coefficient U_L for solar collector is useful for mathematical simplification, consider the flat plate collector thermal network for the tow covers this absorbed energy S distributed to thermal losses through the top and bottom and useful energy gain, simplifying calculation of

the overall coefficient of heat loss by converting the losses to the top thermal network, the loss of thermal energy resulting from convection and radiation between parallel plates. In steady state, the transfer of thermal energy between the first cover of T_{c1} temperature and the absorber plate T_p is the same as between any other two adjacent covers, and is also equal to the energy lost to the surroundings from the top cover as showing in the fig. (3.3), Loss of heat from the top is equal to the transfer of heat from the absorber plate to the first cover where :

$$q_{loss,top} = h_{c,p-c1}(T_p - T_{c1}) + \frac{\sigma(T_p^4 - T_{c1}^4)}{\frac{1}{\epsilon_p} + \frac{1}{\epsilon_{c1}} - 1} \quad (3.11)$$

The subscript ($q_{loss,top}$) is the heat loss from the top of the collector and term $h_{c,p-c1}$ represents the convection heat transfer coefficient between absorber plate and glass1 (cover1), and radiation between the plate at a temperature T_p and cover 1 (glass1), and between glass 1 and cover 2 (glass2) at temperatures T_{c1} and T_{c2} respectively and between cover 2 and sky at temperature T_s as illustrated in follow:

The radiation heat transfer coefficient h_r express in following equation:

$$h_{r,p-c1} = \frac{\sigma(T_p+T_{c1})(T_p^2-T_{c1}^2)}{\frac{1}{\varepsilon_p} + \frac{1}{\varepsilon_{c1}} - 1} \quad (3.12)$$

Where $h_{r,p-c1}$ depict the radiative coefficient of temperature transmission between the absorber plate and glass 1 (cover 1), Consequently, the temperature dropped from of the gatherer's top to ambient for one crystal cover. can be described as follows:

$$q_{loss,top} = (h_{c,p-c1} + h_{r,p-c1})(T_P - T_{c1}) \quad (3.13)$$

The (R_1) illustrate loss of temperature from the upper absorber to ambient, where

$$R_1 = \frac{1}{h_w + h_{r,c2-a}} \quad (3.14)$$

Where h_w the loss coefficient for convectional heat transfer caused by wind and radiation, and $h_{r,c2-a}$ coefficient of heat transmission from the top collector to the surrounding air, where

$$h_w = \frac{8.6v^{0.6}}{L^{0.4}} \quad (3.15)$$

Where v is the wind, speed (m/sec) and L is the length of collector (m)

The resistance R_2 between the coverings (glass1 and glass2) is similarly provided by

$$R_2 = \frac{1}{h_{c,c1-c2} + h_{r,c1-c2}} \quad (3.16)$$

and the resistance R_3 for a solar collector's thermal resistance analysis can be expressed as

$$R_3 = \frac{1}{h_{r,p-c1} + h_{c,p-c1}} \quad (3.17)$$

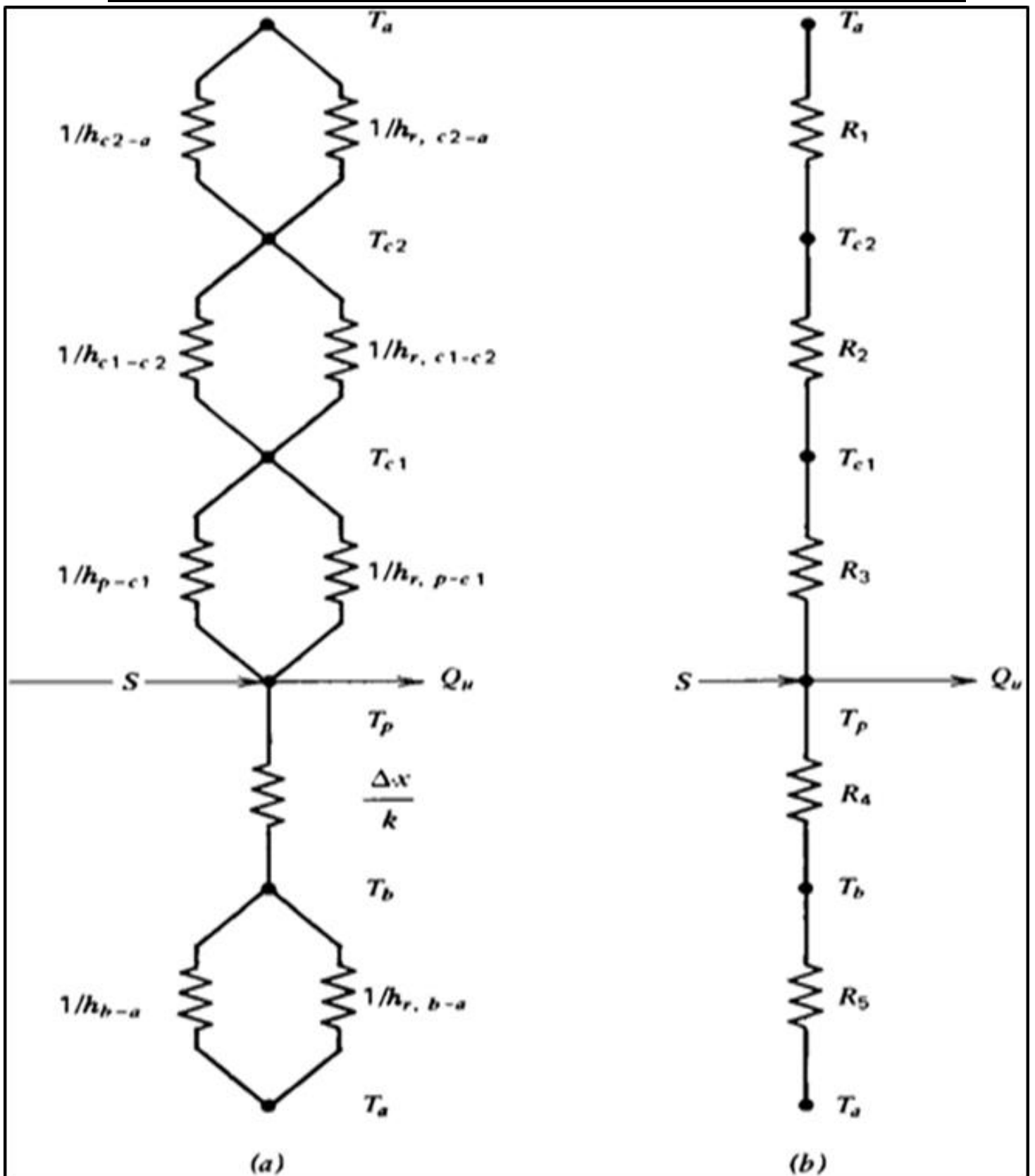


Fig. 3.5: solar collector thermal resistance system with two layers [42].

The highest loss factor from the collection plate to the environment in this two-cover solar system is

$$U_t = \frac{1}{R_1 + R_2 + R_3} \quad (3.18)$$

The resistances R_4 and R_5 both indicate the energy loss from the solar collector's bottom (U_b) and edges (U_e) to ambient. The following equation describes the bottom loss coefficient U_b [41]

$$U_b = \frac{1}{\frac{t_b}{k_b} + \frac{1}{h_{c,b-a}}} \quad (3.19)$$

Where the (t_b) in m is the thickness, (k_b) Represent the thermal conduction (W.K/m) of insulation in the bottom of the gatherer, also, $h_{c,b-a}$ represent the convection coefficient lose between the lowest of the gatherer and the surrounding usually is equivalent to (h_w). The coefficient of heat loss from the gatherer's boundaries is same. U_e can be expressed in the following equation:

$$U_e = \frac{1}{\frac{t_b}{k_e} + \frac{1}{h_{c,e-a}}} \quad (3.20)$$

According to the following correlation, the overall heat loss coefficient U_L in a solar collector is equal to the sum of the top, bottom, and edge loss coefficients:

$$U_L = U_t + U_b + U_e \quad (3.21)$$

The convection heat transfer coefficient between absorber plate cover (glass1) ($h_{c,p-c1}$) And between the covers (glass 1&glass2) ($h_{c,c1-c2}$) evaluate from the following formula[41]:

$$h_c = \frac{k}{l} \left(1 + 1.446 \left[1 - \frac{1708}{Ra \times \cos(\beta)} \right] \left[1 - \frac{1708 (\sin(1.8\beta))^{1.8}}{Ra \times \cos(\beta)} \right] + \left[\left(\frac{Ra \times \cos(\beta)}{5830} \right)^{-0.333} - 1 \right] \right) \quad (3.22)$$

Where (β) is the tilt collector's angle, and k represents thermal conductivity of air between (plate-glass 1) and (glass1-glass2)

And the (Ra) is the Rayleigh number evaluated from the following equations:

$$Ra_{(p-c1)} = \frac{g\beta' pr(T_p - T_{c1})L^3}{\nu^2} \quad (3.23)$$

$$Ra_{(c1-c2)} = \frac{g\beta' pr(T_{c1} - T_{c2})L^3}{\nu^2} \quad (3.24)$$

Where (L) , is the remoteness between (plate-G1) and (G1-G2) in m, g - gravity (m/sec^2) , ν - viscidness of air (m^2/sec) , pr - prandtel amount of air and β'

volumetric coefficient where $\beta' = \frac{T_p + T_{c1}}{2}$ and $\beta' = \frac{T_{c1} + T_{c2}}{2}$ and T_p , T_{c1} , T_{c2} are plate, glass 1 and glass 2 heat, in K. The assets of air in the opening between(plate-glass1) and (glass1-glass2) taken at $\frac{T_p + T_{c1}}{2}$ and $\frac{T_{c1} + T_{c2}}{2}$ correspondingly.

3.7 The internal convection heat transfer coefficient of water flow (h_i) in riser tubes [43]

$$Q_u = \dot{m}C_p(T_o - T_i) = U_o A_o (T_p - T_m) \quad (3.25)$$

The thermal balance for the riser tube of the solar collector

Internally convection heat transfer coefficient calculation (h_i) Coupled eq (3.26)

&eq (3.29) the Nusselt number Nu determined from eq (3.27) where

$$Nu = \frac{h_i d_i}{k_w} \quad (3.27)$$

3.8 The useful energy and the efficiency of solar collector

The usable energy can be computed from the in terms of the resources the absorber absorbs and the energy it loses, where:

$$Q_u = A_c F_R [I_T (\tau\alpha) - U_L (T_i - T_a)] \quad (3.28)$$

The instant specific capacitance, which may be calculated from, converts all of the incident radiation on the collection surface into usable energy.:

$$\eta_i = F_R [(\tau\alpha) - U_L \frac{T_i - T_a}{I_T}] \quad (3.29)$$

Transmittance-absorbent product ($\tau\alpha$) = 0.87 [43] calculated in the appendix(B).

3.9 Thermal performance factor (performance ratio) (TPF)

Performance ratio for constant pumping is defined as

$$TPF = \frac{(Nu_{triangular}/Nu_{circular})}{(f_{triangular}/f_{circular})^{0.1666}} \quad (3.30)$$

Where the $Nu_{triangular}$ Is the Nusselt number for flow in a triangular tubes, $Nu_{circular}$ Nusselt number of flows in circular tubes, $f_{triangular}$ friction factor for flow in a triangular tubes, $f_{circular}$ Friction factor for flow in circular tubes.

CHAPTER FOUR

EXPERIMENTAL

WORK

Chapter Four

Experimental Work

4.1 Introduction

The summary of this chapter provides details about the experimental test and the measuring equipment used in it as show in fig. (4.1). The experimental apparatus is intended to examine the thermal conductivity and reaction to solar radiation of round tubes and triangular tubes in order to determine which tubes are more effective at effective to heating water. Circular tubes placed on a flat plate are compared to triangular tubes placed inside the grooves of a V-grooves absorber plate in the first case, and circular tubes placed on a flat plate are compared to triangular tubes placed inside grooves in the second case. This comparison is in four flow streams, at a flow rate of (2, 3, 5, and 7) LPM, and in three cases. The first case compares triangular tubes put inside the grooves of a V-grooves absorber plate to circular tubes placed on a flat plate. The second case compares circular tubes placed on a flat plate to triangular tubes positioned beside the grooves of the V-grooves absorber plate. The third case compares triangular tubes put over the grooves of the V- grooves absorber plate to circular tubes placed on a flat plate. In the closed system, distilled water is employed as the liquid. execution of an experimental activity at Nasr City, Dhi Qar Governorate, in the coordinates 31.54° N latitude and 46.12° L.

In this study, experimental work was done. Experimental work was carried out in this analysis for the next status:

1. The 45 south-facing flat plate solar collector is installed.
2. The rising circular tubes are placed on an absorber flat plate.
3. In order to determine which of the triangular riser tubes is more effective in thermal conductivity to water heating inside it, the triangular riser tubes are

placed in three different configurations: first, the triangular tubes are placed inside the grooves, second, the triangular tubes are placed beside the grooves, and third, the triangular tubes are placed over grooves of the V- grooves absorber plate in the solar collector.

4.2 Experimental Work Description

The investigational work contains of the next apparatuses:

- a) A plane platter solar hoarder.
 - circular riser tubes.
 - circular header tubes.
 - a flat absorber plate.
 - two glass coverings.
 - the insulators.
 - container of aluminum.
- b) A solar collector with a V-corrugated absorber plate
 - triangular riser tubes.
 - V-corrugated absorber plate.
 - circular header tubes.
 - two glass coverings.
 - container of aluminum.
 - the insulators.
- c) Pipes.
- d) Valves.
- e) Measuring tools.
- f) Tanks.
- g) Sensors.
- h) Aluminum construction.
- i) Insulators that protect pipes and tanks.
- j) Aluminum construction.

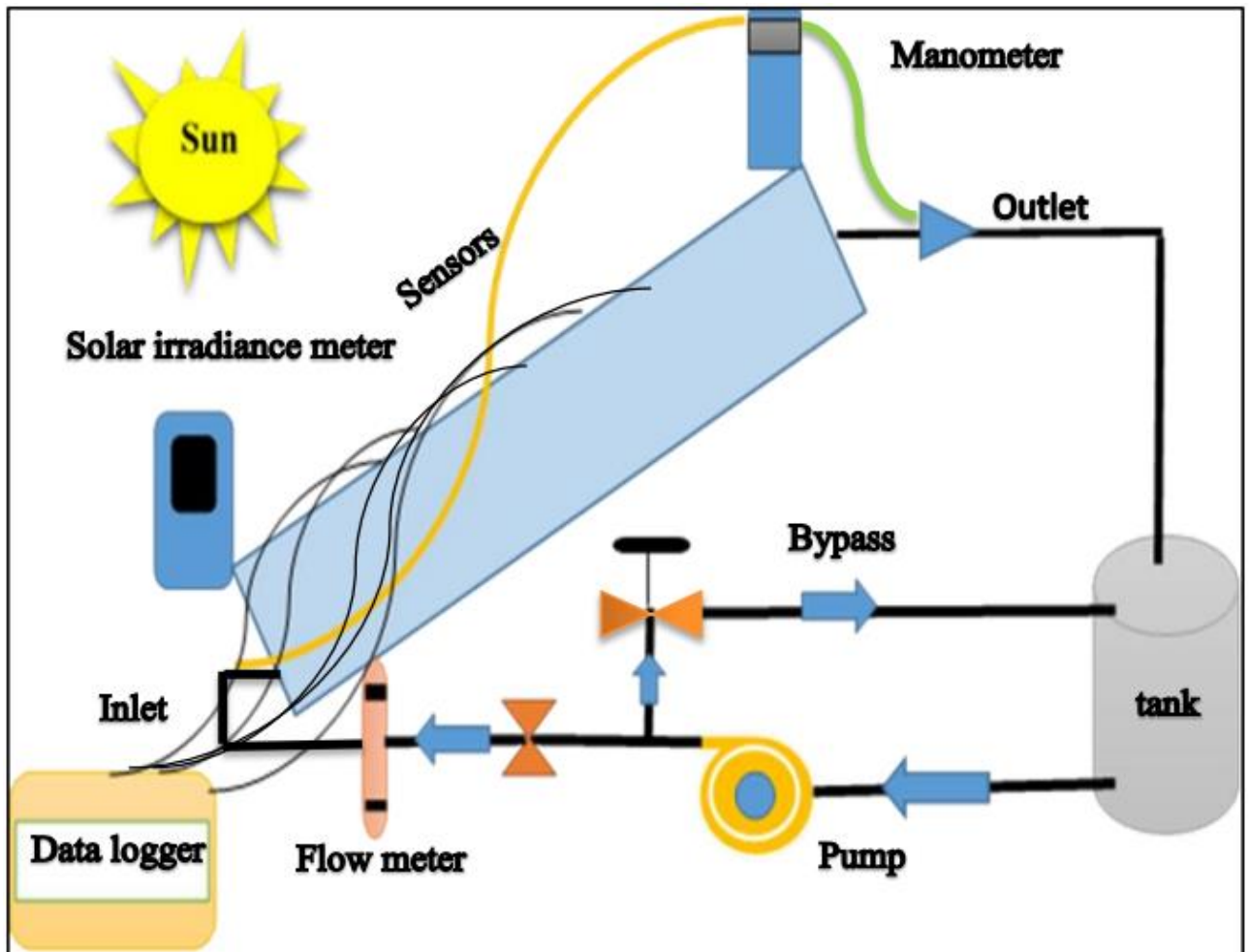


Fig. 4.1: Schematic of test rig construction and the measurement devices

4.2.1 Specifications of Flat Plate Solar collector

The steps below show how to build the solar collector shown in fig. (4.2), and be constructed using the techniques listed below (4.1). The first step is to prepare the riser tubes, which are four copper tubes divided into two with an inner diameter of 0.0115 m and an outer diameter of 0.0125 m and a length of 0.8 m fastened on the absorber flat plate in parallel arrangement, the distance between the center line and the other is 0.1m, and the lower and upper headers are copper tubes with an inner diameter of 0.0175 m and an outer diameter of 0.015 m and length 0.5 m , The absorber plate was mounted in an aluminum container and separated from the bottom and sides by 0.05 m of glass wool insulation thickness

to reduce conductive loss. The absorber plate was made of aluminum metal with dimensions of $L=1$ m and $W=0,5$ m, thickness of absorber plate was 0.0005 m. It had a matt black paint coating with absorption (0.92-0.98) to increase the fraction of available solar radiation absorbed by the plate and to minimize the loss of long wavelength radiation from the absorbing surface. Also to minimize convection losses from the top of the flat plate solar collector the container closed by two 0.004 m thick window glass, sheet due to glass has the high property of transmitting around 90 per cent of short-wave radiation incidence and preventing long-wave radiation emitted from the heat absorber plate to escape into the atmosphere, the distance between the plate and the glass1 is 0.045 m while the distance between the two glasses is 0.02 m , Also, the outer dimensions of the solar collector are 1.1 m in length and width 0.6 m and height 0.15 m. And the stand manufactured from Aluminum for the purpose positioning and the solar collector is tilted to south facing with 45° .

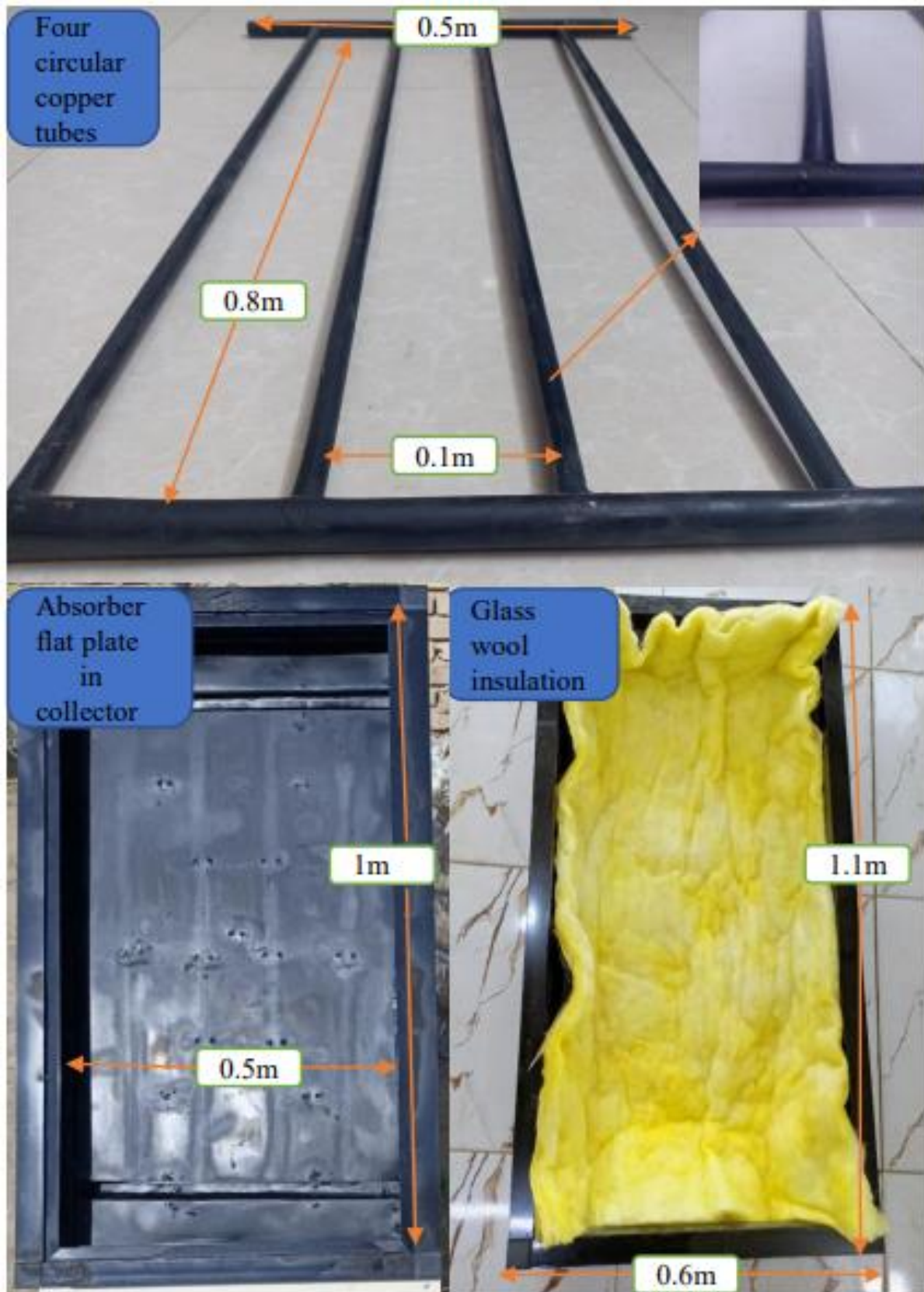


Fig. 4.2: flat plate solar collector components.

Table- 4.1: The specification of flat plate and V-grooves plate solar collectors

Component		Dimension	Remark
Collector		1.10m*0.60m*0.15m	
Absorber plate		1.00m*0.50m*0.0005m	Material: black painted Aluminium
Riser tubes	Circular tubes	The inner diameter is 0.0115m, The outer diameter is 0.0125m, The length is 0.8m Tube center to center distance 0.1m	Material: copper Number of tubes: four Type of tubes: circular riser tubes
	Triangular tubes	Triangular tubes of equal sides side length of triangular tube is 0.013m Triangular tube length is 0.8m The triangular tube center to triangular tube center distance 0.1m	Material: copper Number of tubes: four Type of tubes: triangular riser tubes
Header pipes		Inner diameter 0.0175 m, outer diameter 0.0185 m, length 0.5m	Material: copper Number of tubes: two
Bottom insulation		0.050 m thick	Material: glass wool
Edges insulation		0.050 m thick	Material: glass wool
Cover window Glass		1.00m*0.50m*0.004m	Material: clear window glass Number of covers: two
Tilt angle		45°	

4.2.2 Specifications V-grooves Plate Solar collector

Build of V-grooves Plate Solar collector it is like the build of flat Plate Solar collector but it is contained four triangular riser tubes and four V-grooves, as shown in fig. (4.3). The position of the triangular tubes is changed in three cases in order to compare them with the circular tubes, In each case. in the first case, the triangular tubes are placed inside the grooves, in the second case the triangular tubes placed beside the grooves and the third case the triangular tubes placed over the grooves of the V- grooves plate in solar collector.

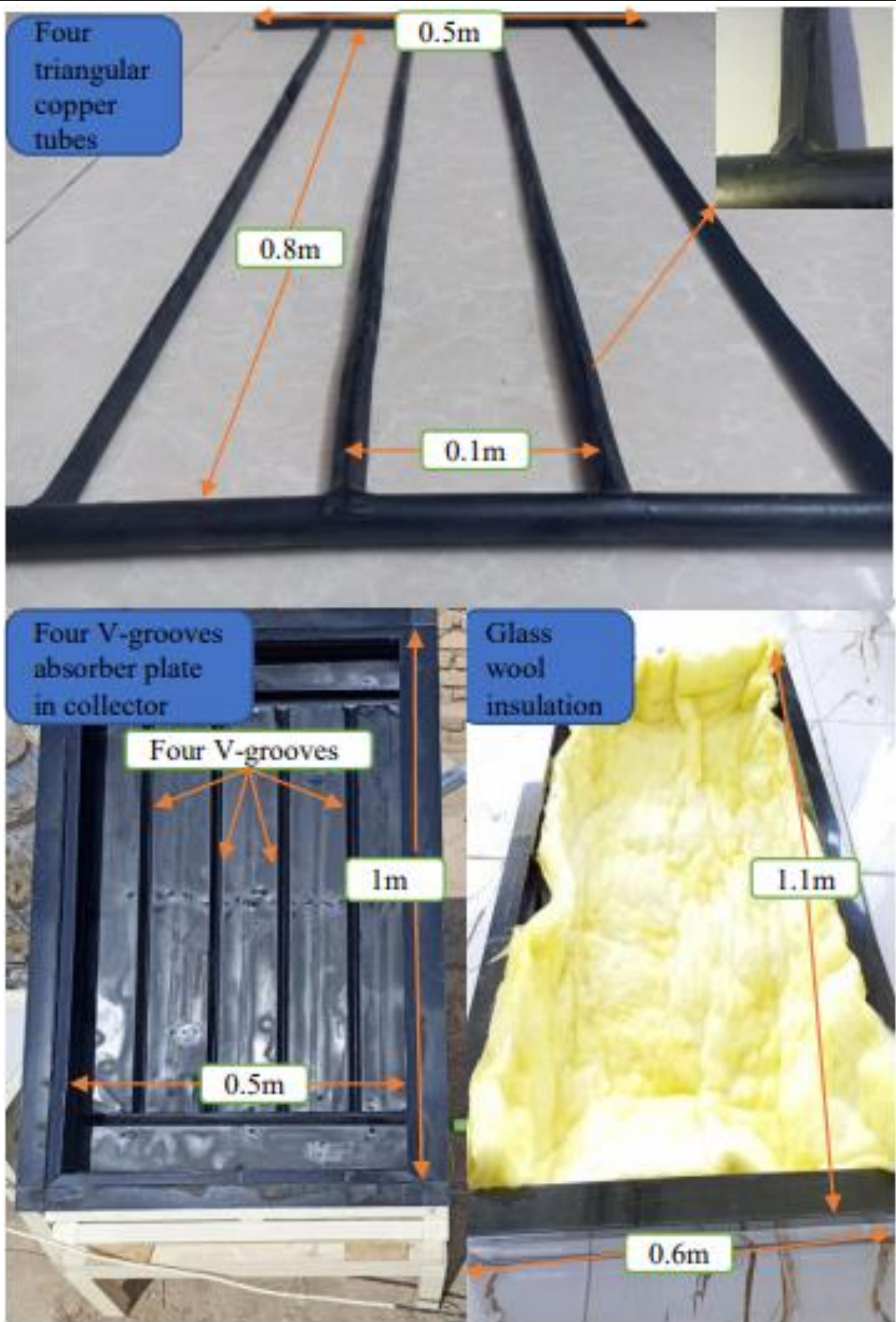


Fig. 4.3: V- grooves plat solar collector components.

4.2.3 Experimental setup of the system

The Fig. (4.4) show the flat plate solar collector and V-grooves plate solar collector, The distance between the first and second glass covers is 0.02 m, and when the rate of solar radiation goes through two glass covers and particularly strikes the aluminum absorber plate that is situated beneath the two glass covers, while there is a 0.02 m gap between the flat plate and the second glass cover, large portions of the sun energy falling on the flat plate are absorbed and transformed into heat energy. The utilized pump aids in circulating the fluid between the solar collector and the tank where the circulation system for the fluid is of the kind of closed system, where the heat is passed to the riser's tubes to liquids, which increases the temperature of the fluid moving within the tubes. the performance was checked Solar collectors in Nasr City in Dhi Qar Governorate, experimentally at that location of with (31.54° N latitude and 46.12° longitude). The data are recorded under transient conditions and a 45° south tilt. In this research. There are four types of solar collector:

- a) The flat plate solar collector that contains circular tubes as show in fig. (4.5).
- b) The V-grooves plate solar collector that contains triangular tubes inside the grooves as show in fig. (4.6).
- c) The V-grooves plate solar collector that contains triangular tubes beside the grooves as show in fig. (4.7).
- d) The V-grooves plate collector that contains triangular tubes over the grooves as show in fig. (4.8).

The three V-grooves plate solar collector used to compare it with a circular tube solar collector to find out which of the three collectors more efficient in thermal conductivity, The specifications for the two collectors are given in table (4.1).

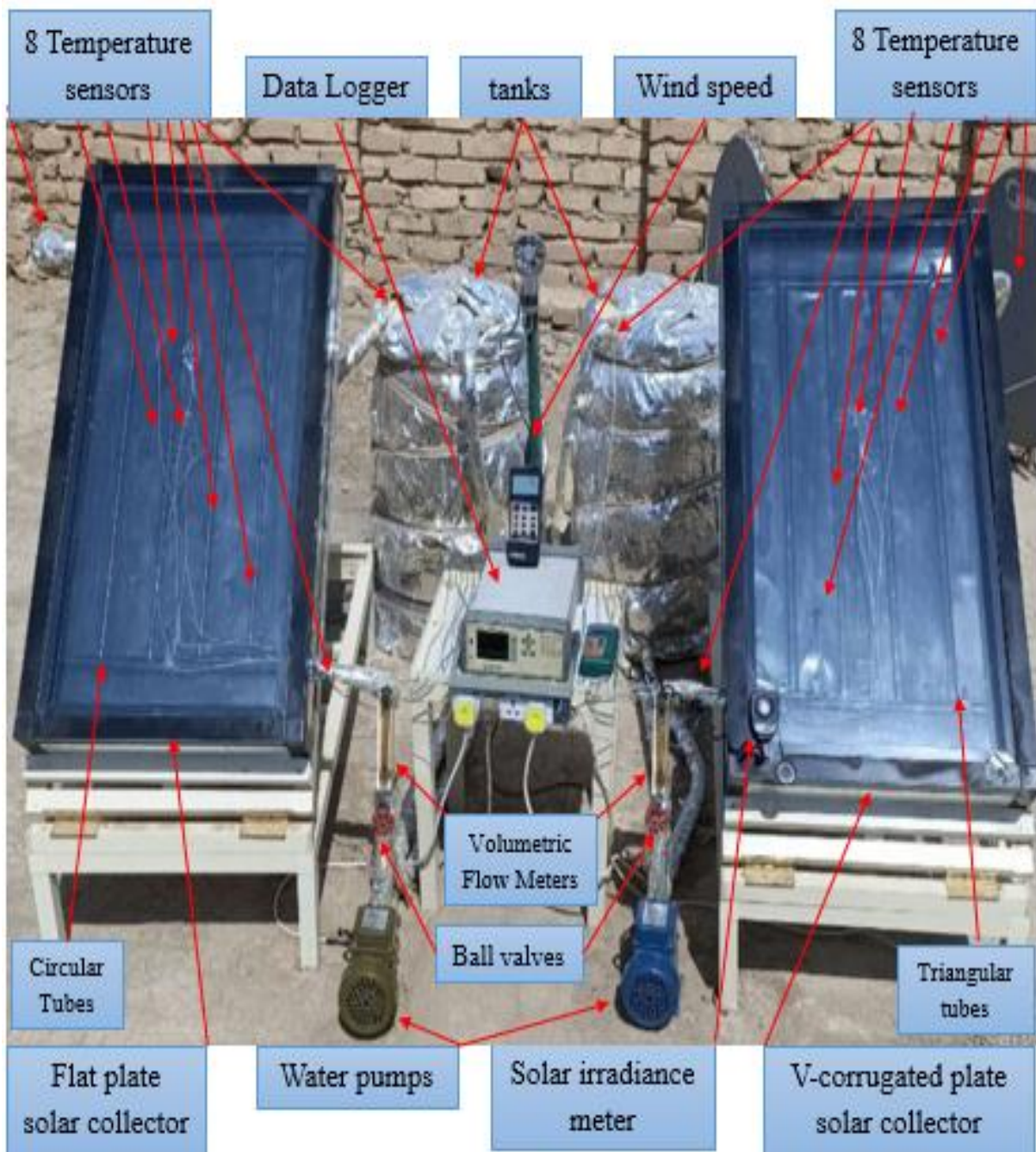


Fig. 4.4: FPC and V-grooves plate solar collector with measurements devices

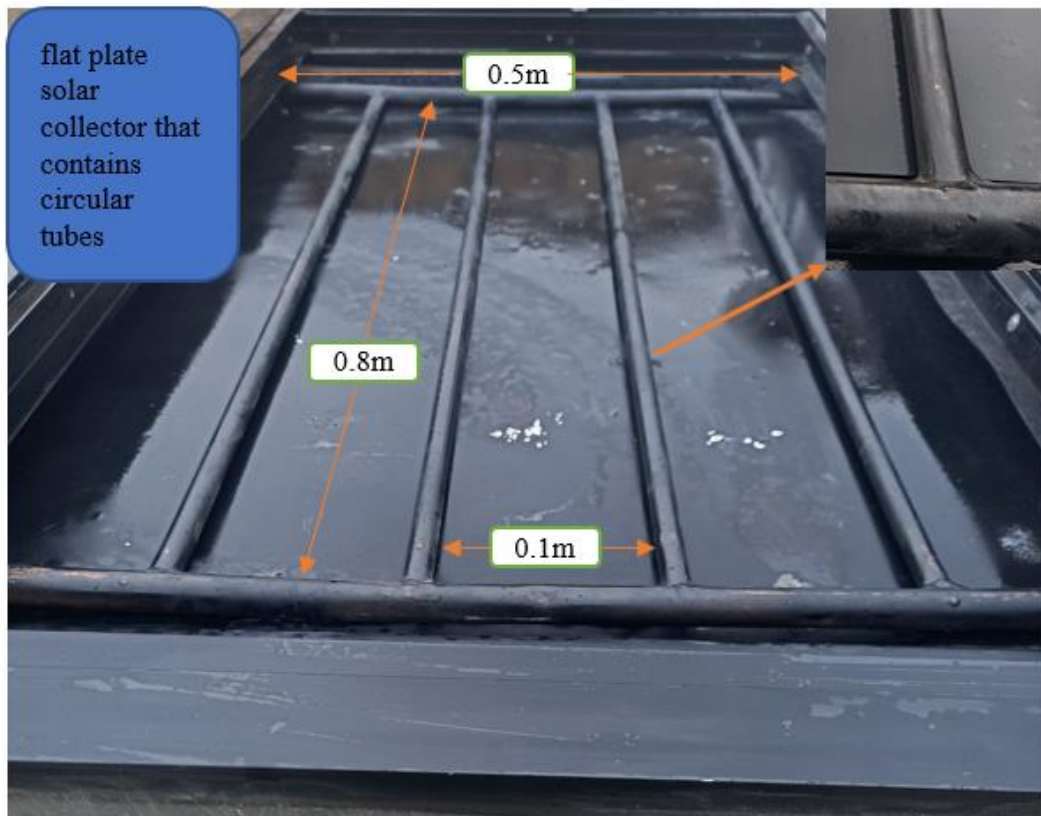


Fig. 4.5: The flat plate solar collector that contains circular tubes.

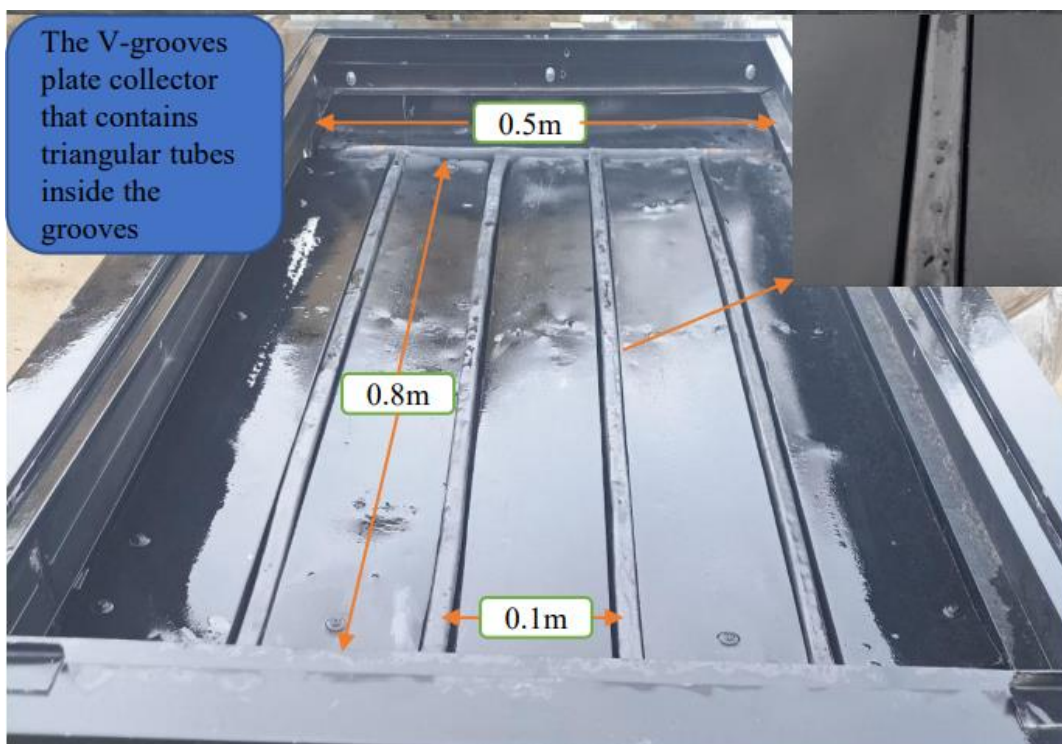


Fig. 4.6: The V-grooves plate solar collector that contains triangular tubes inside the grooves.



Fig. 4.7: The V-grooves plate solar collector that contains triangular tubes beside the grooves

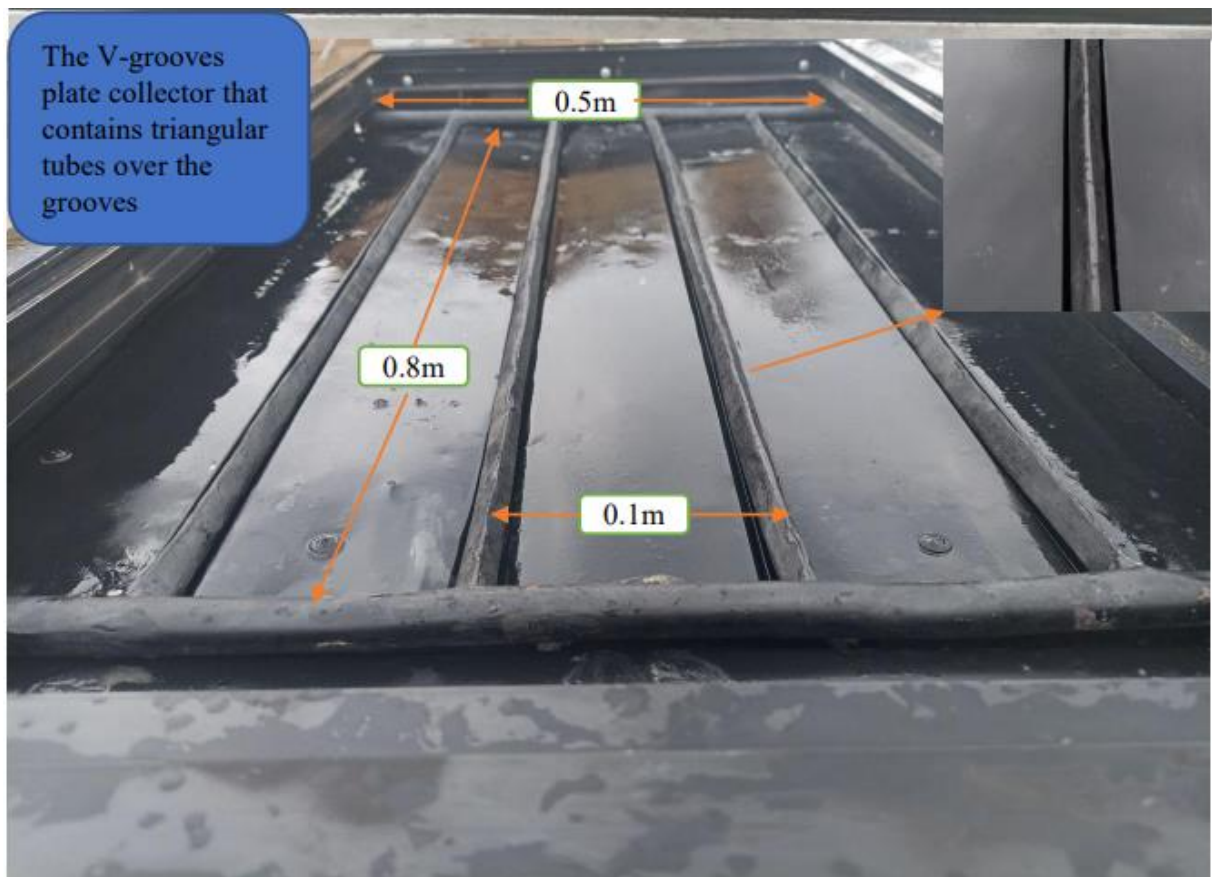


Fig. 4.8: The V-grooves plate collector that contains triangular tubes over the grooves

4.2.4 Water pumps

As seen in figure (4.9), each solar collector in this study had its own pump, and an electric motor-driven centrifugal pump was employed to transport water all through the actual experimental system. The table below provides details about water pump specifications (4.2).



Fig. 4.9: Water pumps

4.2.5 Pipes

Plastic Pipes (1/2 inch) is used to connect all major parts of the test device show in fig. (4.9), the pump with the storage tank and inlet manifold, and the storage tank with the outlet manifold. As well as for the connection between the water tank and the pump, and between the pump and the solar collector, these pipes were covered by a thermal insulator in order to reduce heat exchange with the atmosphere, which increases the work efficiency in order for the results of the comparison between the two solar collectors to be more efficient.

Table- 4.2: The specifications of centrifugal pumps

AKAD Water pump					
Q	Power	R. P. M	Electrical data		
10 – 30 L/min	0.370 kW	2850	A	V	Hz
			1.8	220	50

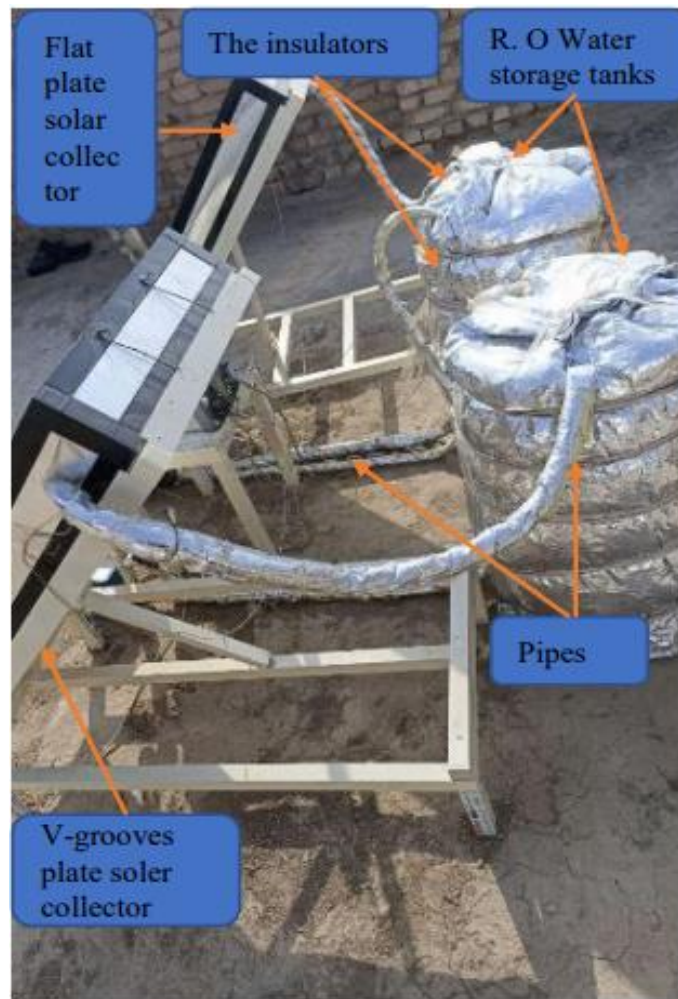


Fig. 4.10: Plastic pipes (1/2 inch) covered by insulators

4.2.6 Valves

In order to control the liquid flow rate, ball valves were used, where the first valve was used between the pump and the solar collector as revealed in figure (4.12) in order to control the required amount of flow, while the second valve was used between the solar hoarder and the water tank in order to return the excess water to the water tank, and in both of solar collectors.

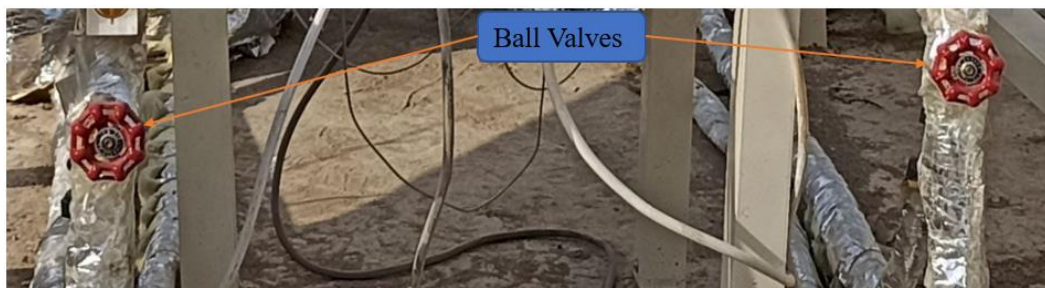


Fig. 4.11: Ball valves

4.2.7 The insulators

In order to avert heat loss of the liquid used in the solar hoarder system, insulators of the type of fleece and spectacles as shown in figure (4.10) were used to cover some of the parts used in the system, such as the water tank and water transmission pipes between the parts of the solar collector. This increased the accuracy of the sensor's readings, which increased the accuracy of comparing the solar collectors used, and therefore increased the efficiency of the work of this work.

4.2.8 The measuring devices

The list that follows includes measuring devices that used

- Inlet and outlet water temperature sensors.
- Glass temperature sensors.
- plate temperature sensors.
- Volumetric water flow meter.
- Solar power meter
- Wind speed.
- Manometer
- Water tank temperature
- Ambient temperature.

The next chapter goes into further information on the equipment that were used to evaluate these parameters.:

a) Data Logger

A data logger device was used model AT4532x as shown in figure (4.12) to measure the temperatures of the water inlet and the water outlet of the solar hoarder, as well as measuring the heat of the flat plate and measuring the V-corrugated absorber plate and measuring the temperature of the used glass, as well as measuring the heat of the liquid in the storage tanks and measuring the temperature of the ambient.



Fig. 4.12 Data Logger

b) Temperature Sensors

As seen in figure (4.13), there were 17 temperature sensors of type K utilized in the solar collectors to measure the temperature in various locations on the test equipment. The sensors had dimensions of 5 x 40 mm, and their sensor cables were 3 m long.



Fig. 4.13: Seventeen temperature sensors type K

Positions of temperature sensors

The temperature sensors used was 16 distributed over all parts of the two solar collectors as shown in fig. (4.14) and as the following:

- Two sensors fixed in the inlet and outlet pipes of the solar collector, to measuring the water temperature at inlet and outlet respectively.
- Three sensors fixed on the absorber platter surface to measure the temperature of the absorber plate.
- One sensor secure (fixed) on the glass 1 covers the absorber plate to measure surface Glass1 temperatures.
- One sensor secure (fixed) on the glass 2 covers the solar collector to measure surface Glass2 temperatures.
- One sensor putted in the water tank to measuring the water tank temperature.
- One Air sensor to measuring the temperature of the ambient.

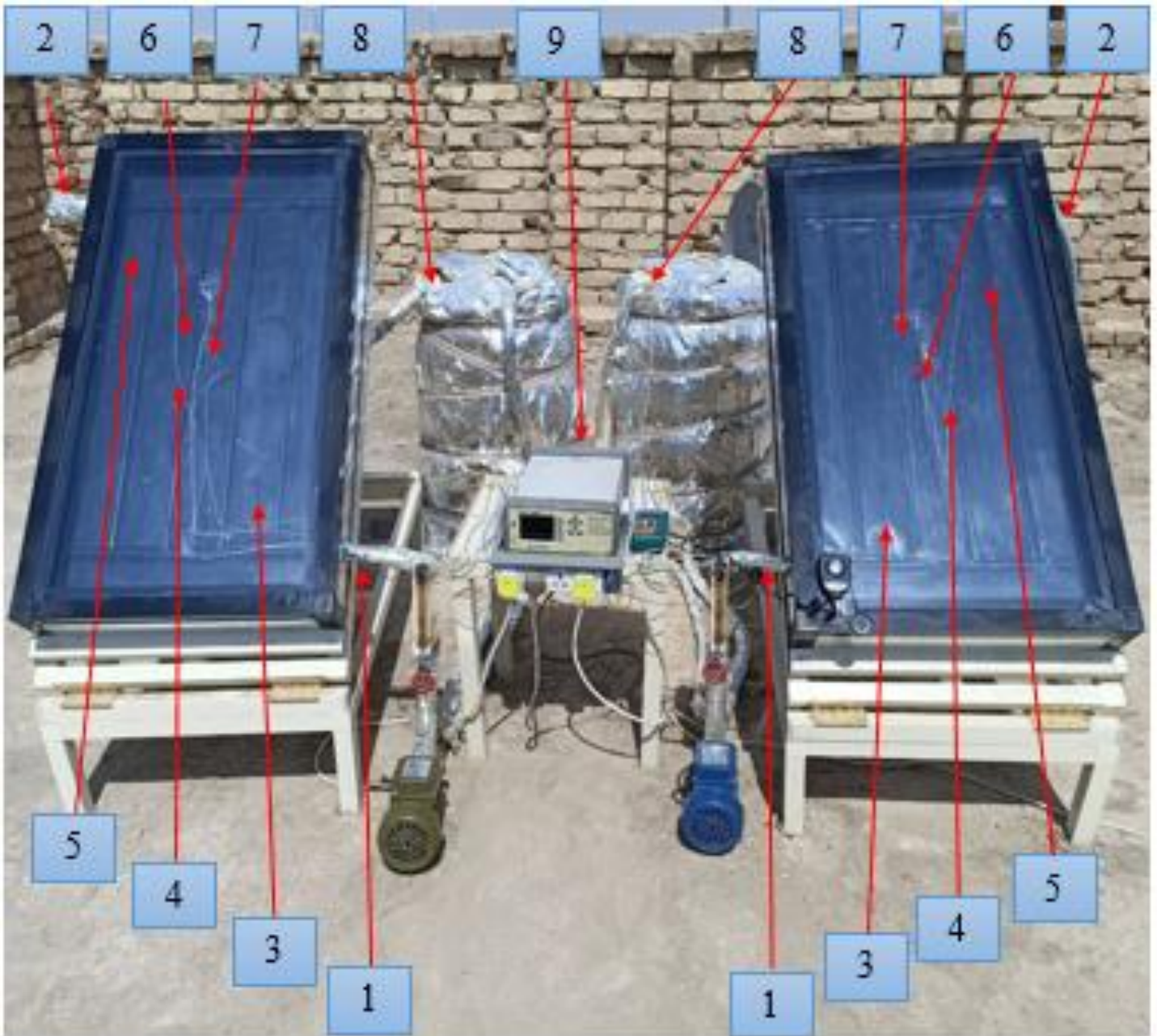


Fig. 4.14: Positions of temperature sensors

c) Volumetric water flow meter

The volumetric flow meter employed in this study, which has a range of 1 to 10 liters per minute, is installed in the solar collector inlet pipe, between the inlet valve and the solar collector (see fig. 4.15).



Fig. 4.15 Volumetric water flow meter

d) Pressure measurement

Manometer of variety (from 5 m Bar to 7000 m Bar), Model PCE-917 exposed in the Fig. (4.16) uses to measure the pressure difference between the inlet (p_1) and outlet of the collector (p_2) over linked the pipes of inlet and opening correspondingly.



Fig. 4.16: Manometer.

e) Solar power meter

A solar cell (also known as a solar panel) and an ohmmeter are employed in the model (TENMARS TM-207) depicted in Fig. (4.17) to measure the presence of solar radioactivity. w/m^2 .



Fig. 4.17 solar power meter

f) Wind speed

In addition to using the internet and the weather information, the wind speed meter model (Lutron AM-4206 M) was utilized as shown in Fig. 4.18 to measure the wind speed at the device test location.



Fig. 4.18 Wind speed

Experimental procedure

This study includes three systems of triangular tubes placed inside and beside and over the grooves of Black V- grooves absorber plate in solar collector to compare it with circular tubes placed on the absorber flat plate of the solar collector each other

Circular tubes system with flat plate, symbol A

Triangular tubes system with V- grooves absorber plate and the triangular tubes placed inside the grooves, symbol B

Triangular tubes system with V- grooves absorber plate and the triangular tubes placed beside the grooves, symbol C,

Triangular tubes system with V- grooves absorber plate and the triangular tubes placed over the grooves, symbol D,

and used distilled water as the working fluid.

The working procedure

The following steps were performed for every day work:

- 1) Fill an insulated tank with 20 liters of fresh distilled water for each working day.
- 2) Equip measuring instruments to read and record data from experimental work
- 3) Turn on the data logger to record the temperature reading and set it to take data every (30 minutes).
- 4) Turn on the water pumps and adjust the flowmeter to the required flow rate by means of an adjustable valve and open the bypass valve.
- 5) Turn on the solar radiation device and setting at w/m^2 .
- 6) The experimental work was conducted for ten hours from 7:00 am to 5:00 pm
- 7) This procedure was repeated for four days, and on each day the flow was different, where (2,3,5 and 7) LPM respectively.
- 8) The readings are taken for the temperature sensors, the rate of solar radiation, and the measurement of wind speed for every half hour of work 7:00 am to 5:00 pm. These above steps were used to

1- compare the performance of circular tubes system of flat plate, symbol A, compared it with triangular tubes placed inside the grooves of V- grooves

absorber plate, symbol B as shown in Fig. (4.6), which of them most efficient thermal conductivity to in heating water used. And in four cases of flow water in (2,3,5 and7) LPM.

2- compare the performance of circular tubes system of flat plate, symbol A, compared it with triangular tubes placed beside the grooves of V-corrugated absorber, symbol C as shown in Fig. (4.7), which of them most efficient thermal conductivity to in heating water used. And in four cases of flow water in (2,3,5 and7) LPM.

3- compare the performance of circular tubes system of flat plate, symbol A, compared it with triangular tubes placed over the grooves of V-corrugated absorber, symbol D as shown in Fig. (4.8), which of them most efficient thermal conductivity to in heating water used. And in four cases of flow water in (2,3,5 and 7) LPM.

CHAPTER FIVE

RESULTS AND DISCUSSIONS

Chapter Five

Results and Discussions

5.1 Introduction

This chapter discusses the experimental results that were obtained through this research work and provides a detailed explanation about them, as this experimental work includes two types of solar collectors (flat plate solar collector and V-grooves plate solar collector). And evaluate the performance of the solar collectors by comparing the solar collector, which contains circular riser tubes, with the solar collector, which contains triangular riser tubes, and in three cases firstly the triangular riser tubes inside grooves, secondly the triangular riser tubes beside grooves and thirdly the triangular riser tubes over grooves, Comparing it to find out which of the solar collectors more efficiency in thermal conductivity of the rising tubes used, and thus heating the water inside the rising tubes. As the working period for each comparison case is four days and for each day a different flow condition (2,3,5 and 7) LPM respectively. where temperatures, intensity of solar radiation and wind speed are recorded every half an hour of work and for both collectors used for the purpose of comparison between them, where the number of comparisons is three comparative cases, so the working days are ten working days. where the work time from 7:00 am until 5 pm.

5.2 Experimental results

The experimental work examines the effectiveness of heating water for the V-grooves plate solar collector in terms of heat transfer (Nusselt number), and in three cases (when the triangular riser tubes inside the grooves, when the triangular riser tubes beside the grooves, and when the triangular riser tubes above the grooves), and compares it with the effectiveness of the solar collector, which contains circular riser tubes.

5.3 The results of solar radiation

The local solar radioactivity data from the atmosphere was measured by using a Solar power meter, in the September for ten hours by day from 7:00 am until 5:00 pm as shown in Fig. (5.1), And for a period of twelve days, during which every four days for a comparison between the flat plate solar collector and the kind of V- corrugated plate solar collectors and for three kinds (that contain triangular riser tubes inside the grooves, that contain triangular riser tubes beside the grooves and that contain triangular riser tubes over the grooves) respectively. where it was found that the solar radiation was at its peaky in the middle of the day, While the solar radiation begins to rise and in a slight form 7:00 am and slightly after that, it begins to rise more than 8:00 am about until reaching its peak in the middle of the day at about 12:00 pm, and then begins to descend slightly gradually For about an entire hour, and then the solar radiation decreases more until it reaches about 4:00 pm , after which the descent was less intense because the sun's disk has become almost horizontal in relation to the solar collector, where the greatest solar radiation is approximately between the 11:00am to 1:00 pm, Which gives more efficient thermal conductivity to the solar collectors , with the difference efficiency between the solar collectors used, because the difference in the shapes of the absorber plates used and the difference in the shapes and locations of the rising tubes used in the solar collectors

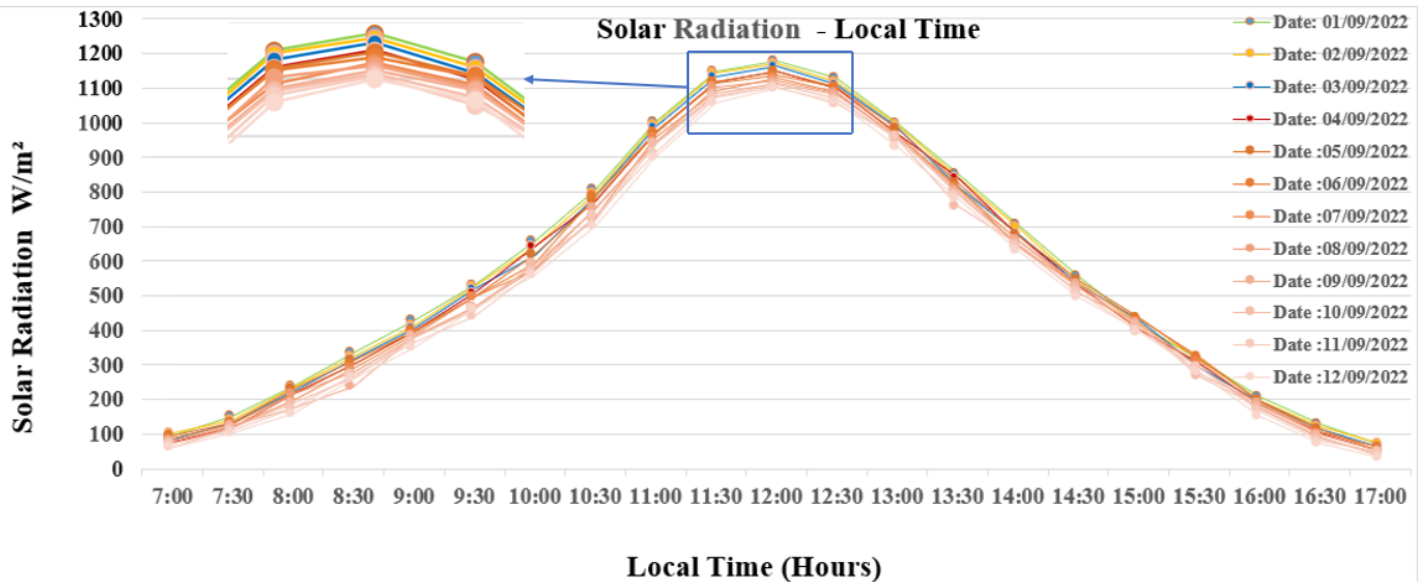


Fig. 5.1: solar radiation for (1-12)/ September /2022.

5.4 The result of outlet temperature

5.4.1 Outlet temperature comparison of the circular and triangular riser tubes inside the grooves

Through the results shown in the fig. (5.2) and in the water flow (2,3,5 and7) LPM respectively, it was found that the V- grooves plate solar collector it was more efficient in heating water than the flat plate solar collector ,that the fall of the sun's rays on the aluminums plates used inside the solar collectors converts it into heat energy that is transmitted from the plates to the riser tubes used , and because the contact area between the triangular riser tubes inside the grooves of the V-corrugated absorber plate was larger than the contact area between the circular riser tubes on the flat plate. The results show the solar collector that contains triangular riser tubes is more efficient than the solar collector that contains circular riser tubes and thus the temperature heating water inside triangular riser tubes is greater, as Fig. (5.2) indicate that the maximum outlet temperature of the triangular riser tubes compared with the circular riser tubes is ($89C^{\circ}$), The outlet temperature begins to rise from operating the solar hoarders 7:00 am (with the variation in the rise of the outlet heat of the collectors used) , until the temperature

of the outlet reaches a steady state, which is approximately from (1:00pm - 3:00pm) hour , That the reason for the steady state of the outlet water was, the greatest solar radioactivity fallen on the two solar collectors was 12:00 pm approximately, as shown in the fig. (5.1), while the most steady state of the outlet temperature water for the solar hoarders was two hours (1:00pm -3:00pm) and for the two solar collectors used, because the amount of heat exchange for the water used between the solar collectors and the storage tanks requires a one hour or more after maximum incident solar radiation on the solar collectors until it reaches to steady state , where notice through the fig. (5.2) , that the maximum steady state of the outlet water is between the two hours (1:00 pm-3:00pm). After that, the outlet temperature of the solar collectors is gradually reduced because the decrease intensity of the solar radioactivity falling on it, also the outlet temperature of the water storage tanks is greater because the high insulation of the water storage tanks and pipes used, and after steady state the outlet temperature of the solar hoarders begins drop until the end work day at the hour 5:00pm.

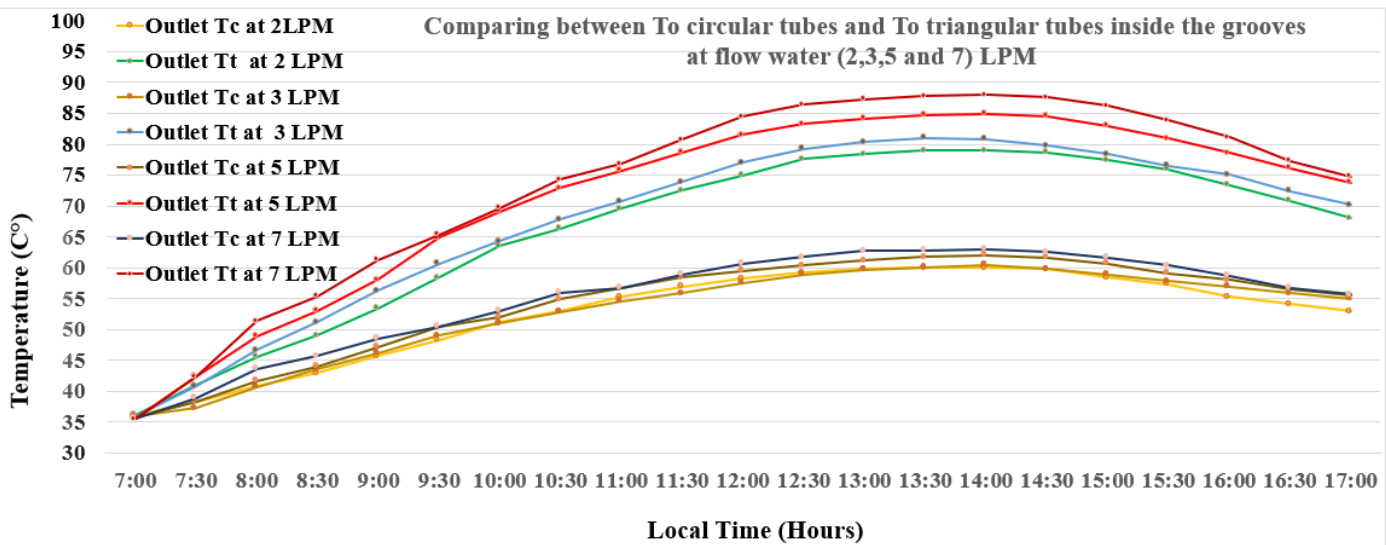


Fig. 5.2: Comparing between T_{out} circular tubes and T_{out} triangular tubes inside the grooves at flow water (2,3,5 and 7) LPM for (1-4)/ September /2022 respectively.

5.4.2 Outlet temperature comparison of the circular and triangular riser tubes beside the grooves

From the comparison of the outlet temperature for the flat plate solar collector that contains circular riser tubes and V- grooves absorber plate solar collector that contain triangular riser tubes beside grooves, and in the water flow (2,3,5,7) Lpm respectively, it was found that V- grooves plate solar collector it was more efficient in heating water from the flat plate solar collector, because the fall of the sun's rays on the aluminums plates used inside the solar collectors converts it into heat energy that is transmitted from the plates to the riser tubes used, and because of the grooves in the V- grooves absorber plate, which makes its surface area larger than the absorber flat plate, which makes the amount of solar radiation falling on it larger, which is converted into thermal energy that is transmitted through the V- grooves absorber plate to the triangular riser tubes, which increases the heating of the water inside the triangular riser tubes, that is increases the efficiency of the V- grooves absorber plate, and because the contact area between the triangular riser tubes beside the grooves of the V- grooves absorber plate was larger than the contact area between the circular riser tubes on the flat plate, and the results shows in fig. (5.3) explain that the maximum outlet temperature of the triangular riser tubes compared with the circular riser tubes is (78C°), The outlet temperature begins to rise from operating the solar collectors 7:00am (with the variation in the rise of the outlet temperature of the collectors used) , until the temperature of the outlet reaches a steady state, which is approximately from (1:00pm - 3:00pm) hour , That the reason for the steady state of the outlet water was the greatest solar radiation fallen on the two solar collectors was 12:00 pm approximately, as shown in the figure (5.1), while the most steady state of the outlet temperature water for the solar collectors was two hours (1:00pm -3:00pm) and for the two solar collectors used, because the amount of heat exchange for the water used between the solar collectors and the storage tanks requires a one hour

or more after maximum incident solar radiation on the solar collectors until it reaches to steady state, where we notice through the fig. (5.3), that the maximum steady state of the outlet water is between the two hours (1:00pm -3:00pm). Following steady state, the outlet temperature of the solar collectors starts to decrease until the end of the workday at 5:00pm. This is because the intensity of the solar radiation falling on the collectors is gradually decreasing. In addition, the outlet temperature of the water storage tanks is higher due to the high insulation of the water storage tanks and pipes used.

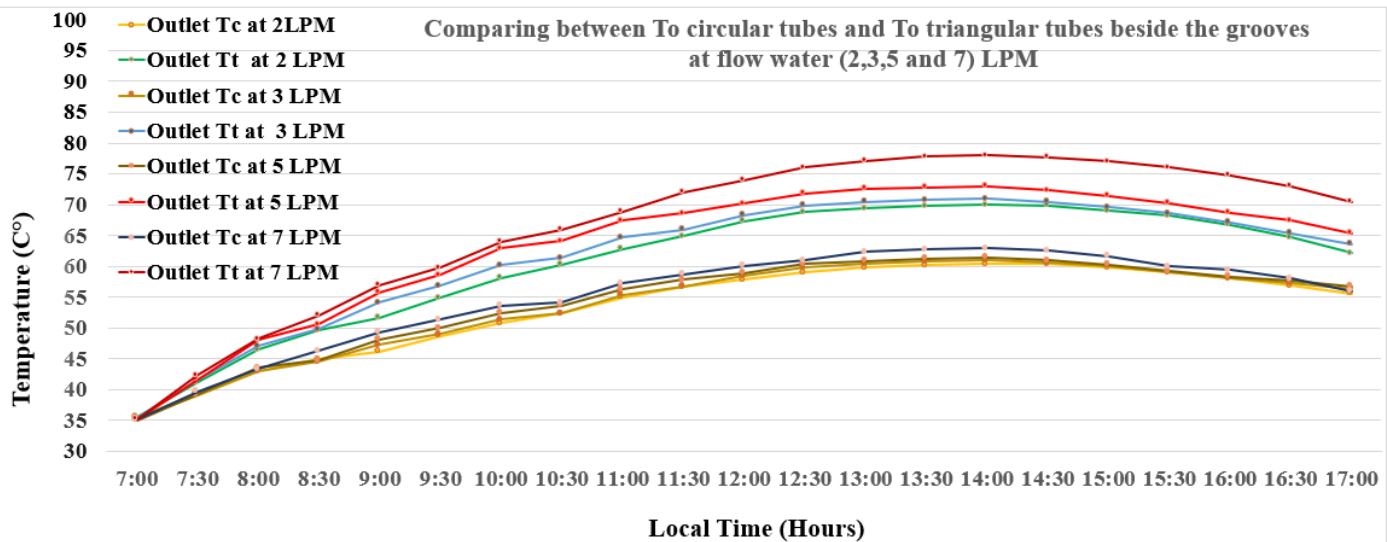


Fig. 5.3: Comparing between T_{out} circular tubes and T_{out} triangular tubes beside the grooves at flow water (2,3,5 and 7) LPM for (5-8)/ September /2022 respectively.

5.4.3 Outlet temperature comparison of the circular and triangular riser tubes over the grooves

Through the comparison of the outlet temperature for the flat plate solar collector that contains circular riser tubes and V- grooves absorber plate solar collector that contain triangular riser tubes over grooves, and in the water flow (2,3,5,7) Lpm respectively, the results shows that the V- grooves plate solar collector it was more efficient in heating water than the flat plate solar collector, because the global

warming generated by the grooves in the V- grooves absorber plate increases the temperature of the used V- grooves absorber plate, that is increases the temperature of the triangular riser tubes, and thus increases the temperature of the water inside the triangular riser tubes used, Which increases the efficiency of the V- grooves absorber plate solar collector, and that the fall of the sun's rays on the aluminums plates used inside the solar hoarders converts it into heat energy that is transmitted from the plates to the riser tubes used , and Fig. (5.4) designate that the maximum outlet temperature of the triangular riser tubes compared with the circular riser tubes is (73C°), The outlet temperature begins to rise from operating the solar collectors 7:00am (with the variation in the rise of the outlet temperature of the collectors used) , until the temperature of the outlet reaches a steady state, which is approximately from (1:00pm - 3:00pm) hour , That the reason for the steady state of the outlet water was, the greatest solar radiation fallen on the two solar collectors was 12:00 pm approximately, as shown in the fig. (5.1), while the most steady state of the outlet temperature water for the solar collectors was two hours (1:00pm 3:00pm) and for the two solar collectors used, because the amount of heat exchange for the water used between the solar collectors and the storage tanks requires a one hour or more after maximum occurrence solar radioactivity on the solar hoarders until it reaches to steady state ,Following steady state, the outlet temperature of the solar hoarders starts to decrease until the end of the workday at 5:00pm, because the outlet temperature of the water storage tanks is higher due to the high padding level of the water storing tanks and pipes used, and because the gradual reduction in the amount of solar radiation

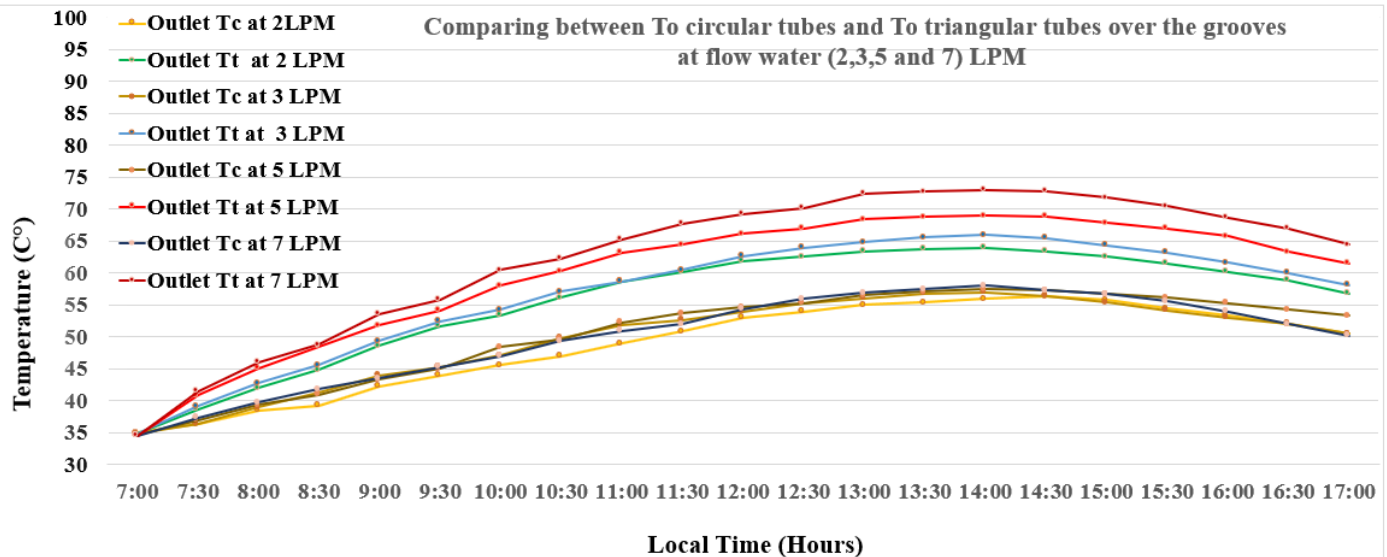


Fig. 5.4: Comparing between T_{out} circular tubes and T_{out} triangular tubes over the grooves at flow water (2,3,5 and 7) LPM for (9-12)/ September /2022 respectively.

5.4.4 The outlet temperature comparison for the Tt inside and Tt beside and Tt over grooves

Through comparing three cases of the outlet temperature (the outlet temperature of the V- grooves absorber plate solar collector that contains triangular tubes inside the grooves divided by the outlet temperature of the plane plate solar hoarder that contains circular tubes placed on a flat plate, the outlet temperature of the V- grooves absorber plate solar collector that contains triangular tubes beside the grooves divided by the outlet temperature of the plane plate solar hoarder that contains circular tubes placed on a plane plate, the outlet temperature of the V- grooves absorber plate solar collector that contains triangular tubes over the grooves divided by the outlet temperature of the flat plate solar hoarder that contains circular tubes placed on a flat plate), ($T_{ot_{inside\ grooves}}/T_{oc}$, $T_{ot_{beside\ grooves}}/T_{oc}$, $T_{ot_{over\ grooves}}/T_{oc}$), and in four cases of flow (2,3,5,7) Lpm respectively. The results shows and as show in Figures (5.5),(5.6),(5.7) and(5.8) indicate that the ($T_{ot_{inside\ grooves}}/T_{oc}$) it was more efficient in heating water than the ($T_{ot_{beside\ grooves}}/T_{oc}$) that was more efficient in heating water than the ($T_{ot_{over\ grooves}}/T_{oc}$) and in

four cases of flow (2,3,5,7) Lpm respectively, Because in the first case($T_{\text{inside grooves}}/T_{\text{oc}}$) the triangular tubes were inside the grooves, which increases the contact between the triangular tubes and the grooves for two sides of the triangular tubes and the third side of the triangular tubes are exposed to sunlight directly. But in the second case ($T_{\text{beside grooves}}/T_{\text{oc}}$), one contact side between the triangular tubes and the V- corrugated absorber plate. But in the third case ($T_{\text{over grooves}}/T_{\text{oc}}$), the triangular tubes are in contact with the V- grooves absorber plate just in the two angles of the triangular tubes. While the case of circular tubes was placed on a flat plate without grooves, which reduces the surface area of the flat plate exposed to sunlight because it does not contain grooves. And that the fall of the sun's rays on the aluminum's plates used inside the solar collectors converts it into heat energy that is transmitted from the plates to the riser tubes used and through which the water is heated, the outlet temperature rises as soon as the solar collectors are turned on at 7:00am (with variations in the rise of the outlet temperature of the utilized collectors) and continues to rise until it achieves a constant state. The highest solar radiation fell on the solar collectors at 12:00 pm, as shown in fig. (5.1), and the steadiest state of the outlet temperature water for the solar collectors was two hours (1:00pm -3:00pm). This was the cause for the steady state of the outlet water. Because it takes an hour or more after the solar collectors' maximum incident solar radiation to reach steady state, the amount of heat exchange for the water consumed between the solar hoarders and the storage tanks, Because the outlet temperature of the water storage tanks is higher due to the high insulation level of the used water storage tanks and pipes and because of the gradual reduction in the amount of solar radiation, the outlet temperature of the solar collectors begins to decrease after steady state and continues to do so until the end of the workday at 5:00pm.

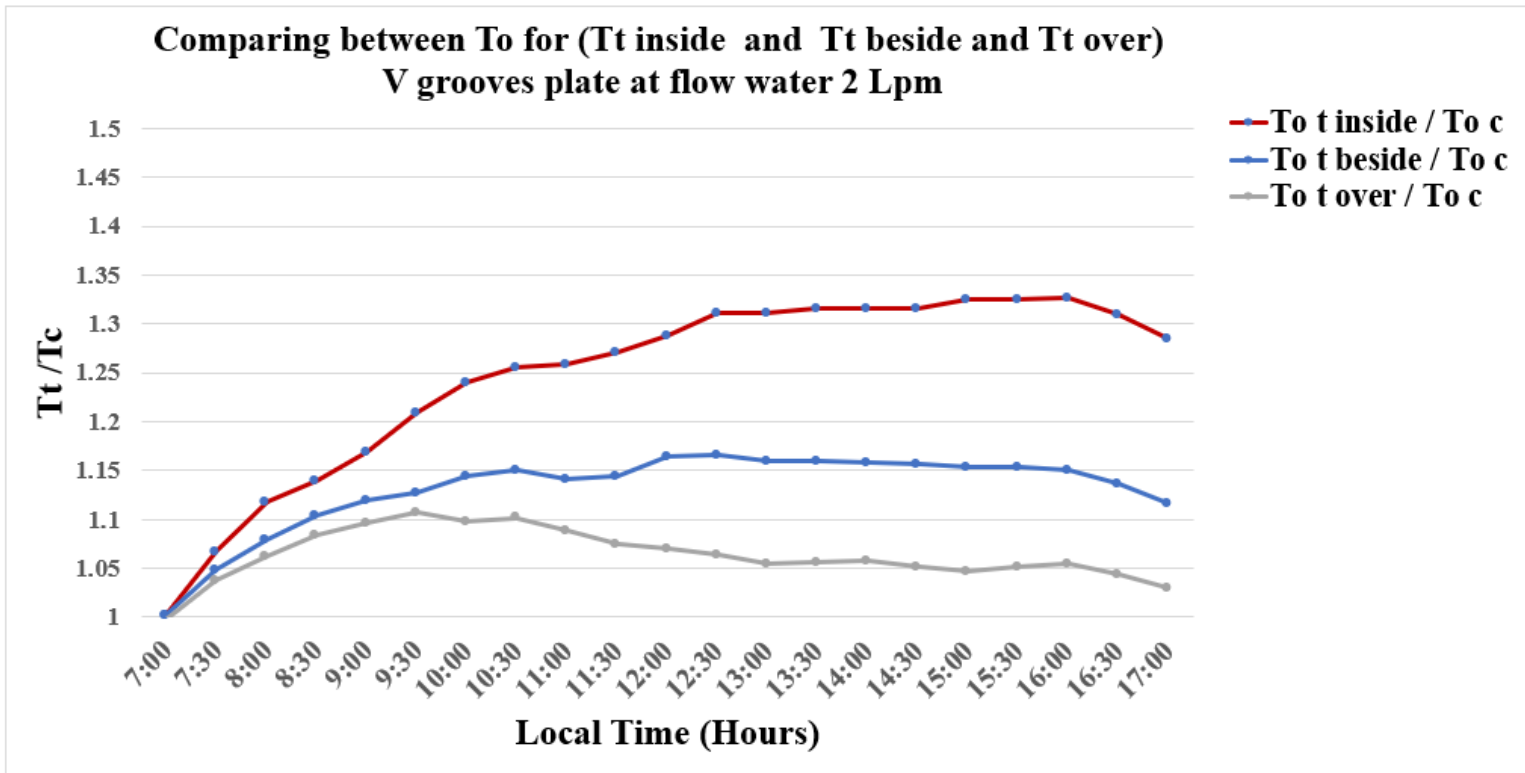


Fig. 5.5: Comparing between To for (Tt_{inside} , Tt_{beside} ,Tt_{over}) V grooves plate at flow water 2 Lpm

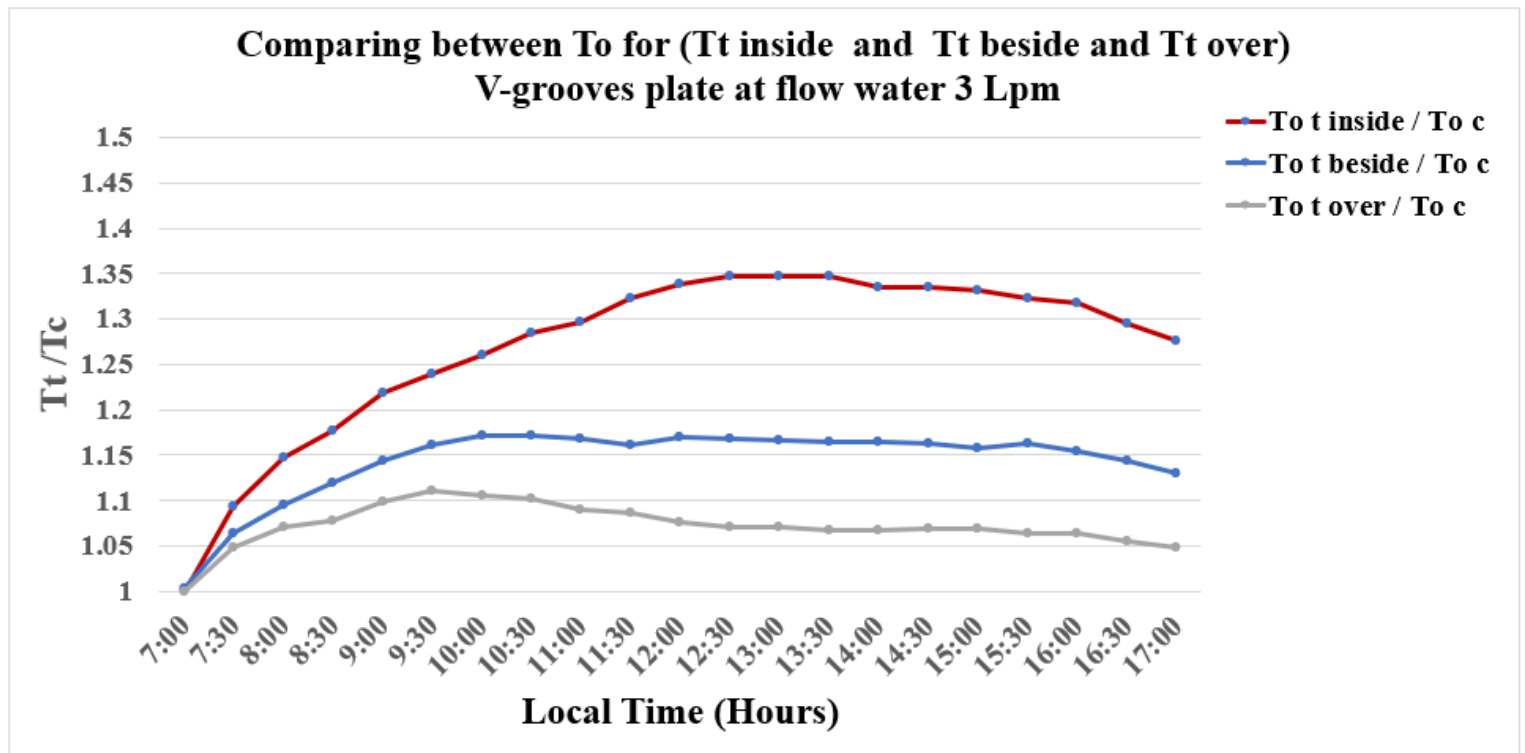


Fig. 5.6: Comparing between To for (Tt_{inside} , Tt_{beside} ,Tt_{over}) V grooves plate at flow water 3 Lpm

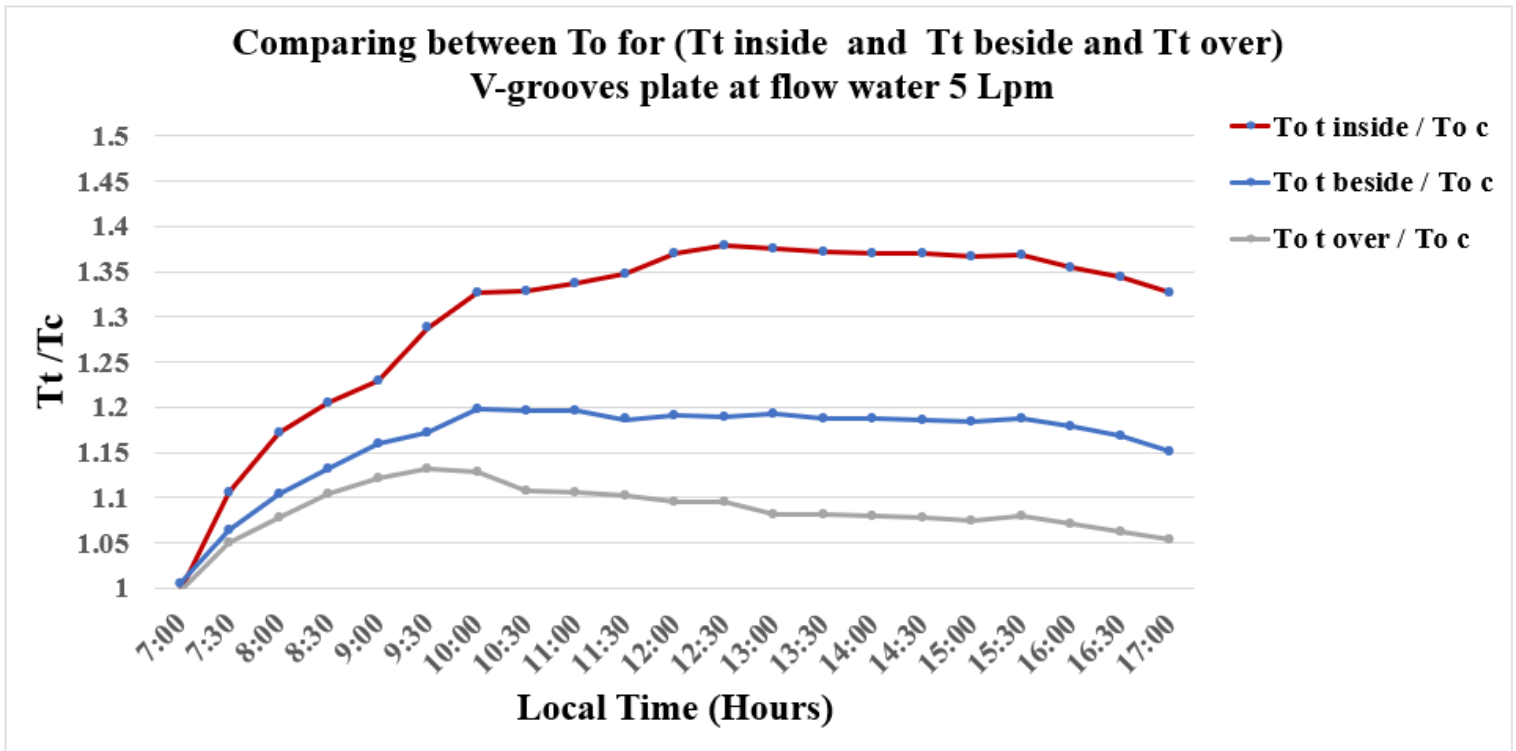


Fig. 5.7: Comparing between To for ($T_{t_{inside}}$, $T_{t_{beside}}$, $T_{t_{over}}$) V grooves plate at flow water 5 Lpm

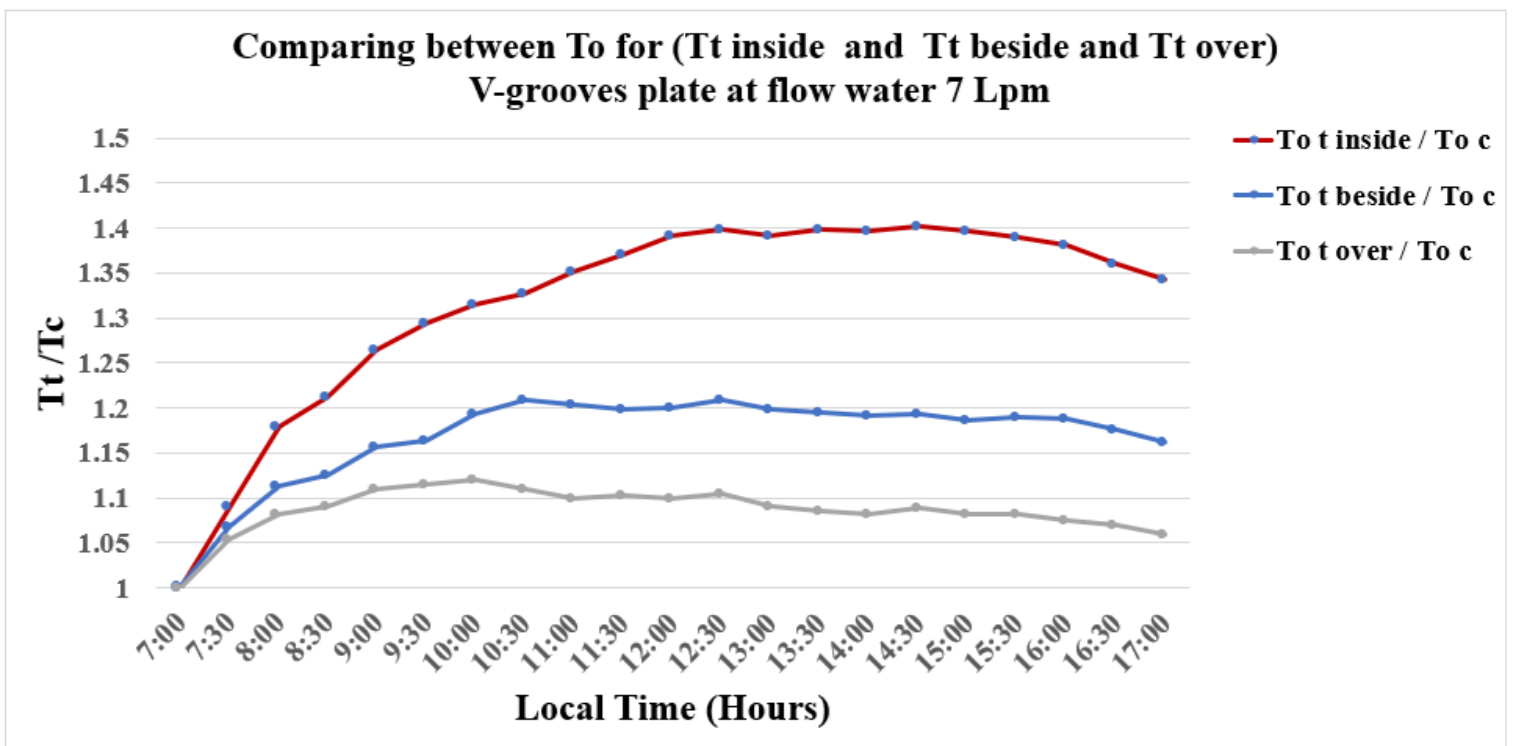


Fig. 5.8: Comparing between To for ($T_{t_{inside}}$, $T_{t_{beside}}$, $T_{t_{over}}$) V grooves plate at flow water 7 Lpm

5.5 The results of temperature difference

The difference in temperature between the outlet and inlet of the water is affected by the flow rate of the work fluid. Figures (5.9) to (5.12) show the difference in the temperature of the water outlet, where its outlet has four volumetric flow rates (2,3,5 and 7 LPM), It was found that the reduction in the stream rate leads to an increase in the water temperature difference between the outlet and the inlet, because the transmission of heat from the tube to the liquid takes time, as at low flow rates it leads to a decrease in the speed of the liquid and thus to the absorption of more solar energy in order to increase the temperature. The maximum temperature difference was (10.8 C°) at (2 LPM) as shown in the figure (5.9) Where the difference in temperature increased approximately at (12:00 PM) and decreased after that, the figures (5.9) to (5.12) indicate a difference in the outlet and inlet temperatures of the tubes (triangular tubes inside the grooves, triangular tubes beside the grooves, triangular tubes over the grooves and circular tubes placed on the flat plate) at volumetric flow rates (2,3,5 and 7 LPM), where The maximum difference in temperature was 10.8 C°, 8 C°, 6.5 C° and 5 C° of triangular tubes inside the grooves, at (2,3,5 and 7 LPM) respectively.

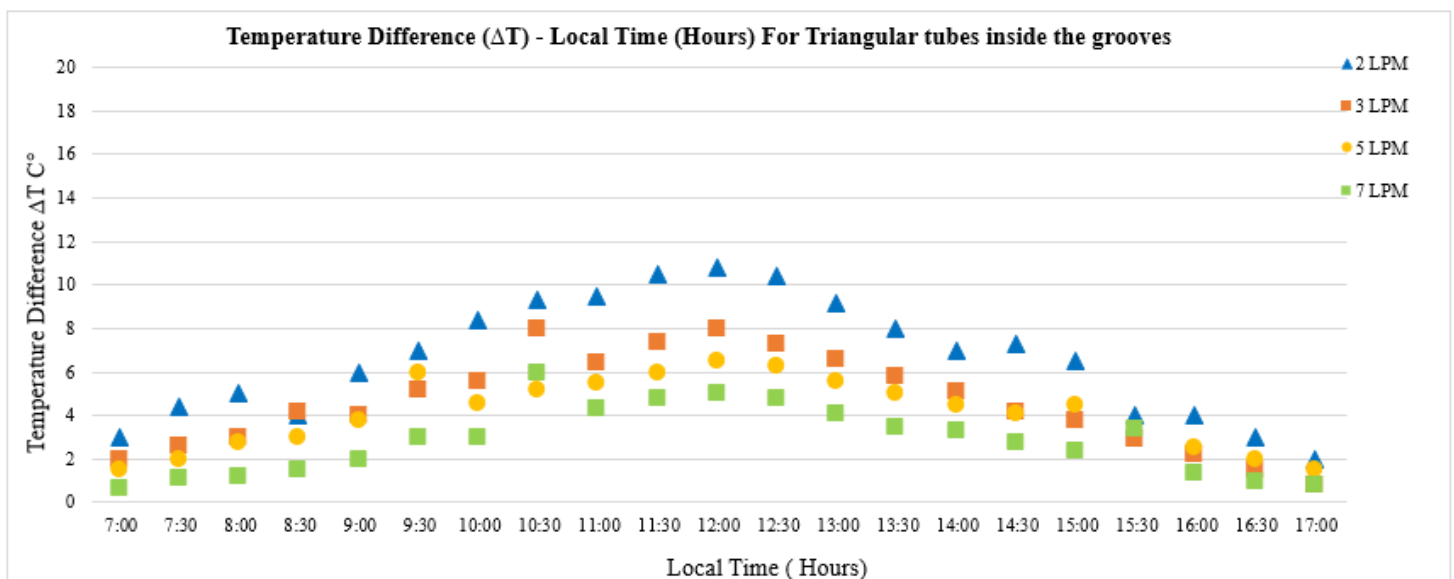


Fig. 5.9: Temperature Difference for Triangular tubes inside the grooves

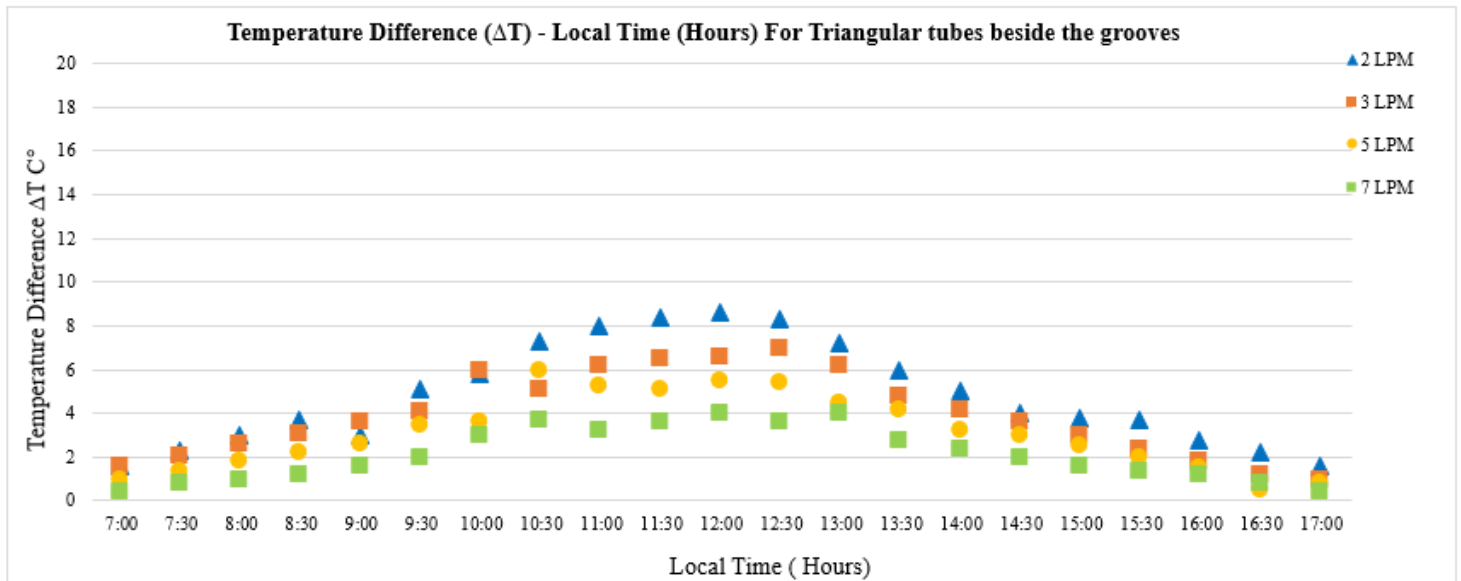


Fig. 5.10: Temperature Difference for Triangular tubes beside the grooves

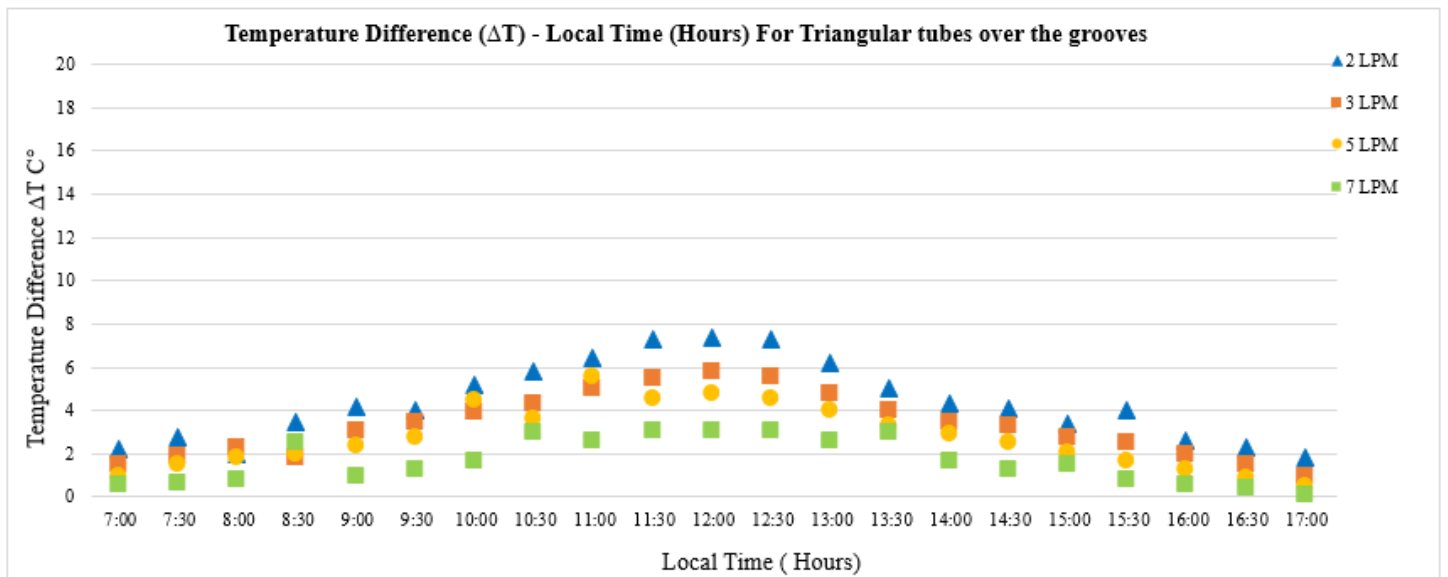


Fig. 5.11: Temperature Difference for Triangular tubes over the grooves

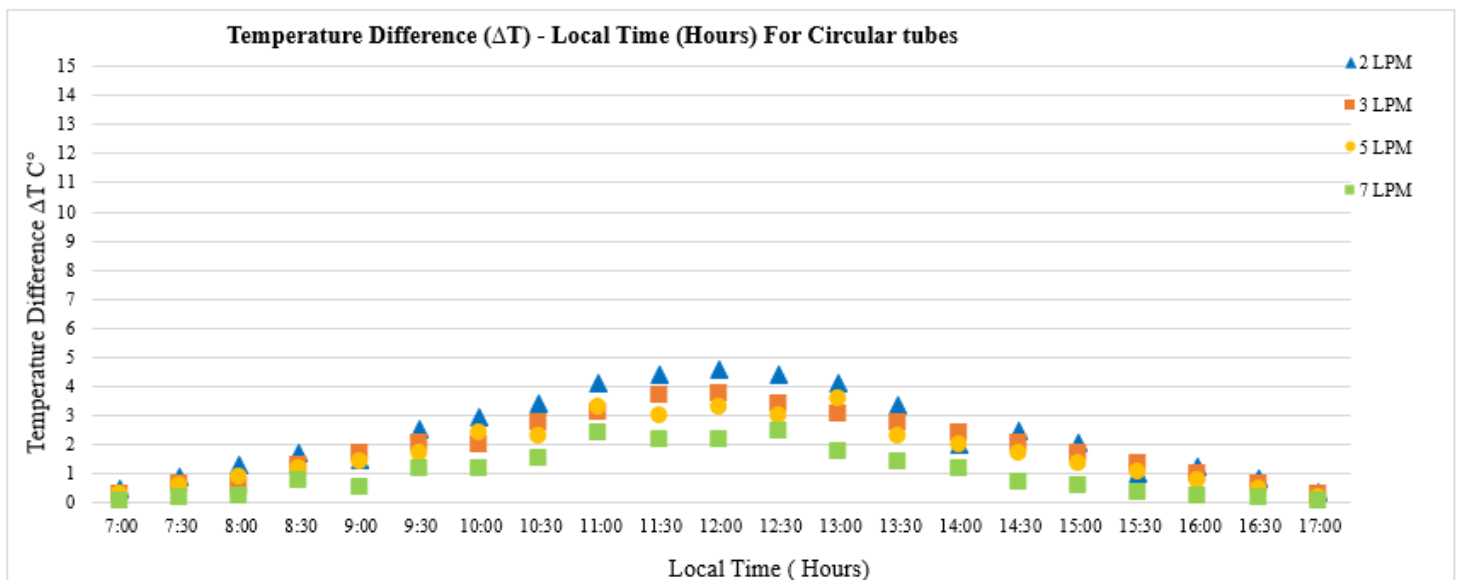


Fig. 5.12: Temperature Difference for Circular tubes

5.6 The heat transfer variation

In this section, the variation of heat transfer in term Nusselt Number(Nu) with Local Time and variation of Nusselt Number(Nu) with Reynolds number is shown in order to reveal the effect of four types of tubes (triangular tubes inside the grooves, triangular tubes beside the grooves, triangular tubes over the grooves and circular tubes) on heat transfer in term Nusselt Number, the figures (13) to (16) show the variation of Nusselt number in four types of tubes with local time, the maximum heat transfer rates in the triangular riser tube that placed inside the grooves and the triangular riser tube that placed beside the grooves and the triangular riser tube that placed over the grooves with respect to circular riser tubes that placed on the flat plate at four flow rates (2,3,5 and 7PM). The figures (13) to (16) also show that the rate of heat transfer of triangular tubes inside the grooves is greater than the rate of heat transfer of triangular tubes beside the grooves, and it is greater than the rate of heat transfer of triangular tubes over the grooves, and it is greater than the rate of heat transfer of circular tubes, because the contact area between triangular tubes and the V- grooves absorber plate is greater than the contact area between circular tubes and flat plate, and the surface area exposed to radiation The solar of the V- grooves absorber plate is greater

than the surface area of the flat plate. The figure (17) shows that the Nusselt (Nu) obtained from the (triangular tubes inside the grooves, triangular tubes beside the grooves and triangular tubes over the grooves) tends to be higher than the one obtained from the circular tubes on flat plate with respect to circular tubes laminar flow for $500 < Re > 1900$, where the Nusselt Number in the triangular riser tubes inside the grooves enhanced to 30%, 35.5%, 40% and 52.7% with respect to circular tube at laminar flow for $500 < Re > 1900$.

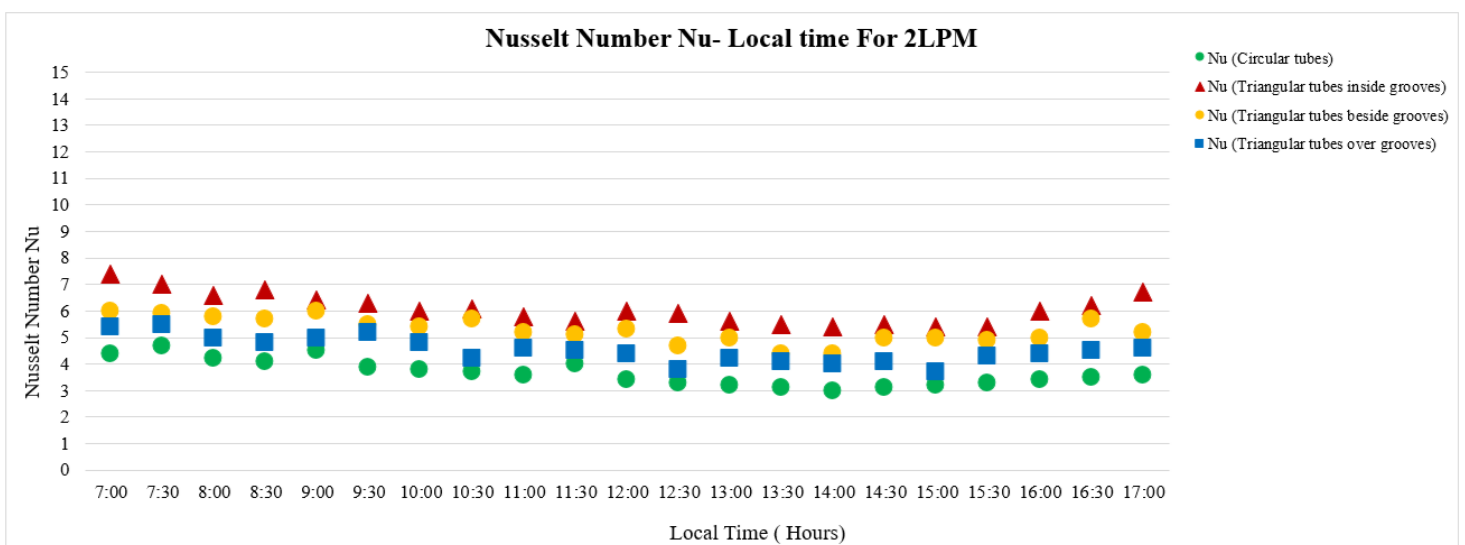


Fig. 5.13: The variation of Nusselt Number with local Time For 2L/min.

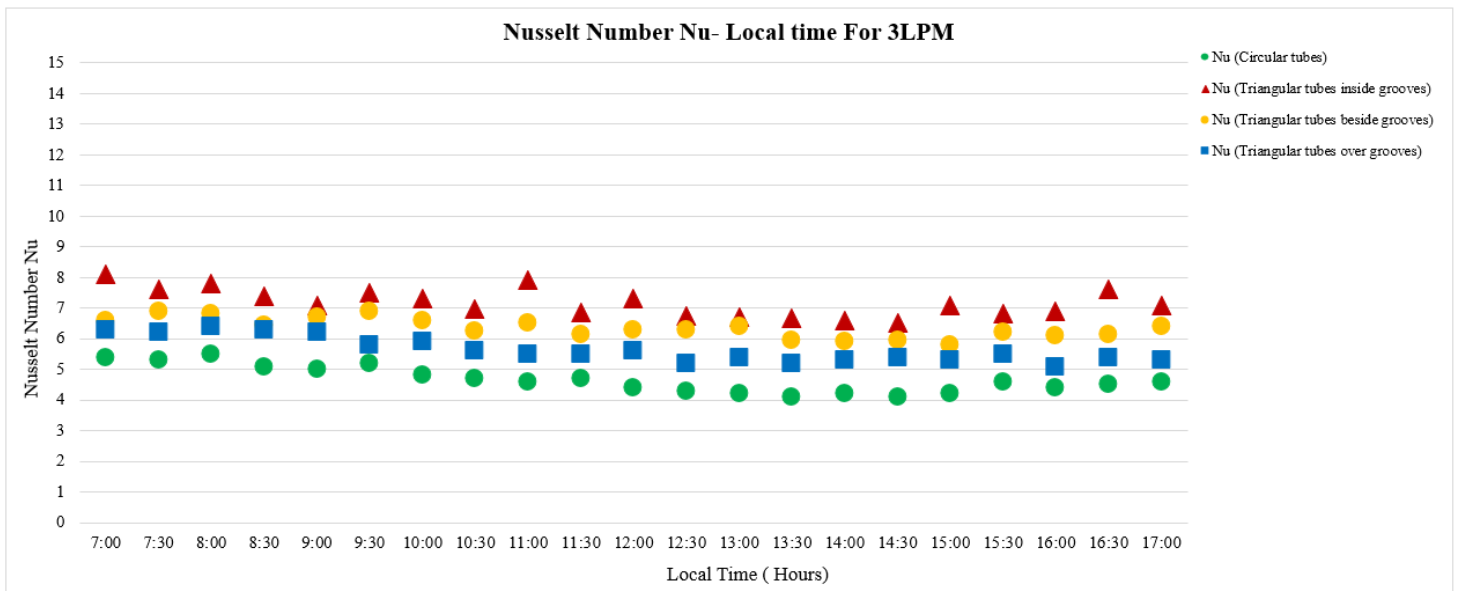


Fig. 5.14: The variation of Nusselt Number with local Time For 3L/min.

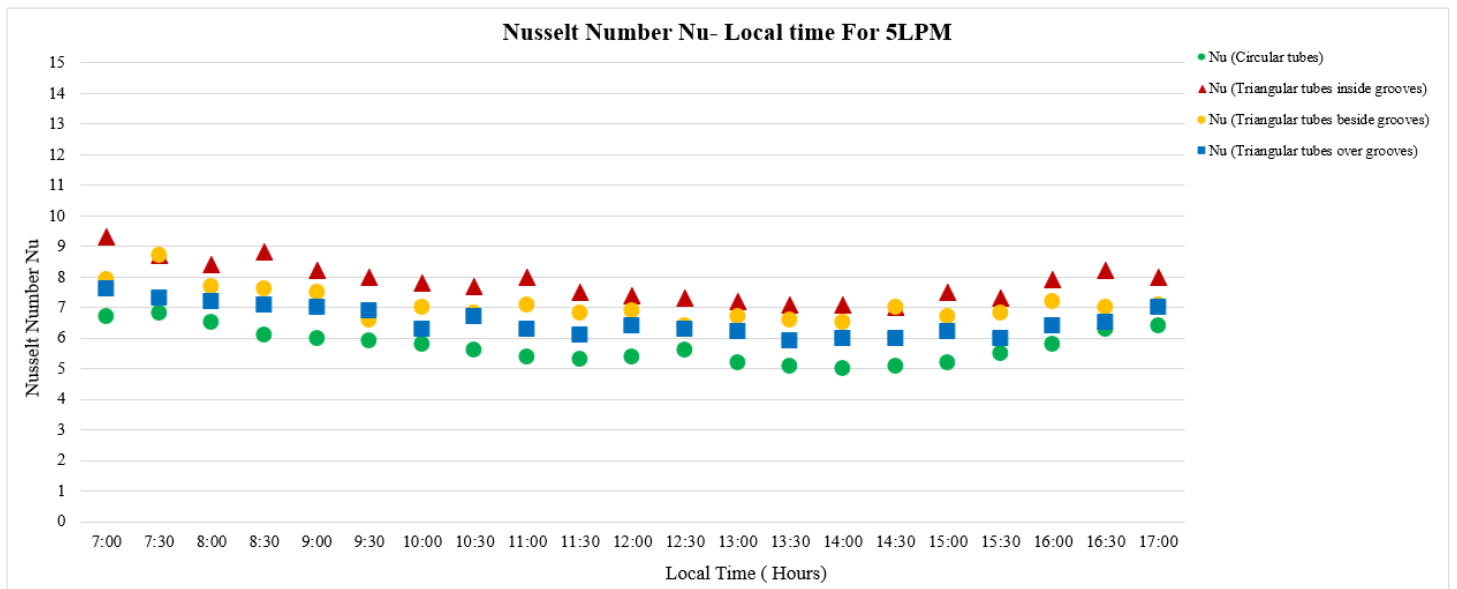


Fig. 5.15: The variation of Nusselt Number with local Time For 5L/min.

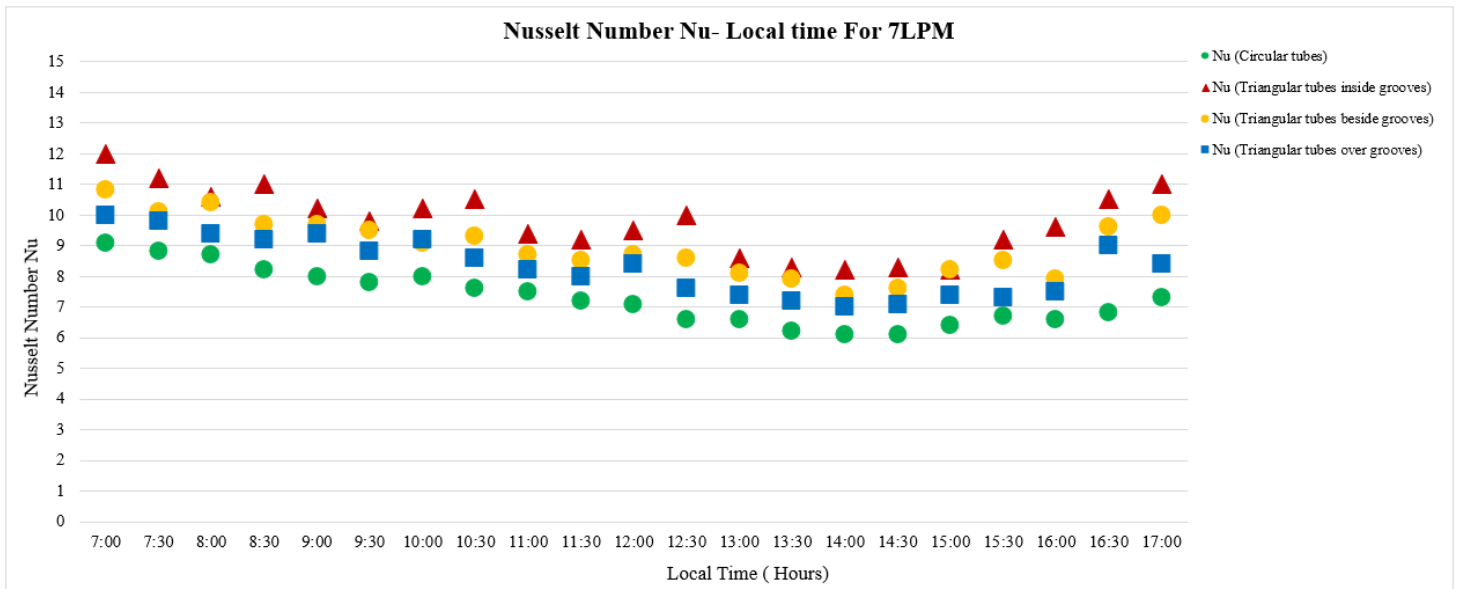


Fig. 5.16: The variation of Nusselt Number with local Time For 7L/min.

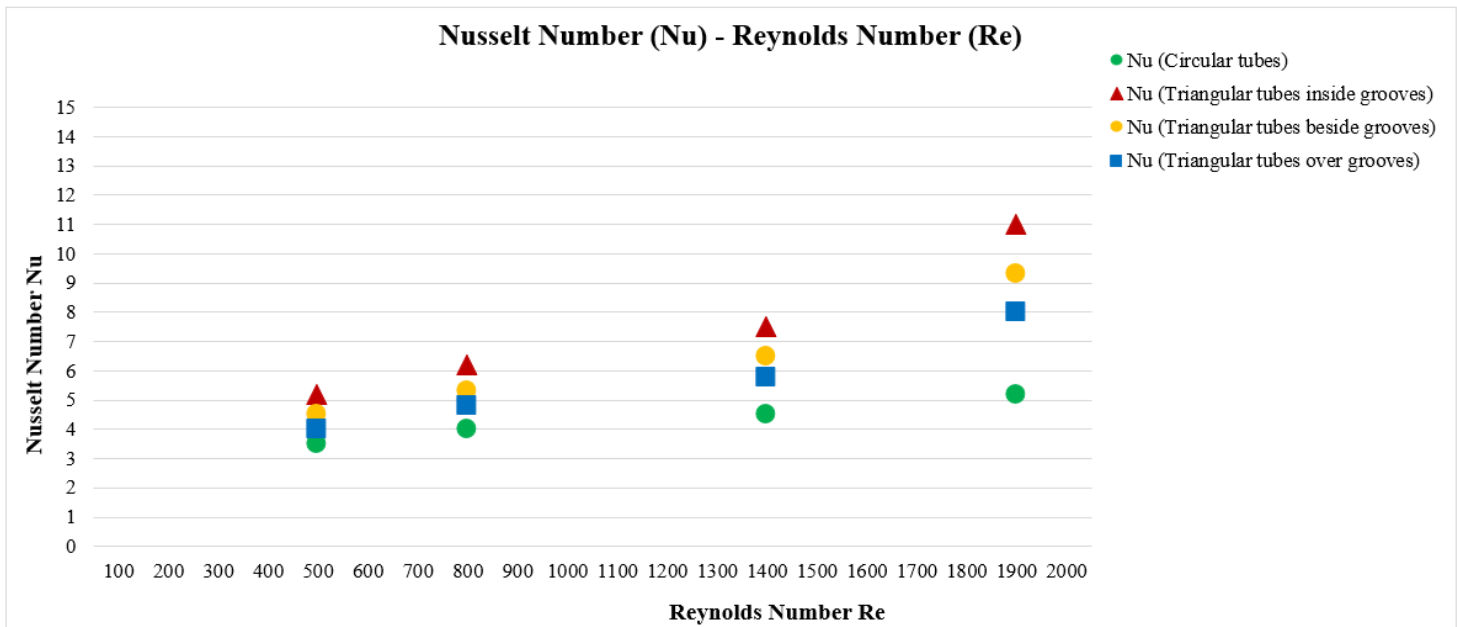


Fig. 5.17: Nusselt number (Nu) variation with Reynolds Number Re for (circular tubes, triangular tubes inside the grooves, triangular tubes beside the grooves and triangular tubes over the grooves)

5.7 The Results of pressure loss

In terms of friction factor (f) the effect of three types of triangular tubes used (triangular tubes _{inside the grooves} , triangular tubes _{beside the grooves} and triangular tubes _{over the grooves}) on the change in pressure (Δp) was represented and compared to the circular tube, the application leads to an increase in the friction factor compared to the circular tube with a decrease in Reynolds number (Re) , enhances the use of Triangular tube heat transfer surface area and increases friction and turbulence due to the angles of the triangle, which causes a decrease in pressure. Figures (5.18) to (5.21) show the variation of the friction factor with the local time of the (triangular tubes _{inside the grooves}, triangular tubes _{beside the grooves} and triangular tubes _{over the grooves}) and the circular tubes used, with four flow rates (2,3,5 and 7 LPM) The figure (5.18) show the variation of the friction factor (f) with Reynolds number Re , the figures (5.18) to (5.21) show the friction factor associated with triangular tubes and its comparison with circular tubes and with four volumetric flow rates (2,3,5 and 7 LPM) for the local time from 7:00 am to 5:00 pm ,The friction factor was higher with triangular tubes placed inside grooves compared with other circular and triangular tubes. The effect of triangular tubes on the coefficient of friction shown in the figure (5.22), the coefficient of friction increases with the decrease of Reynolds number, and the maximum friction factor is created in triangular tubes compared to circular tubes, the friction factor (f) in triangular tubes is about 13%-20% above circular tubes.

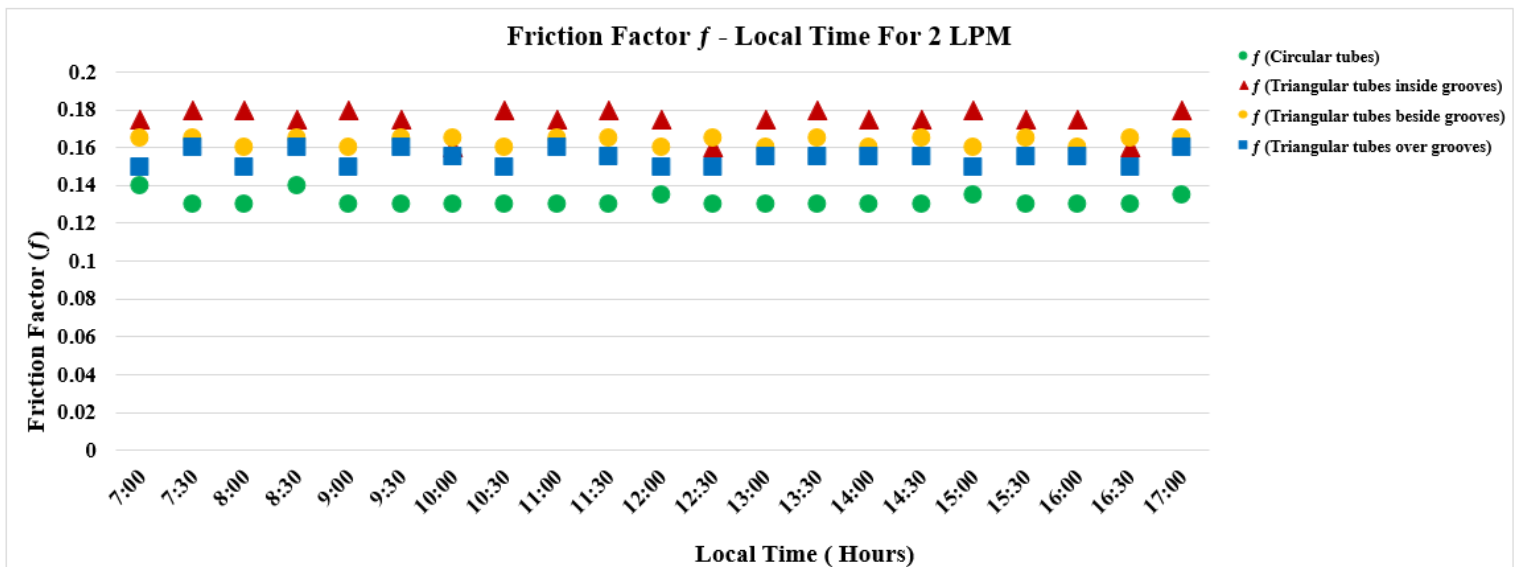


Fig. 5.18: The Friction Factor variation with Local Time For 2 LPM

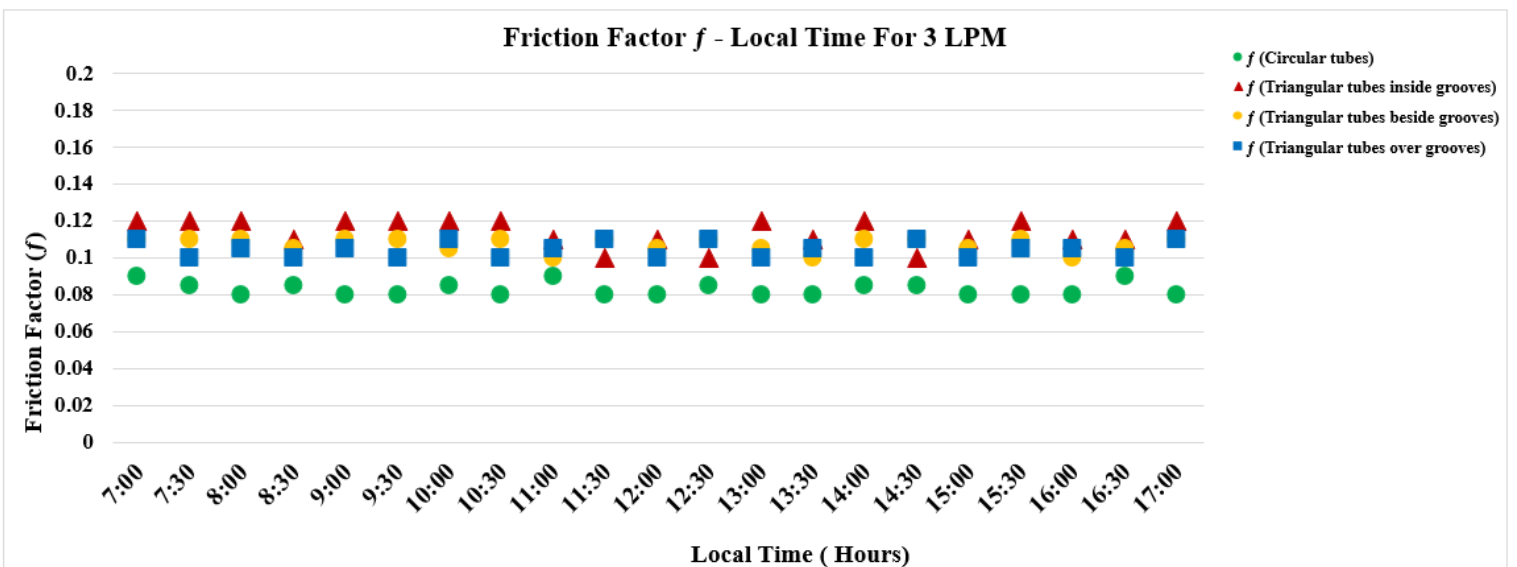


Fig. 5.19: The Friction Factor variation with Local Time For 3 LPM

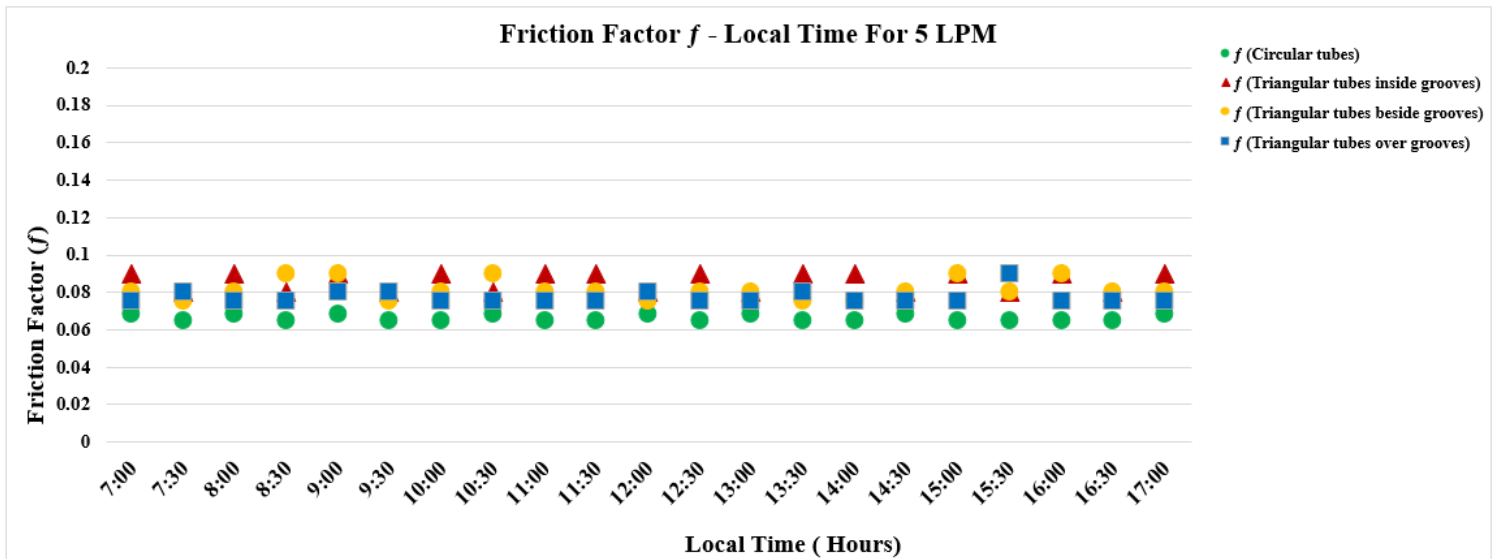


Fig. 5.20: The Friction Factor variation with Local Time For 5 LPM

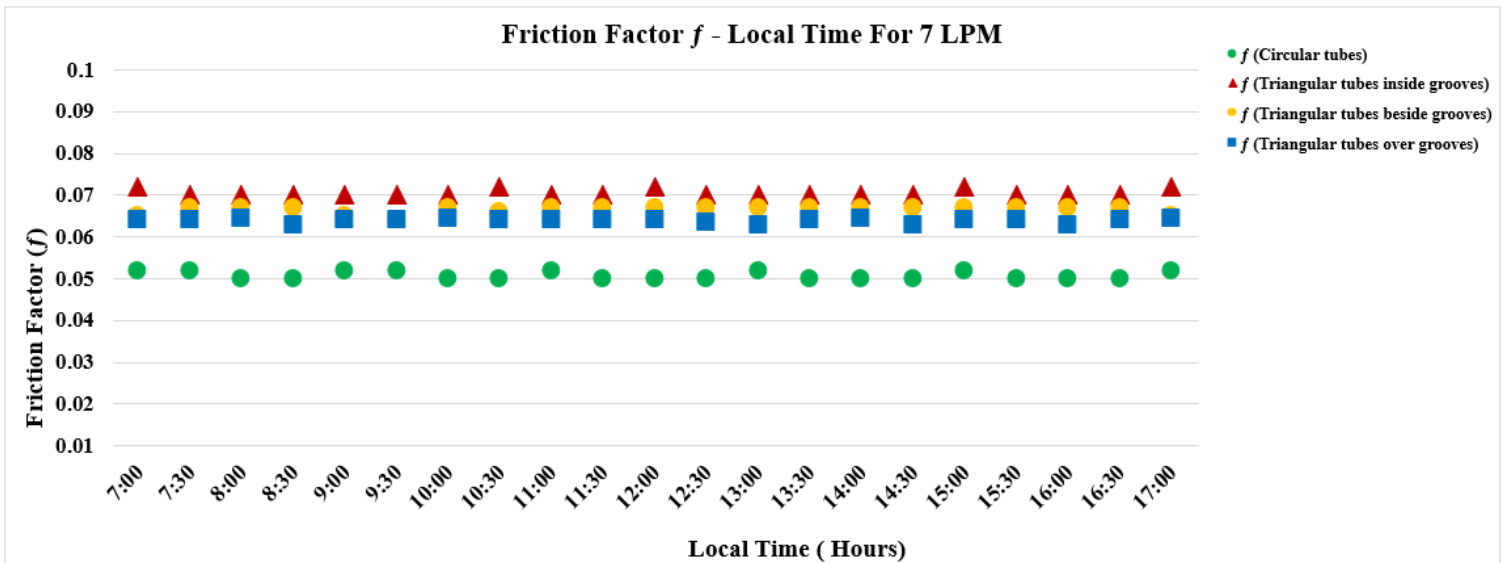


Fig. 5.21: The Friction Factor variation with Local Time For 7 LPM

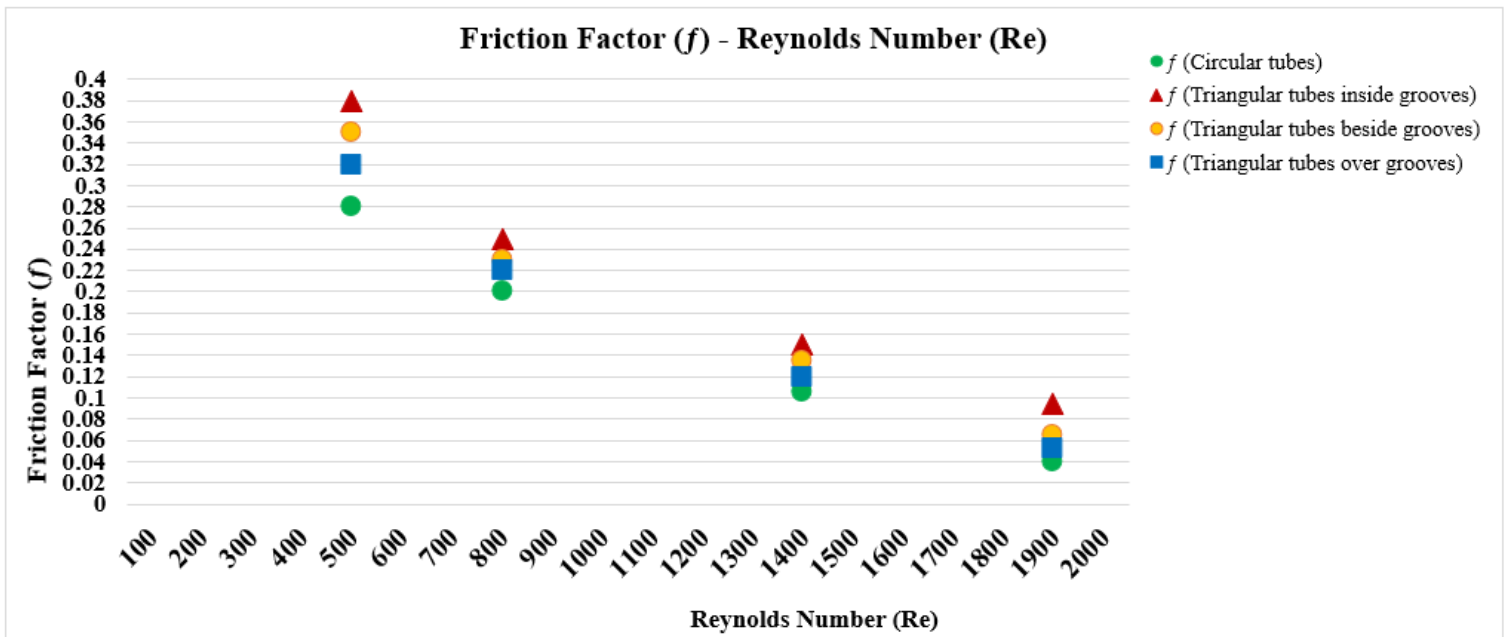


Fig. 5.22: The Friction Factor variation with Reynolds Number Re for (circular tubes, triangular tubes inside the grooves, triangular tubes beside the grooves and triangular tubes over the grooves)

5.8 Thermal Performance factor TPF

The heat transfer rate and friction factor are calculated simultaneously for circular and triangular tubes under the same conditions and with the same pumping power in equation 3.35. The thermal performance factor (TPF) illustrates the practical benefit derived from this equation. Triangle and circular tube thermal performance coefficients are shown in Figures (5.23) to (5.26) with local time and four volumetric flow rates (2,3,5,7 LPM). The fluctuation of the thermal performance factor of circular and triangular tubes with Reynolds number is depicted in Fig. 5.27. Figures (5.23) to (5.26) demonstrated that the thermal performance factors (TPF) for triangle-shaped tubes that were placed inside grooves, next to grooves, and over grooves were higher than those for circular tubes. The thermal performance of the triangular tubes in the grooves is higher than that of the other used tubes with the same pumping force, as shown in Fig. (5.27). This is due to the larger thermal contact area between the triangular tubes

inside the grooves and the plate used as well as the additional fluid turbulence, as well as the better fluid mixing, which results in higher heat transfer rates, The maximum thermal performance factor of the triangular tubes inside the grooves was 1.8.

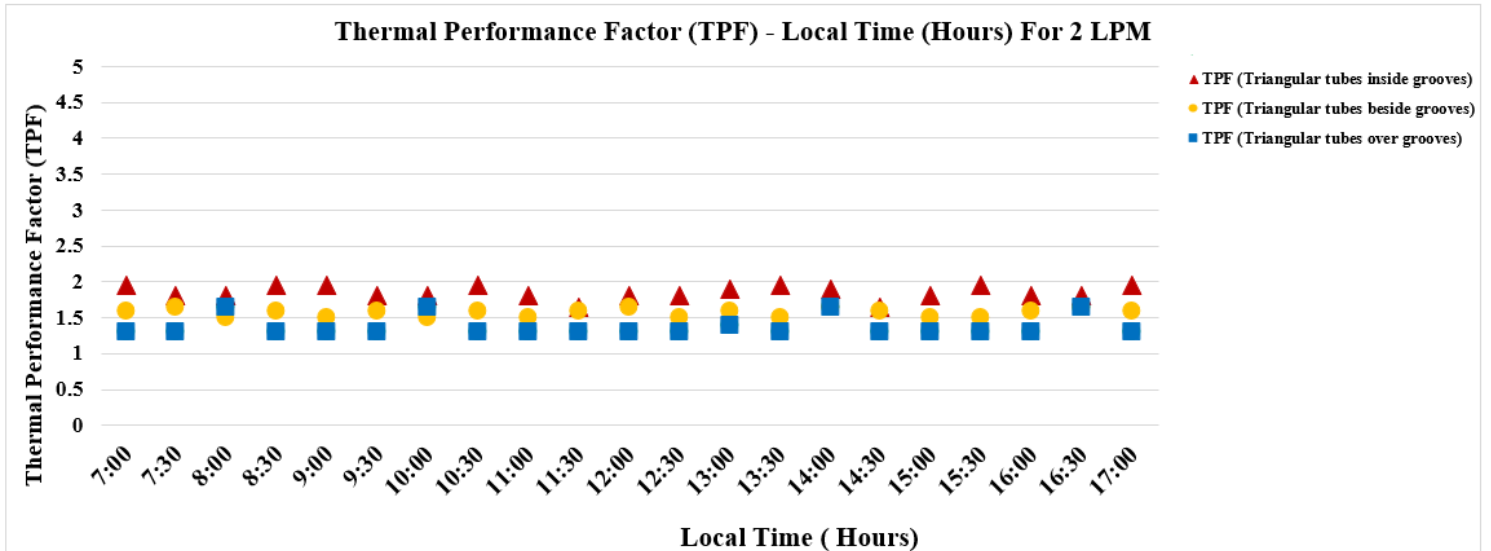


Fig. 5.23: Thermal Performance Factor (TPF) with Local Time For 2LPM.

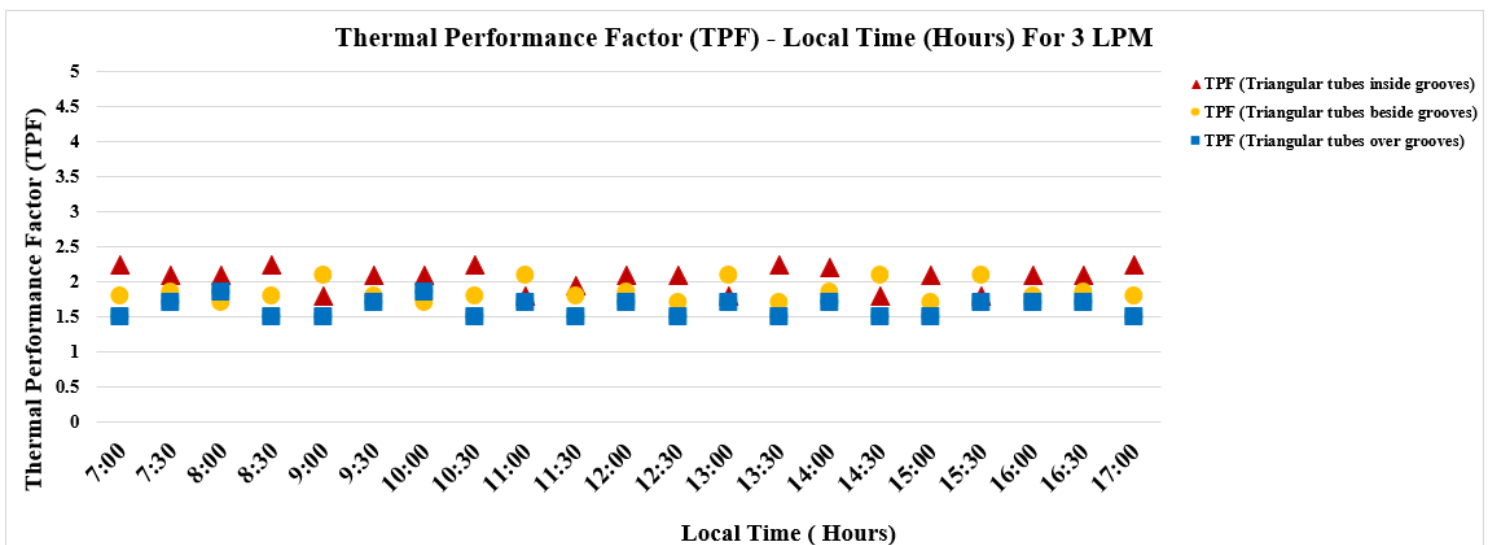


Fig. 5.24: Thermal Performance Factor (TPF) with Local Time For 3LPM.

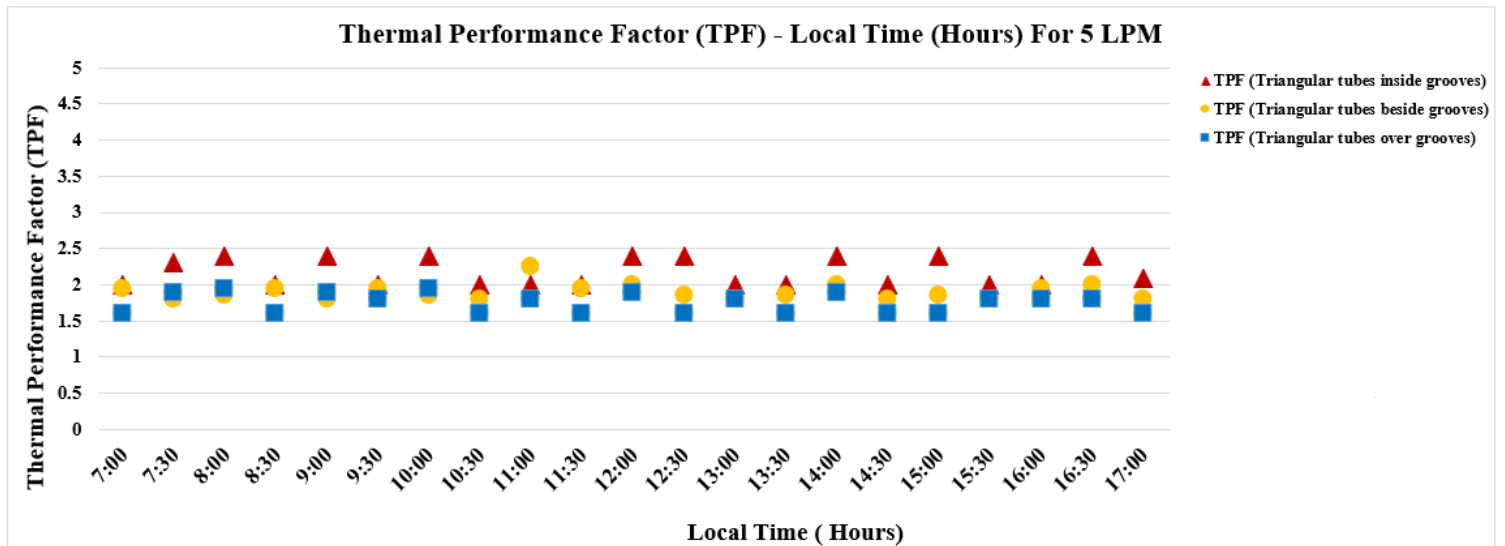


Fig. 5.25: Thermal Performance Factor (TPF) with Local Time For 5LPM.

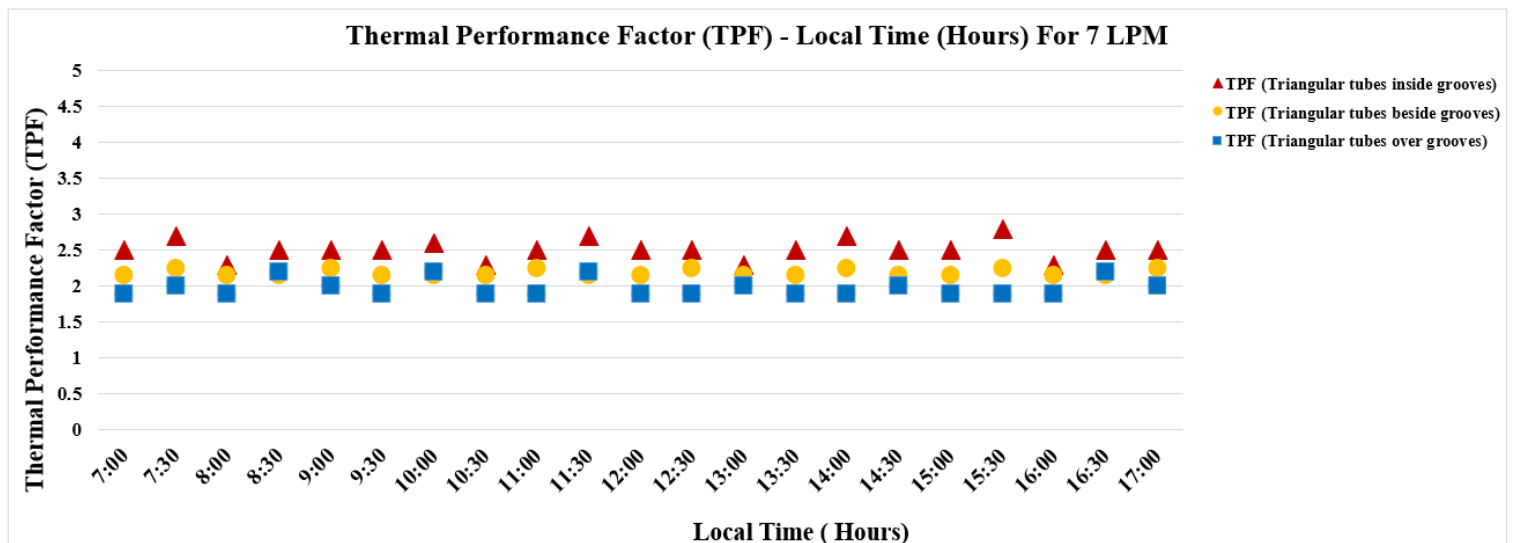


Fig. 5.26: Thermal Performance Factor (TPF) with Local Time For 7LPM.

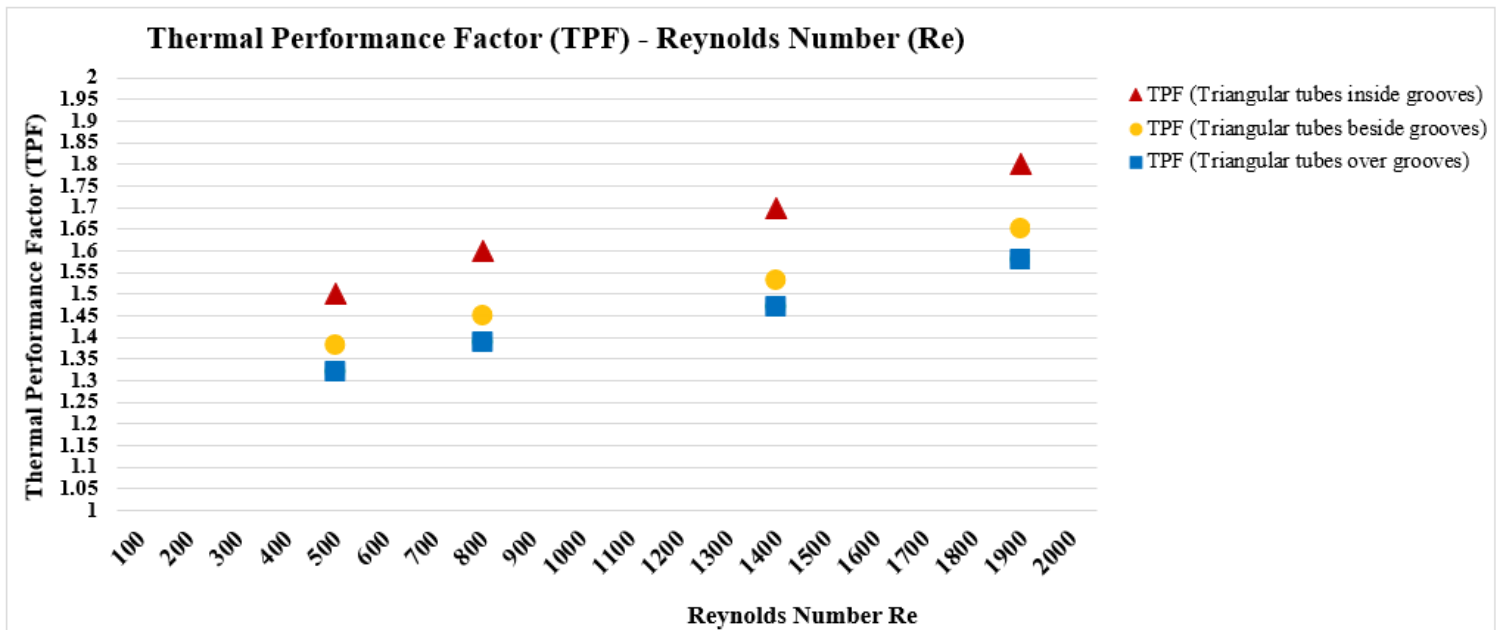


Fig. 5.27: Thermal Performance Factor with Reynolds Number Re for triangular tubes inside the grooves, triangular tubes beside the grooves and triangular tubes over the grooves)

5.9 Collector efficiency

Fig. (5.28) shows the effect of tubes (triangular tubes inside the grooves, triangular tubes beside the grooves, triangular tubes over the grooves and circular tubes placed on the flat plate) on the efficiency of the solar collector with Reynolds number. The figure shows the maximum efficiency (η) in the triangular tubes placed inside the grooves at a constant pumping force and a steady state. This is the fact that the tubes placed inside the grooves have the largest contact between the triangular tubes and the grooves of the V- grooves absorber plate, which ensures greater thermal conductivity between the V-grooves absorber plate and the triangular tubes inside the grooves, and because the surface area of the V-grooves absorber plate is greater than the surface area of the flat plate because it contains grooves, This increases the amount of solar radiation falling on it, which is converted into thermal energy, which is transmitted by triangular riser tubes to the water used inside them. In addition to the greater friction in triangular tubes than circular tubes, which leads to maximum efficiency. The maximum efficiency 53.4 % was found for the triangular tubes inside the grooves.

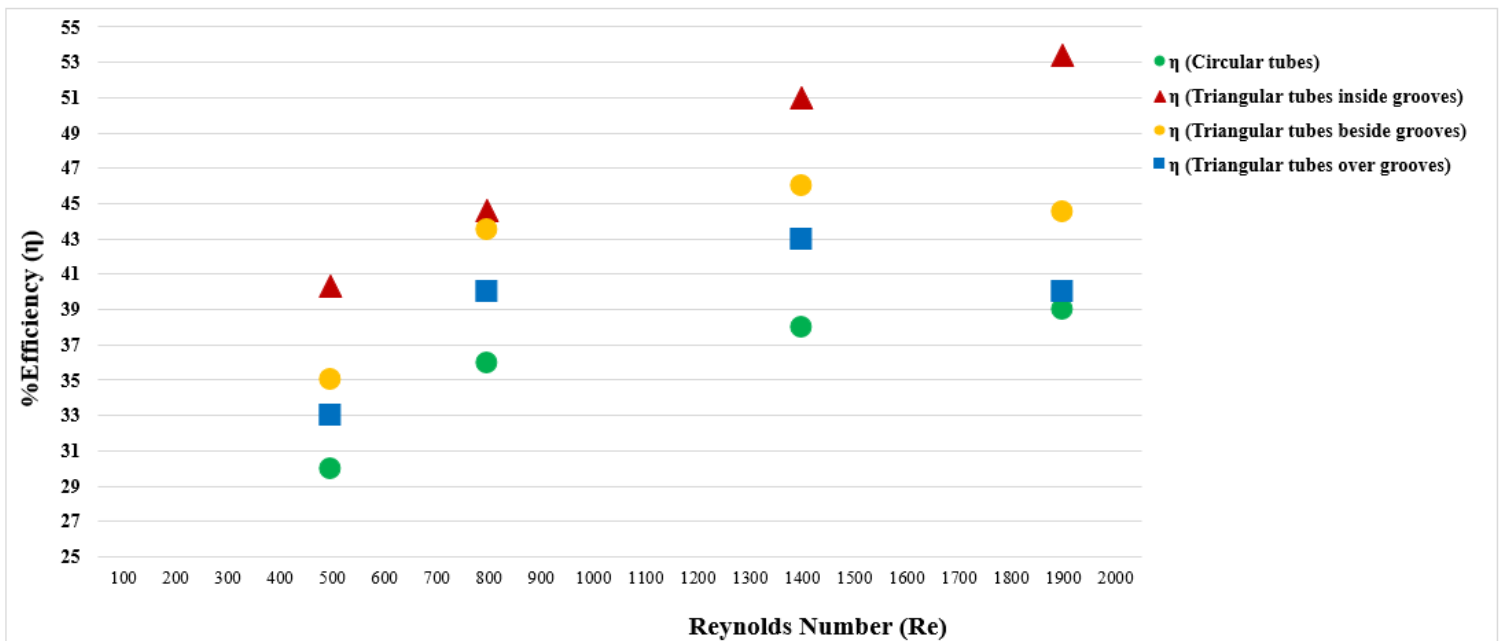


Fig. 5.28: the efficiency of solar collector with Reynolds number Re for (triangular tubes inside the grooves, triangular tubes beside the grooves, triangular tubes over the grooves and circular tubes placed on the flat plate)

5.10 Compare the results obtained with the results of previous research

The comparing with a previous search and in similar circumstances, that includes title (study the effect of using different types of twisted tapes on thermal performance in solar collector). The study included the researcher used different types of twisted tapes inside the tubes of the solar collector. and studied experimentally the effect of the use of twisted aluminum strips as turbulence promoters on the heat transfer rate in terms of the Nusselt number (Nu), pressure loss in terms of friction factor(f), thermal performance factor TPF and the efficiency (η) of a flat plate solar collector. This research focuses on the process of energy conversation under steady state conditions in the laminar flow regime and uses distilled water as the working fluid. The experimental side consists of the manufacture of a flat plate solar collector and four different types of twisted tapes with vortex generators (VG) in twist ratio $Y=2$ (twisted tape with curvature vortex generator in front flow TTFF, twisted tape with curvature vortex generator in opposite flow TTOF, twisted tape with straight vortex generator TTS and typical twisted tape TT), dimensions of the vortex generator 2mm high and 1mm thick. The measuring instruments used in this experiment were solar irradiance meter, volumetric flow meter, manometer, temperature record meter, and temperature sensors. The experiments are carried out in Babal, Iraq with latitude

32° ,13',27 N and longitude 44° ,22',36 E, the volumetric flow rates used are (7, 5,3 and 1.5) L / min and the number of Reynolds varies between 400 and 2000. The experimental result showed that the decrease in flow rate was found to increase the difference in water temperature between the outlet and the inlet of tubes fitted with twisted tape, the higher difference in temperature was (18.3 ° C) in tubes fitted with TTFF at volumetric flow rate 1.5 L / min and at the same time the maximum outlet temperature of the fitted tube (TTFF) was 98 ° C 1.5 L / min . In addition , heat transfer in term Nusselt number(Nu) and pressure loss in term friction factor (f) improved compared to other cases in the tube fitted with (TTFF), the Nusselt Number in tube fitted with (TTFF) enhanced to 31%,38.2%,40% and 54.2% with respect to plain tube at laminar flow for Reynolds Number Re ranges from 400 to 2000 respectively and the friction factor increases as the Reynolds number Re decreases and the higher friction factor is achieved in the tube equipped with (TTFF, TTOF and TTS) compared to the (TT) and smooth tube, the friction factor (f) in the tube equipped with TTFF increases by about 18% to 30% above the plain tube. The experimental results also showed that the TPF thermal performance factor for TTFF was higher than the other twisted tapes with the same pumping capacity, the maximum thermal performance factor was 1.4 and the maximum efficiency of the TTFF tube was 64.7%. From this conclude that the results obtained through the experimental study the effect of triangular cylinder with V-grooves absorber on performance of solar collector are similar to the results obtained from this research

CHAPTER SIX

CONCLUSIONS AND RECOMMENDATIONS

Chapter Six

Conclusions and Recommendations

The aim of this research was to study the effect of triangular tubes on the efficiency of solar collectors using a V- corrugated absorber plate and in three cases (the triangular tubes inside the grooves, the triangular tubes beside the grooves and the triangular tubes over the grooves), for the laminar flow regime ($500 < Re < 1900$).) under stable conditions and constant pumping power, at different volumetric flow rates(2, 3, 5 and 7) LPM and study the effect on heat transfer rates and pressure loss. This chapter summarizes the main conclusion of this study, and suggestions for further research are mentioned.

6.1 The conclusions

The study arrived at the main following conclusions:

1. The temperature difference between the outlet and the inlet decreased with the increase in the volumetric flow rate of water (2,3,5 and 7 LPM) respectively, because the greater the volumetric flow velocity of water, the period of passage of water inside the riser tubes is faster, and this reduces the volume of heat exchange between the water and the pipes. The riser through which the water passes. The maximum temperature difference achieved for triangular tubes inside the grooves was 10.8°C , 8°C , 6.5°C and 5°C for volume flow rates (2,3,5 and 7 LPM) respectively.
2. The water outlet temperature of the solar collector, which contains triangular tubes placed inside the grooves, increases more than the outlet water temperature of the triangular tubes placed beside the grooves, which in turn is greater than the outlet water temperature of the triangular tubes placed over the grooves, and the previous three cases of triangular tubes in which the outlet temperature is greater than the outlet temperature of the circular tubes, because the contact area between

the triangular tubes and the V- grooves absorber plate is larger than the contact area between the circular tubes and the flat plate used, and the surface area of the V- grooves absorber plate is greater than the surface area of the flat plate due to It contains grooves. The maximum outlet temperature of the triangular tubes placed inside the grooves was (89 C°), while the maximum outlet temperature of the triangular tubes placed beside the grooves is (78 C°), and the maximum temperature of the tubes placed over the grooves is (73 C°), and the outlet temperature of the circular tubes placed on the flat plate is (58 C°), in the following water flows (7,5,3 and 2 L/min).

3. Triangular tubes inside the grooves usually amplified the heat transfer rate in term Nu, because the contact area between the triangular tubes inside the grooves is larger than the interaction area between the other triangular tubes and the V- grooves absorber plate used (Triangular tubes beside the grooves, Triangular tubes over the grooves), as well as for the circular tubes. the solar collector that contains triangular tubes placed inside the grooves achieved the maximum heat transfer rate compared to the solar collector that contains circular tubes, where the Nusselt Number in the triangular riser tubes inside the grooves enhanced to 30%,35.5%,40% and 52.7% with respect to circular tube at laminar flow for Reynolds Number Re ranges ($500 < Re < 1900$) respectively
4. The pressure drop in the triangular tubes was higher than that of the circular tubes due to the difference in the shape of the tubes and its containment of the angles of the triangular tubes, the friction coefficient in the triangular tubes was greater than the circular tubes, where the friction factor increased about 15% - 25% with an increase in the Reynolds number of Re
5. Thermal performance factor (TPF) in the triangular tubes inside the grooves was higher than the circular tubes because the contact area between the triangular tubes and the V- grooves plate is greater than the contact area between the circular tubes and the flat plate, as well as because of the different shapes of the tubes and the triangular tubes containing the corners, which increases the water turbulence and the maximum TPF for the triangular tubes was 2.6

6. The fact that the triangular tubes inside the grooves have a larger contact area with the V- grooves absorber plate from the contact area of the circular tubes with the flat plate, and the V- grooves absorber plate has a larger surface area than the flat plate because it contains the grooves, and this increases the solar falling on it, which increases the efficiency of the solar collector. also increase the pressure of the fluid due to the angles of the triangular tubes, which ensures better mixing of the fluid which increases the heat transfer rate leading to increased collector efficiency. The maximum efficiency was 53.4 % in the triangular riser tubes inside the grooves at persistent impel relation and laminar flow regime ($500 < Re < 1900$).

6.2 The recommendations

Next are the recommendations for future work:

1. Investigating the effect of triangular tubes on the performance of the solar collector by using water and nanofluids as a working fluid.
2. Studying the effect of triangular tubes on the thermal performance of a solar collector in different flows
3. Using different shapes of riser tubes and study the performance effects of the solar hoarder
4. performance Investigation the V- corrugated absorber plat on the solar collector

REFERENCES

References

- [1] “Index,” in *Solar Energy Engineering*, Elsevier, 2009, pp. 755–760. doi: 10.1016/B978-0-12-374501-9.00024-8.
- [2] M. Hallquist, “HEAT TRANSFER AND PRESSURE DROP CHARACTERISTICS OF SMOOTH TUBES AT A CONSTANT HEAT FLUX IN THE TRANSITIONAL FLOW REGIME,” 2011.
- [3] M. I. Omisanya, A. K. Hamzat, S. A. Adedayo, I. A. Adediran, and T. B. Asafa, “Enhancing the thermal performance of solar collectors using nanofluids,” in *IOP Conference Series: Materials Science and Engineering*, Jun. 2020, vol. 805, no. 1. doi: 10.1088/1757-899X/805/1/012015.
- [4] C. C. Newton, “Electronic Theses, Treatises and Dissertations The Graduate School,” 2007.
- [5] P. Bisht, M. Joshi, and A. Gupta, “Comparison of Heat Transfer between a Circular and Rectangular Tube Heat Exchanger by using Ansys Fluent,” 2014. [Online]. Available: <http://inpressco.com/category/ijtt/>
- [6] V. G. Shelke and C. v Patil, “Analyze the Effect of Variations in Shape of Tubes for Flat Plate Solar Water Heater.” [Online]. Available: www.ijser.in
- [7] M. Thakare and M. v Khot, “International Journal of Current Engineering and Technology Performance investigation of formed tubes of different geometry for a Flat-plate solar collector.” [Online]. Available: <http://inpressco.com/category/ijcet>
- [8] N. P. Salunke, J. Khatik, and A. Professor, “A REVIEW ON THE RECENT ADVANCEMENTS IN IMPROVING THE PERFORMANCE OF THE FLAT PLATE COLLECTOR,” 2018. [Online]. Available: www.ijcrt.org
- [9] G. K. Badgujar and S. G. Kamble, “Performance Analysis of Flat Plate Collector by changing Geometry of Absorber tube A Review,” 2007. [Online]. Available: www.ijirset.com

- [10] S. Basavanna and K. S. S. Shashishekar, "CFD ANALYSIS OF TRIANGULAR ABSORBER TUBE OF A SOLAR FLAT PLATE COLLECTOR," 2013. [Online]. Available: www.ijmerr.com
- [11] M. Saad Abbass and N. Sanke, "Employees of the Najaf Technical Institute, Foundation of Technical Education , Ministry of Higher Education and Scientific Research."
- [12] M. Moravej, "AN Experimental Study of the Performance of a Solar Flat Plate Collector with Triangular Geometry," 2021.
- [13] S. v Yeole, Y. J. Vaidya, and S. M. Patil, "Title: Analyze the Effect of Various Shapes of Riser Tubes on Flat Plate Solar Water Heater Efficiency," *International Research Journal of Engineering and Technology*, 2022, [Online]. Available: www.irjet.net
- [14] R. Kumar and M. A. Rosen, "Thermal performance of integrated collector storage solar water heater with corrugated absorber surface," *Appl Therm Eng*, vol. 30, no. 13, pp. 1764–1768, Sep. 2010, doi: 10.1016/j.applthermaleng.2010.04.007.
- [15] S. Li, H. Wang, X. Meng, and X. Wei, *Comparative study on the performance of a new solar air collector with different surface shapes*, vol. 114. Elsevier Ltd, 2017, pp. 639–644. doi: 10.1016/j.applthermaleng.2016.12.026.
- [16] Jalaluddin, E. Arif, and R. Tarakka, "Experimental study of an SWH system with V-shaped plate," *Journal of Engineering and Technological Sciences*, vol. 48, no. 2, pp. 207–217, 2016, doi: 10.5614/j.eng.technol.sci.2016.48.2.7.
- [17] M. S. Chaudhari, D. B. Nalawade, and M. Jagadale, "International Journal of Current Engineering and Technology Heat Transfer Enhancement of Solar Flat Plate Collector by Using V Corrugated Fins and Various Parameters." [Online]. Available: <http://inpressco.com/category/ijcet>
- [18] T. A. Yassen, N. D. Mokhlif, and M. A. Eleiwi, "Performance investigation of an integrated solar water heater with corrugated absorber surface for domestic use," *Renew Energy*, vol. 138, pp. 852–860, Aug. 2019, doi: 10.1016/j.renene.2019.01.114.

- [19] M. H. Tariq, F. Khan, and T. A. Cheema, “Analytical and Experimental Investigation of a Triangular-Channeled Solar Water Heater,” Dec. 2021, p. 17. doi: 10.3390/engproc2021012017.
- [20] Y. Jiang *et al.*, “A comparative study on the performance of a novel triangular solar air collector with tilted transparent cover plate,” *Solar Energy*, vol. 227, pp. 224–235, Oct. 2021, doi: 10.1016/j.solener.2021.08.083.
- [21] R. Shukla, K. Sumathy, P. Erickson, and J. Gong, “Recent advances in the solar water heating systems: A review,” *Renewable and Sustainable Energy Reviews*, vol. 19, pp. 173–190, 2013. doi: 10.1016/j.rser.2012.10.048.
- [22] R. D. Maldonado, E. Huerta, J. E. Corona, O. Ceh, A. I. León, and I. Henandez, “Design and construction of a solar flat collector for social housing in México,” in *Energy Procedia*, 2014, vol. 57, pp. 2159–2166. doi: 10.1016/j.egypro.2014.10.182.
- [23] S. Hossain, A. W. Abbas, J. Selvaraj, F. Ahmed, and N. B. A. Rahim, “Experiment of a flat plate solar water heater collector with modified design and thermal performance analysis,” in *Applied Mechanics and Materials*, 2014, vol. 624, pp. 332–338. doi: 10.4028/www.scientific.net/AMM.624.332.
- [24] R. Bakari, R. J. A. Minja, and K. N. Njau, “Effect of Glass Thickness on Performance of Flat Plate Solar Collectors for Fruits Drying,” *Journal of Energy*, vol. 2014, pp. 1–8, 2014, doi: 10.1155/2014/247287.
- [25] B. Salim, “THEORITICAL ANALYSIS OF FLAT PLATE SOLAR COLLECTOR PLACED IN MOSUL CITY BY USING DIFFERENT ABSORBING MATERIALS AND FLUIDS Practical Comparison of Turbulent Flow Heat Losses for Different Air Duct Materials and Air Velocity. View project E-LEARNING DEVELOPMENT View project,” 2014. [Online]. Available: <https://www.researchgate.net/publication/323245254>
- [26] A. M. Lenz, S. N. M. de Souza, C. E. C. Nogueira, F. Gurgacz, M. Prior, and F. A. Pazuch, “Análise da energia absorvida e eficiência de um coletor solar de placa plana,” *Acta Scientiarum - Technology*, vol. 39, no. 3, pp. 279–284, 2017, doi: 10.4025/actascitechnol.v39i3.29352.

- [27] V. Goel, P. Guleria, and R. Kumar, "Effect of apex angle variation on thermal and hydraulic performance of roughened triangular duct," *International Communications in Heat and Mass Transfer*, vol. 86, pp. 239–244, Aug. 2017, doi: 10.1016/j.icheatmasstransfer.2017.06.008.
- [28] P. N. Shrirao, S. S. Pente, and A. N. Mahure, "International journal of basic and applied research Comparative Thermal Analysis of a Flat Plate Solar Collector using Aerofoil Absorber Tubes with Conventional Circular Absorber Tubes," *Number 12 UGC Approved Journal*, vol. 8, 2018, [Online]. Available: www.pragatipublication.com
- [29] H. Qasim, and H. Q. Mohammed "Experimental Study of Solar Water heating by using Air Bubbles Injection", *Journal of engineering and applied sciences*, vol. 706 no 04, February. 2020, doi: 10.13140/RG.2.2.30392.70408.
- [30] J. Shandal and Q. A. Abed, "A review on development of solar thermal flat plate collector," in *IOP Conference Series: Materials Science and Engineering*, Nov. 2020, vol. 928, no. 2. doi: 10.1088/1757-899X/928/2/022051.
- [31] A. Shakir Baqir, A. Majeed, A. al -Kreem, and A. H. Yousif, "Study the effect of twisted tapes on thermal performance solar collector with using curvature vortex generators," 2020. [Online]. Available: <https://www.researchgate.net/publication/344324530>
- [32] H. S. Khwayyir, A. S. Baqir, and H. Q. Mohammed, "Effect of air bubble injection on the thermal performance of a flat plate solar collector," *Thermal Science and Engineering Progress*, vol. 17, Jun. 2020, doi: 10.1016/j.tsep.2019.100476.
- [33] H. Hameed, M. Mohammed, and A. Saeed, "Performance of A New Model of Air Heating System: Experimental Investigation", *Journal of Mechanical Engineering Research and Developments*, vol.44, no 06 May 2021. [Online]. Available: <https://www.researchgate.net/publication/351367031>
- [34] Y. K. Al-Azmi, R. Y. Sakr, O. E. Abdelatif, and I. M. M. Elsemary B A Graduate Student, "Experimental Investigation of an Evacuated Tube Heat Pipe Solar Collector Using Different Fluids," 2022.

- [35] M. H. Tariq, F. Khan, and T. A. Cheema, "Analytical and Experimental Investigation of a Triangular-Channeled Solar Water Heater," Dec. 2021, p. 17. doi: 10.3390/engproc2021012017.
- [36] S. v Yeole, Y. J. Vaidya, and S. M. Patil, "Title: Analyze the Effect of Various Shapes of Riser Tubes on Flat Plate Solar Water Heater Efficiency," *International Research Journal of Engineering and Technology*, 2022, [Online]. Available: www.irjet.net
- [37] Sunil V. Yeole, Ajay U. Awate, Chandrakant R. Patil, "Investigate the impact of Riser Tube Shape Variations on Flat Plate Solar Water Heater Performance Using CFD Analysis," *Mathematical Statistician and Engineering Applications*, Vol. 71 no. 09 June 2022. doi: 471-Article Text-742-1-10-20220819.
- [38] E. A. Handoyo, D. Ichsani, Prabowo, and Sutardi, "Experimental studies on a solar air heater having v-corrugated absorber plate with obstacles bent vertically," in *Applied Mechanics and Materials*, 2014, vol. 493, pp. 86–92. doi: 10.4028/www.scientific.net/AMM.493.86.
- [39] V. P. Tyagi, "HEAT TRANSFER AND SKIN FRICTION IN A CHANNEL-LAMINAR FLOW WITH VARIABLE PHYSICAL PROPERTIES," *International Journal of Heat and Mass Transfer*. Vol. 8, Pages 1481-1490. no 19 February 1965. doi.org/10.1016/0017-9310(65)90033-5
- [40] J. F. Jf, L. J. Marks, J. A. S. E. Stewart, M. L. Dorsy, W. Watson-wright, and J. S. F. Lawrsrrcs, "FluidMechanics-Streeter.pdf."1992, doi: 10.1016/0041-0101(92)90430-D.
- [41] J. A. Duffie and W. A. Beckman, *Solar engineering of thermal processes*. Wiley, 2013.
- [42] W. A. B. John A. Duffie, *Wiley: Solar Engineering of Thermal Processes, 4th Edition - John A. Duffie, William A. Beckman*. 2013.
- [43] M. Murugan, R. Vijayan, A. Saravanan, and S. Jaisankar, "Performance enhancement of centrally finned twist inserted solar collector using corrugated booster reflectors," *Energy*, vol. 168, pp. 858–869, 2019, doi: 10.1016/j.energy.2018.11.134.

- [44] R. J. Moffat, “Describing the uncertainties in experimental results,” *Exp Therm Fluid Sci*, vol. 1, no. 1, pp. 3–17, 1988, doi: 10.1016/0894-1777(88)90043-X.

APPENDICES

Appendix (A)

A. The calibration of the experiment-related equipment

A.1 Calibration of solar collector meter:

The Figure (A.1) addresses the irradiance meter powered by the sun adjustment. In the staff of specialized designing/Najaf, the sun-oriented meter is adjusted with the sun powered research station for energy. The information was gathered for at regular intervals between 7:00 AM and 5:00 PM.

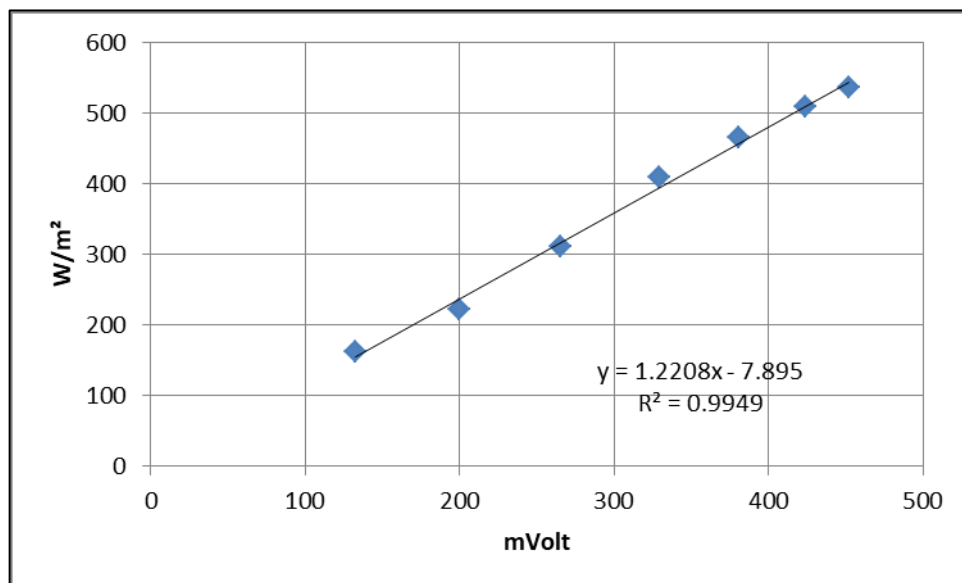


Fig. A.1: sun radiation meter calibration.

A.2 Calibration of volumetric flow meter

The volume stream meter is adjusted utilizing round and hollow graduated glass stopwatch and vessels. Area beneath shows the adjustment measures with test results. Utilizing a calibrator time weight used to adjust the volume stream meter with stopwatch and graduated glass vessel, The adjustment is finished by streaming the water through a stream meter at various stream rates and

simultaneously estimating the stream time expected by volume by the bucket to fill the right measure of working liquid.

samples for calibrating volume flow meters

The flow rate meter's volumetric flow rate reading =1 liter/min

Inspection 1:

Monitoring time =1 minute

The volumetric flow rate in graduate vessel = 0.98liter/min.

Inspection no (2):

Monitoring time =1 minute

Gradient vessel volumetric flow rate = 0.973 liter/min.

Inspection no (3):

Monitoring time =1 minute.

Volumetric flow rate in a graduating vessel = 0.962liter/minute

Inspection 4:

Monitoring time =1 minute.

The Volumetric flow rate in graduate vessel = 0.985 liter/minute.

The average of volumetric flow rates

$V = (v_1 + v_2 + v_3 + v_4) / 4 = (0.98 + 0.973 + 0.962 + 0.985) / 4 = 0.975$ liter/minute the error of the volume flow meter = $1 - 0.975 = 0.025$ liter/minute

% Error = $(1 - 0.975) \times 100 = 2.5\%$

A.3 Calibration of temperature sensors of 8- channel data logger and 4K type thermocouples with digital thermometers:

Four thermocouples (T1-T4) °C for a digital thermometer and two sets of sensors (S1-S8) °C, (S9-S16) °C for two 8-channel data loggers are calibrated using mercury thermometers. The tables (A-1), (A-2) and (A-3) include the calibration findings (A-3)

Table A.1: Calibration results of first 8- channels data logger with 8 sensors

Mercury Thermometer °C	S1°C	S2°C	S3°4	S4°C	S5°C	S6°C	S7°C	S8°C
20	20.4	20.4	20.3	19.8	19.7	20.3	20.4	19.6
25	25.5	25.4	24.6	24.7	25.4	25.3	25.4	24.7
30	30.4	30.3	30.5	29.7	30.4	30.3	30.4	29.6
35	35.4	35.4	35.3	35.4	34.6	35.4	35.2	34.7
40	40.3	40.2	40.2	40.2	39.9	39.8	40.2	40.3
45	45.2	45.4	44.7	44.6	45.2	45.2	45.3	44.9
50	50.3	50.4	49.6	49.7	50.1	50	50.3	50.2
55	55.4	55.3	54.6	55.1	55.3	54.6	55.2	55.3
60	60.3	60.4	60.3	60.1	59.7	60.2	60.2	60.2
65	64.5	65.4	64.5	64.5	65.5	64.6	64.8	64.6

TableA.2: Calibration results of second 8- channels data logger with 8 sensors

Mercury Thermometer °C	S9 °C	S10 °C	S11 °C	S12 °C	S13 °C	S14 °C	S15 °C	S16 °C
20	20.4	19.4	20.4	19.8	20.4	19.7	20.3	19.8
25	24.8	25.4	25.4	25.3	25.4	24.7	25.3	25.3
30	30.4	30.5	30.3	29.7	30.3	29.8	29.6	30.4
35	35.5	35.3	35	34.6	35.3	34.7	34.9	34.7
40	40.4	40.3	40	39.7	39.6	40.4	39.8	39.8
45	45.4	45	44.7	44.6	45.4	44.8	45.4	45.3
50	50.3	50	50.4	49.6	49.8	50.1	50.3	50.2
55	55.3	55.2	55	54.6	54.7	55.4	55.3	54.6
60	60.4	60.3	60	60.4	59.7	59.8	60	60.4
65	64.3	65	64.7	64.7	64.8	64.5	65	64.4

Table A.3: The calibration of 4 k- type

Mercury Thermometer°C	T1°C	T2°C	T3°C	T4°C
25	25.9	26	26	26
30	31	29.2	31	31
35	36	35.6	36	36.3
40	41	40.9	41	41
45	44.1	46	46	46
50	49.2	51	51	51
55	54.1	54	56	56
60	60	61	61.2	59
65	64	64	64.1	66

When plotted, the advantages of sixteen temperature sensors for two 8-channel data lumberjacks and four thermocouples are so near together that they are impossible to distinguish. Bending the straight lines that connect the aforementioned attributes.

a. The correlation values of the first set sensors (S_1 to S_8) as follows:

$$T_{S1}=0.988 \times T_{S1}(\text{real})+0.78 \quad \dots\dots\dots(\text{A.1})$$

$$T_{S2}=0.99 \times T_{S1}(\text{real})+0.3752 \quad \dots\dots\dots(\text{A.2})$$

$$T_{S3}=0.9886 \times T_{S3}(\text{real})+0.4442 \quad \dots\dots(\text{A.3})$$

$$T_{S4}=0.9993 \times T_{S4}(\text{real})-0.0841 \quad \dots\dots (\text{A.4})$$

$$T_{S5}=1.0035 \times T_{S5}(\text{real})-0.0794 \dots\dots .(\text{A.5})$$

$$T_{S6}=0.9851 \times T_{S5}(\text{real})+0.6836 \dots\dots\dots(\text{A.6})$$

$$T_{S7}=0.991 \times T_{S7}(\text{real})+0.6212 \quad \dots\dots\dots(\text{A.7})$$

$$T_{S8}=1.0064 \times T_{S8}(\text{real}) - 0.263 \dots\dots\dots(\text{A.8})$$

Where: $T_s(\text{real})$ = measured values; $T_{s1} \dots s8$ = correction values.

b. The correlation values of the second set sensors (S_9 to S_{16}) as follows:

$$T_{S9}=0.9918 \times T_{S9}(\text{real}) + 0.5703 \dots\dots\dots (\text{A.9})$$

$$T_{S10}=1.0024 \times T_{S10}(\text{real}) + 0.37 \dots\dots\dots (\text{A.10})$$

$$T_{S11}=0.9882 \times T_{S11}(\text{real}) + 0.5897 \dots\dots\dots(\text{A.11})$$

$$T_{S12}=0.999 \times T_{S12}(\text{real}) - 0.1588 \dots\dots\dots .(\text{A.12})$$

$$T_{S13}=0.983 \times T_{S13}(\text{real}) + 0.7612 \dots\dots\dots(\text{A.13})$$

$$T_{S14}=0.003 \times T_{S14}(\text{real}) - 0.2388 \dots\dots\dots(\text{A.14})$$

$$T_{S15}=1.0006 \times T_{S15}(\text{real}) + 0.0642 \dots\dots\dots(\text{A.15})$$

$$T_{S16}=0.9941 \times T_{S16}(\text{real}) + 0.2424 \dots\dots\dots(\text{A.16})$$

c. The correlation values of thermocouples (T_1 to T_4) as follows:

$$T_1 = 0.946 \times T_1(\text{real}) + 2.4633 \dots\dots\dots(\text{A.17})$$

$$T_2 = 0.978 \times T_2(\text{real}) + 1.8011 \dots\dots\dots (\text{A.18})$$

$$T_3 = 0.9767 \times T_3(\text{real}) + 1.8611 \dots\dots\dots(\text{A.19})$$

$$T_4 = 0.981 \times T_4(\text{real}) + 1.155 \dots\dots\dots(\text{A.20})$$

A.4 Calibration differential pressure manometer:

Utilizing a difference pressure gauge and a hydraulic system (air pump), the pressure gauge manometer is calibrated by opening both ports of the gauge and exposing them to the environment in order to achieve a zero-pointer position since no is applied to either port. Pneumatic hose should be connected to the high or positive side. Create the necessary pressure, compare it to a manometer, and record all information for 5 test points. The differential pressure manometer's calibration is shown in fig. (A-2).

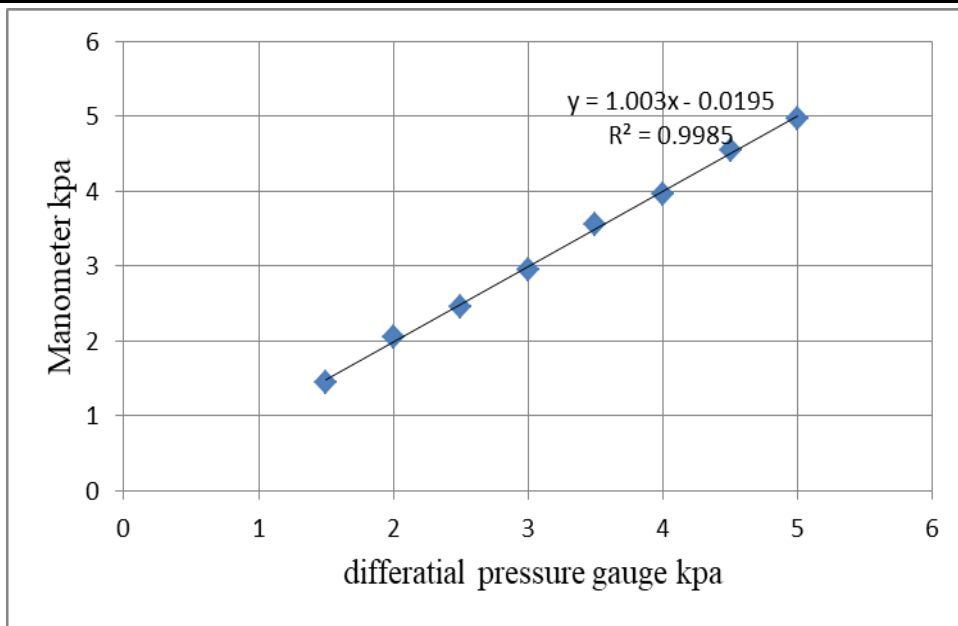


Fig. A.2: calibration of differential pressure manometer

Appendix(B)

B. Uncertainties analysis

Some of the causes of inaccuracy in the current analysis, which are sources of uncertainty in calculating volumetric flow rates, temperatures, pressure decreases, and solar radiation, could cause inaccuracies in the anticipated values:

1. Unsteadiness of electrical power.
2. Indecision in temperature understanding caused from defects in industrial in temperature reader devices and thermocouples.
3. Faults in drift measurements.

R. J. Moffat [44] based on the Kline and McClintock method was used to calculate the error in the obtained results:

Considering the results (R) be a function of m independent variables :
 $S_1, S_2, S_3 \dots S_m$

$$R = R(S_1, S_2, S_3 \dots S_m) \quad (B.1)$$

It is possible to show this relation in linear form as follows for modest changes in the variables:

$$\delta R = R_{S_1} \delta S_1 + R_{S_2} \delta S_2 + R_{S_3} \delta S_3 + \dots + R_{S_m} \delta S_m \quad (B.2)$$

The resulting uncertainty interval (e) may, therefore, be given as:

$$\left(\frac{e_R}{R}\right)^2 = \left[\left(R_{S_1} \frac{e_{S_1}}{S_1} \right)^2 + \left(R_{S_2} \frac{e_{S_2}}{S_2} \right)^2 + \left(R_{S_3} \frac{e_{S_3}}{S_3} \right)^2 + \dots + \left(R_{S_m} \frac{e_{S_m}}{S_m} \right)^2 \right]$$

(B.3)

Where : $R_{S_m} = \frac{\partial R}{\partial S_m} \quad (B.4)$

B.1 Friction factor derivation

$$f = \left(\frac{d_i}{L}\right) \left(\frac{2\Delta P}{\rho_w U^2}\right) \quad (\text{B.1})$$

$$f = 2 \left(\frac{\Delta P}{L}\right) \left(\frac{\rho_w d_i^3}{Re^2 \mu_w^2}\right) \quad (\text{B.2})$$

$$\frac{\partial f}{\partial(\Delta P)} = \frac{2}{L} \left(\frac{\rho_w d_i^3}{Re^2 \mu_w^2}\right)$$

$$\frac{\partial f}{\partial(L)} = 2 \Delta P \left(\frac{\rho_w d_i^3}{Re^2 \mu_w^2}\right) \left(-\frac{1}{L^2}\right)$$

$$\frac{\partial f}{\partial(d_i)} = \frac{2 \Delta P}{L} \left(\frac{\rho_w}{Re^2 \mu_w^2}\right) (3 d_i^2)$$

$$\frac{\partial f}{\partial(Re)} = \frac{2 \Delta P}{L} \left(\frac{\rho_w d_i^3}{\mu_w^2}\right) \left(\frac{-2}{Re^3}\right)$$

Take amount of error on either side of the equation (C.1)

$$\Delta f = \left[\left\{ \frac{\partial f}{\partial(\Delta P)} \Delta(\Delta P) \right\}^2 + \left\{ \frac{\partial f}{\partial(L)} \Delta(L) \right\}^2 + \left\{ \frac{\partial f}{\partial(d_i)} \Delta(d_i) \right\}^2 + \left\{ \frac{\partial f}{\partial(Re)} \Delta(Re) \right\}^2 \right]^{0.5} \quad (\text{B.3})$$

$$\frac{\partial f}{\partial(\Delta P)} \Delta(\Delta P) = \frac{2}{L} \left(\frac{\rho_w d_i^3}{Re^2 \mu_w^2}\right) \Delta(\Delta P)$$

$$= \frac{2\Delta P}{L} \left(\frac{\rho_w d_i^3}{Re^2 \mu_w^2}\right) \frac{\Delta(\Delta P)}{\Delta P}$$

$$= f \frac{\Delta(\Delta P)}{\Delta P} \quad (\text{B.4})$$

$$\frac{\partial f}{\partial(L)} \Delta(L) = 2 \Delta P \left(\frac{\rho_w d_i^3}{Re^2 \mu_w^2}\right) \left(-\frac{1}{L^2}\right) \Delta(L)$$

$$= -2 \left(\frac{\Delta P}{L}\right) \left(\frac{\rho_w d_i^3}{Re^2 \mu_w^2}\right) \frac{\Delta(L)}{L} = -f \frac{\Delta(L)}{L} \quad (\text{B.5})$$

$$\frac{\partial f}{\partial(d_i)} \Delta(d_i) = \frac{2 \Delta P}{L} \left(\frac{\rho_w}{Re^2 \mu_w^2}\right) (3 d_i^2) \Delta(d_i)$$

$$= 3 \left(\frac{\Delta P}{L}\right) \left(\frac{\rho_w d_i^3}{Re^2 \mu_w^2}\right) \frac{\Delta(d_i)}{d_i} = 3f \frac{\Delta(d_i)}{d_i} \quad (\text{B.6})$$

$$\frac{\partial f}{\partial(Re)} \Delta(Re) = \frac{2 \Delta P}{L} \left(\frac{\rho_w d_i^3}{\mu_w^2}\right) \left(\frac{-2}{Re^3}\right) \Delta(Re)$$

$$= \frac{2 \Delta P}{L} \left(\frac{\rho_w d_i^3}{\mu_w^2 Re^2}\right) \left(\frac{-2\Delta(Re)}{Re}\right) = -2f \left(\frac{\Delta(Re)}{Re}\right) \quad (\text{B.7})$$

replacing equations (B.4),(B.5),(B.6) and (B.7) in equation (B.3), we can get:

$$\begin{aligned}
 \Delta f &= \left[\left\{ f \frac{\Delta(\Delta P)}{\Delta P} \right\}^2 + \left\{ -f \frac{\Delta(L)}{L} \right\}^2 + \left\{ 3f \frac{\Delta(d_i)}{d_i} \right\}^2 + \left\{ -2f \left(\frac{\Delta(Re)}{Re} \right) \right\}^2 \right]^{0.5} \\
 &= \left[f^2 \left\{ \frac{\Delta(\Delta P)}{\Delta P} \right\}^2 + f^2 \left\{ \frac{\Delta(L)}{L} \right\}^2 + f^2 \left\{ \frac{3\Delta(d_i)}{d_i} \right\}^2 + f^2 \left\{ \frac{2\Delta(Re)}{Re} \right\}^2 \right]^{0.5} \\
 \Delta f &= f \left[\left\{ \frac{\Delta(\Delta P)}{\Delta P} \right\}^2 + \left\{ \frac{\Delta(L)}{L} \right\}^2 + \left\{ \frac{3\Delta(d_i)}{d_i} \right\}^2 + \left\{ \frac{2\Delta(Re)}{Re} \right\}^2 \right]^{0.5} \\
 \frac{\Delta f}{f} &= \left[\left\{ \frac{\Delta(\Delta P)}{\Delta P} \right\}^2 + \left\{ \frac{\Delta(L)}{L} \right\}^2 + \left\{ \frac{3\Delta(d_i)}{d_i} \right\}^2 + \left\{ \frac{2\Delta(Re)}{Re} \right\}^2 \right]^{0.5} \tag{B.8}
 \end{aligned}$$

where ΔP directly evaluated from forced circulation or $\Delta P = (\rho_{mercury} - \rho_w) \Delta h$ where;

h is difference between mercury and water columns in meter).

$\rho_{mercury}$ is density of mercury in kg/m^3 .

$$\frac{\Delta(\Delta P)}{\Delta P} = \frac{\Delta h}{h} \tag{B.9}$$

$$Re = \frac{\rho_w d_i U}{\mu_w} \quad \text{and} \quad \dot{m} = \frac{\pi}{4} d_i^2 \rho_w U$$

$$\text{Thus} \quad Re = \frac{4 \dot{m}}{\pi d_i \mu_w} \tag{B.10}$$

$$\frac{\Delta(Re)}{Re} = \left[\left\{ \frac{\Delta \dot{m}}{\dot{m}} \right\}^2 + \left\{ \frac{\Delta d_i}{d_i} \right\}^2 \right]^{0.5} \tag{B.11}$$

B.2 Nusselt number derivation

$$Nu = \frac{h_i d_i}{k} \tag{B.12}$$

$$\frac{\Delta Nu}{Nu} = \left[\left\{ \frac{\Delta h_i}{h_i} \right\}^2 + \left\{ \frac{\Delta d_i}{d_i} \right\}^2 + \left\{ \frac{\Delta k}{k} \right\}^2 \right]^{0.5} \tag{B.13}$$

From equations (3.25)& (3.26)

$$h_i = \frac{1}{A_i \left[\frac{q}{T_p - T_m} - \frac{\ln\left(\frac{d_o}{d_i}\right)}{2\pi k_w L} \right]} \tag{B.14}$$

$$\Delta h_i = \frac{1}{A_i} \left[\left\{ \frac{\partial h_i}{\partial q} \Delta q \right\}^2 + \left\{ \frac{\partial h_i}{\partial T_p} \Delta T_p \right\}^2 + \left\{ \frac{\partial h_i}{\partial T_m} \Delta T_m \right\}^2 + \left\{ \frac{\partial h_i}{\partial \left(\ln\left(\frac{d_o}{d_i}\right) \right)} \Delta \left(\ln\left(\frac{d_o}{d_i}\right) \right) \right\}^2 \right]^{0.5}$$

$$\begin{aligned}
 \frac{\Delta h_i}{h_i} &= \frac{1}{A_i} \frac{1}{h_i} [\{ \frac{\partial h_i}{\partial q} \Delta q \}^2 + \{ \frac{\partial h_i}{\partial T_p} \Delta T_p \}^2 + \{ \frac{\partial h_i}{\partial T_m} \Delta T_m \}^2 + \{ \frac{\partial h_i}{\partial (\ln(\frac{d_o}{d_i}))} \Delta (\ln(\frac{d_o}{d_i})) \}^2]^{0.5} \\
 &= \frac{1}{A_i} [\frac{1}{h_i^2} \{ \frac{\partial h_i}{\partial Q} \Delta Q \}^2 + \frac{1}{h_i^2} \{ \frac{\partial h_i}{\partial T_p} \Delta T_p \}^2 + \frac{1}{h_i^2} \{ \frac{\partial h_i}{\partial T_m} \Delta T_m \}^2 + \frac{1}{h_i^2} \{ \frac{\partial h_i}{\partial (\ln(\frac{d_o}{d_i}))} \Delta (\ln(\frac{d_o}{d_i})) \}^2]^{0.5} \\
 &= \frac{1}{A_i} [(\frac{\Delta q}{q})^2 \frac{1}{[\{ \frac{q}{T_p - T_m} \} - \frac{\ln(\frac{d_o}{d_i})}{2\pi k_{WL}}]^2} \frac{1}{h_i^2} + (\frac{\Delta T_p}{T_p})^2 \frac{1}{[\{ \frac{q}{T_p - T_m} \} - \frac{\ln(\frac{d_o}{d_i})}{2\pi k_{WL}}]^2} \frac{1}{h_i^2} + \\
 &(\frac{\Delta T_m}{T_m})^2 \frac{1}{[\{ \frac{q}{T_p - T_m} \} - \frac{\ln(\frac{d_o}{d_i})}{2\pi k_{WL}}]^2} \frac{1}{h_i^2} + (\frac{\Delta (\ln(\frac{d_o}{d_i}))}{\ln(\frac{d_o}{d_i})})^2 \frac{1}{[\{ \frac{q}{T_p - T_m} \} - \frac{\ln(\frac{d_o}{d_i})}{2\pi k_{WL}}]^2} \frac{1}{h_i^2}]^{0.5} \\
 \frac{\Delta h_i}{h_i} &= A_i [\{ \frac{\Delta Q_{out}}{Q_{out}} \}^2 + \{ \frac{\Delta T_p}{T_p} \}^2 + \{ \frac{\Delta T_m}{T_m} \}^2 + \{ \frac{\Delta (\ln(\frac{d_o}{d_i}))}{\ln(\frac{d_o}{d_i})} \}^2]^{0.5} \quad (B.15)
 \end{aligned}$$

B.3 collector efficiency derivation

gatherer effectiveness is assessed in light of the proportion of intensity yield from the sun powered authority to warm contribution of the sun oriented gatherer.

$$\eta = \left(\frac{Q_{out}}{Q_{in}} \right), \quad \eta = \frac{(\frac{\Delta Q}{Q})_{out}}{(\frac{\Delta Q}{Q})_{in}}$$

where the Q_{out} represent the heat gained by the water from the inlet to outlet. Thus Q_{out} is given by:

$$Q_{out} = \dot{m} \times C_p \times (T_o - T_i)$$

$$\left(\frac{\Delta Q}{Q} \right)_{out} = \left(\frac{1}{Q_{out}} \right) [\{ \frac{\partial Q_{out}}{\partial \dot{m}} \Delta \dot{m} \}^2 + \{ \frac{\partial Q_{out}}{\partial T_o} \Delta T_o \}^2 + \{ \frac{\partial Q_{out}}{\partial T_i} \Delta T_i \}^2]^{0.5}$$

$$\left(\frac{\Delta Q}{Q} \right)_{out} = [\{ \frac{\Delta \dot{m}}{\dot{m}} \}^2 + \{ \frac{\Delta T_o}{T_o} \}^2 + \{ \frac{\Delta T_i}{T_i} \}^2]^{0.5} \quad (B.16)$$

Q_{in} is the input heat evaluated from atmospheric temperature and in temperature of water:

$$\left(\frac{\Delta Q}{Q} \right)_{in} = \frac{1}{Q_{in}} [\{ \frac{\partial Q_{in}}{\partial T_i} \Delta T_i \}^2 + \{ \frac{\partial Q_{in}}{\partial T_a} \Delta T_a \}^2 + \{ \frac{\partial Q_{in}}{\partial G_T} \Delta G_T \}^2]^{0.5}$$

$$\left(\frac{\Delta Q}{Q}\right)_{in} = \left[\left\{ \frac{\Delta T_i}{T_i} \right\}^2 + \left\{ \frac{\Delta T_a}{T_a} \right\}^2 + \left\{ \frac{\Delta G_T}{G_T} \right\}^2 \right]^{0.5} \quad (B.17)$$

$$\frac{\Delta \eta}{\eta} = \frac{1}{\eta} \left[\left\{ \frac{\partial \eta}{\partial Q_{in}} \Delta Q_{in} \right\}^2 + \left\{ \frac{\partial \eta}{\partial Q_{out}} \Delta Q_{out} \right\}^2 \right]^{0.5}$$

$$\frac{\Delta \eta}{\eta} = \left[\left\{ \frac{\Delta Q_{in}}{Q_{in}} \right\}^2 + \left\{ \frac{\Delta Q_{out}}{Q_{out}} \right\}^2 \right]^{0.5} \quad (B.18)$$

B.4 Uncertainty analysis for forced circulation condition:

The blunders got in this analysis concentrate on care considering the least counts and the exactness of the gadgets used. Table (B.1) address the mistakes in the gadgets utilized in this tests review.

TableB.1: The errors in the instruments used in experiments

S. No.	Quantity	Value	probable error[Δx]
1.	d _i	0.0115 m	0.0007m
2.	d _o	0.0125m	0.0007m
3.	L	1.5m	0.001m
4.	ṁ	0.025kg/sec	0.00048 kg/sec
5.	T _p	54°C	0.6°C
6.	T _i	36.3°C	0.6°C
7.	T _o	40.2°C	0.6°C
8.	T _m	38.4°C	0.6°C
9.	T _a	30.4°C	0.6°C
10.			
11.	ΔP	58 mbar	0.04mbar

B4.1Friction factor evaluated

From eq. (B.11)

$$\frac{\Delta(\text{Re})}{\text{Re}} = \left[\left\{ \frac{\Delta \dot{m}}{\dot{m}} \right\}^2 + \left\{ \frac{\Delta d_i}{d_i} \right\}^2 \right]^{0.5} = \left[\left\{ \frac{0.00048}{0.025} \right\}^2 + \left\{ \frac{0.0008}{0.0115} \right\}^2 \right]^{0.5} = 6.32\%$$

From eq.(C.9)

$$\frac{\Delta(\Delta P)}{\Delta P} = \frac{0.05 \text{ mbar}}{65 \text{ mbar}} = 7.69 \times 10^{-4}$$

From eq. (B.8)

$$\frac{\Delta f}{f} = \left[\left\{ \frac{\Delta(\Delta P)}{\Delta P} \right\}^2 + \left\{ \frac{\Delta(L)}{L} \right\}^2 + \left\{ \frac{3\Delta(d_i)}{d_i} \right\}^2 + \left\{ \frac{2 \Delta(\text{Re})}{\text{Re}} \right\}^2 \right]^{0.5}$$

$$\frac{\Delta f}{f} = \left[\left\{ 7.69 \times 10^{-4} \right\}^2 + \left\{ \frac{0.001}{1.6} \right\}^2 + \left\{ \frac{3 \times 0.0008}{0.0115} \right\}^2 + \left\{ 2 \times 0.0721 \right\}^2 \right]^{0.5} = 0.326$$

B 4.2. The Nusselt number calculation

From the equation (B.16)

$$\begin{aligned} \left(\frac{\Delta Q}{Q} \right)_{\text{out}} &= \left[\left\{ \frac{\Delta \dot{m}}{\dot{m}} \right\}^2 + \left\{ \frac{\Delta T_o}{T_o} \right\}^2 + \left\{ \frac{\Delta T_i}{T_i} \right\}^2 \right]^{0.5} = \left[\left\{ \frac{0.00048}{0.025} \right\}^2 + \left\{ \frac{0.5}{39.8} \right\}^2 + \left\{ \frac{0.5}{35.6} \right\}^2 \right]^{0.5} \\ &= 2.68\% \end{aligned}$$

From equations (B.14) and (B.15)

$$\begin{aligned} \frac{\Delta h_i}{h_i} &= A_i \left[\left\{ \frac{\Delta Q_{\text{out}}}{Q_{\text{out}}} \right\}^2 + \left\{ \frac{\Delta T_p}{T_p} \right\}^2 + \left\{ \frac{\Delta T_m}{T_m} \right\}^2 + \left\{ \frac{\Delta(\ln(\frac{d_o}{d_i}))}{\ln(\frac{d_o}{d_i})} \right\}^2 \right]^{0.5} \\ &= 1.039 \times 10^{-4} \left[\left\{ 0.0268 \right\}^2 + \left\{ 0.0119 \right\}^2 + \left\{ 0.0133 \right\}^2 + \left\{ \frac{0}{0.0883} \right\}^2 \right]^{0.5} \\ &= 1.382 \times 10^{-6} \end{aligned}$$

$$\begin{aligned} \frac{\Delta \text{Nu}}{\text{Nu}} &= \left[\left\{ \frac{\Delta h_i}{h_i} \right\}^2 + \left\{ \frac{\Delta d_i}{d_i} \right\}^2 \right]^{0.5} = \left[\left\{ \frac{\Delta h_i}{h_i} \right\}^2 + \left\{ \frac{\Delta d_i}{d_i} \right\}^2 \right]^{0.5} \\ &= \left[\left\{ 1.382 \times 10^{-6} \right\}^2 + \left\{ 0.0695 \right\}^2 \right]^{0.5} = 5.42\% \end{aligned}$$

B.4.3 Efficiency calculation

From the equations (1.17) and (1.18)

$$\left(\frac{\Delta Q}{Q}\right)_{\text{in}} = \left[\left\{ \frac{\Delta T_i}{T_i} \right\}^2 + \left\{ \frac{\Delta T_a}{T_a} \right\}^2 + \left\{ \frac{\Delta G_T}{G_T} \right\}^2 \right]^{0.5} = \left[\{ 0.0140 \}^2 + \{ 0.0174 \}^2 + \{ 0.0141 \}^2 \right]^{0.5} = 2.64\%$$

$$\frac{\Delta \eta}{\eta} = \left[\left\{ \frac{\Delta Q_{\text{in}}}{Q_{\text{in}}} \right\}^2 + \left\{ \frac{\Delta Q_{\text{out}}}{Q_{\text{out}}} \right\}^2 \right]^{0.5} = \left[0.0264 \right]^2 + \left[0.0268 \right]^2 \right]^{0.5} = 4.35\%$$

Appendix(C)

C. List of publications

1. Accept the publication of the paper (Experimental study of heat transfer by using triangular cylinder inside V- corrugated plate solar collector) in the journal (Journal of Optoelectronics Laser).



ARTICLE ACCEPTANCE LETTER

Date: 17, September, 2022

Dear Authors,

Thank you very much for your submission to our journal.

We are pleased to inform you that your paper has been reviewed, and **accepted** for publication in upcoming issue **2022** of the journal based on the Recommendation of the Editorial Board without any major corrections in the content submitted by the researcher. This letter is the official confirmation of acceptance of your research paper.

Title: Experimental study of heat transfer by using triangular cylinder inside V- corrugated plate solar collector

Authors: Abdulabbas A. Wali¹, Ahmed Hashim Yousif².

¹ Department of Power Mechanics, Technical College Najaf, Al-Furat Al-Awsat Technical University, Najaf 31001, Iraq

² Mechanical Department, Technical Institute of Al-Diwaniyah, Al-Furat Al-Awsat Technical University (ATU), Al-Qadisiyah 58001, Iraq

Kindly acknowledge the Paper acceptance.

Best wishes,

A handwritten signature in black ink, appearing to read "M. Rashed".

Editor In-Chief

Guangdianzi Jiguang/Journal of Optoelectronics Laser

<http://www.gdiz.org/index.php/OJL>

<https://www.scopus.com/urn:sid/29685>

Email: gdizjournal@gmail.com

Experimental Study of Heat Transfer by Using Triangular Cylinder Inside V- Corrugated Plate Solar CollectorAbdulabbas A. Wali¹ & Ahmed Hashim Yousif²¹Department of Power Mechanics, Technical College Najaf, Al-Furat Al-Awsat Technical University, Najaf 31001, Iraq²Mechanical Department, Technical Institute of Al-Diwaniyah, Al-Furat Al-Awsat Technical University (ATU), Al- Qadisiyah 58001, Iraq**ABSTRACT**

The experimental work in this paper to compare the performance of solar collector containing triangular tubes placed inside grooves of V-corrugated absorber plate with solar collector containing circular tubes placed on a flat plate, under the same environmental conditions, and at four flow conditions (2,3,5,7) LPM. And the results were 1- The solar collector that contain triangular tubes placed inside grooves of V-corrugated absorber plate are more efficient in thermal conductivity than the solar collector that contain circular tubes placed on the flat plate, because the contact area between the triangular tubes and the V-corrugated absorber plate is greater than the contact area between the circular tubes and the flat plate, which increases the heat transfer from the V-corrugated plate to the triangular tubes, which increases the heating of the water used. 2-2-Increasing the flow water in the pipes of the both solar collectors, increasing the flow water in the pipes of the both solar collectors, increases the temperature of the water used, which increases the efficiency of the solar collector. As it was used in this research, (2,3,5,7) l/min respectively.

Keyword: Solar Collector, V- corrugated absorber plate, triangular tubes, circular tubes, heat transfer, thermal conductivity, grooves

I. INTRODUCTION

One of the simplest designs and installation of the solar applications is the FPSC which has a wide interest of researchers for its high efficiency as comparison with its low initial cost and high flexibility for building and development. Flat plate solar collector is used for low temperature heating applications. Domestic solar water heater is one of the popular examples of its use. These collectors are more reliable, simple in operation and low maintenance required. These collectors are extensively used all over the world. The further applications of this collector are pool heating, laundry, space heating, drying agriculture products etc.

Muhammad, et al. [1] utilizes the collector's energy by constructing a new V-shaped solar collector with triangular channels, different operational settings, and a mass flow rate and solar heat flow for the supply of hot water for the home. Through the influence of the water temperature, the solar efficiency was determined analytically and compared with the test results. Additionally, this study contains theoretical and practical investigations into the thermal effectiveness of the suggested absorber as well as the heat exchange impact. All three sides of the triangular channels used in this study are simultaneously exposed to solar radiation, allowing for the collection of more heat energy and resulting in greater temperatures and improved collector performance.

The researchers Mangesh Thakare * and M.V.Khot [2] used round, triangular, square, and oval-shaped tubes are among the different tube forms used in solar flat plate collectors. The improvement of solar flat plate collector performance was the main goal of this investigation. Utilize molded tubes in various shapes to predict outcomes and conduct tests to enhance the efficiency of flat panel solar collectors. The different figures were acquired by studies using tubes of different forms, including square, triangular, circular, and oval tubes. According to the efficiency table, the triangular tube has the maximum efficiency when compared to other tubes. Additionally, it has been found that efficiency varies with sunshine intensity and is directly related to flow rate.

Ganesh K. Badgujar, et al. [3] performed a performance investigation of the flat plate collector using different absorber tube geometries, including square, circular, semicircular, triangular, oval, and rectangular tubes. The triangle tube, which was used, had the highest heat transfer efficiency compared to the other tubes used, and the efficiency of the solar collector was directly proportional to the flow rate of the fluid used. Additionally, the efficiency of the solar collector could be increased by altering the absorption by using a substance. High conductivity also improves collector performance by reducing the area of FPC while increasing tube diameter and raiser length. Through this work, it can be deduced that the flat plate solar collector's efficiency increases with an increase in the contact surface area between the flow tube and the liquid.

Researchers H.Ambarita, R.E.T. Siregar, AD Ronowikarto, E.Y. Setyawan [4] used , CFD was used to determine how the inclination angle affected the effectiveness of the flat plate solar collector. This study came to the conclusion

2. Accept the distribution of the exploration (Study the effect of using triangular cylinder besides v-corrugated plate solar collector on heat transfer experimentally) in the journal (Journal of Northeastern University)



Journal of Northeastern University
E-ISSN: 1005-3026
<https://dbdxcb.cn/>

Date: 07-11-2022
Paper Id: JNU_2022_124

ACADEMIC PAPER ACCEPTANCE LETTER

Dear Authors:

Abdulabbas A. Wali^{1,*}, Ahmed Hashim Yousif^{2,†}

¹Department of Power Mechanics, Technical College Najaf, Al-Furat Al-Awsat Technical University, Najaf 31001, Iraq

²Mechanical Department, Technical Institute of Al-Diwaniyah, Al-Furat Al-Awsat Technical University (ATU), Al-Qadisiyah 58001, Iraq.

Title: Study the effect of using triangular cylinder besides v-corrugated plate solar collector on heat transfer experimentally

Date of Acceptance : 07-11-2022
Type of Paper : **Research Paper**

After peer review process, your article has been provisionally accepted for publication in **Journal of Northeastern University** in the forthcoming issue of 2022.

All papers are published in English language. All submitted manuscripts are subject to peer-review by the leading specialists for the respective topic.

Regards



Editorial Manager
Journal of Northeastern University
ISSN: 1005-3026



<https://www.scopus.com/sourceid/16040>

<https://dbdxcb.cn/>

3. Accept the distribution of the exploration (Experimental study for enhanced heat transfer from triangular cylinder over V-corrugated plate solar collector) in the journal (Advanced Engineering Science)

Gongcheng Kexue Yu Jishu/
Advanced Engineering Science

November 12, 2022

ARTICLE ACCEPTANCE LETTER

Article ID: AES- 2022-0376

Article Title: Experimental study for enhanced heat transfer from triangular cylinder over V-corrugated plate solar collector.

Authors: Abdulabbas A. Wali^{1,*)}, Ahmed Hashim Yousif^{2,*)}

¹Department of Power Mechanics, Technical College Najaf, Al-Furat Al-Awsat Technical University, Najaf 31001, Iraq

²Mechanical Department, Technical Institute of Al-Diwaniyah, Al-Furat Al-Awsat Technical University (ATU), Al- Qadisiyah 58001, Iraq.

Thank you very much for your submission to our journal.

We are pleased to inform you that your paper has been reviewed, and accepted for publication. Your article will be published in upcoming current issue.

Thank you for making the journal a vehicle for your research interests.



Best wishes, Editor-in-Chief



Advanced Engineering Science
ISSN: 2096-3246

<https://advancedengineeringscience.com/>

<https://www.scopus.com/sourceid/21100805730>

<https://www.scimagojr.com/journalsearch.php?q=21100805730&tip=sid&clean=0>

الخلاصة

الهدف من هذا البحث هو دراسة عملية لتأثير استخدام الأنابيب المثلية مع صفيحة المنيوم تحتوي على أخاديد بشكل V، وتأثيرها على معدل انتقال الحرارة بدلالة رقم نسلت Nu ، وخسائر الضغط بدلالة معامل الاحتكاك f ، ومعامل الأداء الحراري TPF ، والكفاءة للمجمع الشمسي، هذا البحث ركز على عملية حفظ الطاقة تحت ظروف مستقلة للجريان الطبقي وللماء المقطر كمائع إختباري.

الجانب العمل يشتمل على تصنيع مجمع شمسي يحتوي على صفيحة من الالمنيوم والتي تحتوي على اخاديد بشكل V، ومجمع شمسي اخر يحتوي على صفيحة مسطحة من الالمنيوم، وكذلك تصنيع نوعين من الانابيب (الانابيب الدائرية والانابيب المثلية). أجهزة القياس المستخدمة كانت جهاز قياس الاشعاع الشمسي، جهاز قياس التدفق الحجمي للمائع، جهاز قياس فرق الضغط، جهاز قياس درجات الحرارة مع حساسات الحرارة، التجارب أجريت في محافظة ذي قار حسب خط العرض $N 31.54^\circ$ وخط الطول $E 46.12^\circ$ مدى التدفق الحجمي المستخدم في التجارب كان (2,3,5,7) لتر/ثانية ورقم رينولد Re يتغير من 500 الى 1900، والنتائج الاختبارية بينت ان انخفاض معدل التدفق الحجمي يزيد في فرق درجة الحرارة بين درجة حرارة الدخول والخروج للماء، وكان اعلى فرق في درجة الحرارة للتدفق الحجمي هو $10.8^\circ C$ كان عند التدفق 2 لتر/ثانية في الانابيب المثلية الموضوعة في داخل الاخاديد وبنفس الوقت ان اعلى ارتفاع في درجة الحرارة $89^\circ C$ خروج كان عند التدفق 7 لتر/ثانية للأنابيب المثلية الموضوعة في داخل الاخاديد. بالإضافة الى ان معدل انتقال الحرارة بدلالة رقم نسلت Nu ، خسائر الضغط بدلالة معامل الاحتكاك f ازداد في الانابيب المثلية في داخل الاخاديد مقارنة مع الانابيب الدائرية كذلك ان رقم نسلت ازداد (30%, 35.5%, 40% and 52.7%) بالمقارنة مع الانابيب الدائرية للجريان الطبقي ورقم رينولد $500 < Re < 1900$ اضافة الى ان معامل الاحتكاك يقل بزيادة رقم رينولد (Re)، حيث يزداد معامل الاحتكاك في الانابيب المثلية في داخل الاخاديد بالمقارنة مع الانابيب الدائرية حيث تكون الزيادة (15% -25%). وبينت النتائج العملية أن أعلى معامل أداء حراري وكفاءة يكون في الأنابيب المثلية الموضوعة في داخل الأخاديد بالمقارنة مع الحالات الأخرى. حيث أن أعلى معامل أداء حراري كان 2.6 وأعلى كفاءة كانت 53.4%.



دراسة تجريبية لمجمع الألواح الشمسية المسطحة باستخدام الأخاديد على شكل V مع تصميم أنابيب متعددة الأشكال

رسالة مقدمة إلى

قسم هندسة تقنيات ميكانيك القوى في الكلية التقنية الهندسية-نجف / جامعة الفرات الأوسط التقنية
كجزء من متطلبات نيل درجة الماجستير في هندسة تقنيات ميكانيك الحرارية

تقدم بها

عبد العباس عبد النبي والي حمادي القره غولي

إشراف

الأستاذ الدكتور

أحمد هاشم يوسف

1444 هـ



جمهورية العراق
وزارة التعليم العالي والبحث العلمي
جامعة الفرات الاوسط التقنية
الكلية التقنية الهندسية-النجف

دراسة تجريبية لمجمع الألواح الشمسية المسطحة باستخدام الأخاديد
على شكل V مع تصميم أنابيب متعددة الأشكال

عبد العباس عبد النبي والي حمادي القره غولي
ماجستير في هندسة تقنيات ميكانيك القوى